

ISSN: 2164-5388 Volume 12, Number 4, October 2022



Open Journal of Biophysics

BIOPHYSICS

ISSN: 2164-5388



9 772164 538002 04

<https://www.scirp.org/journal/ojbiphy>

Journal Editorial Board

ISSN Print: 2164-5388 ISSN Online: 2164-5396
<https://www.scirp.org/journal/ojbiph>

Editor-in-Chief

Prof. W. John Martin Institute of Progressive Medicine, USA

Associate Editors

Dr. Veysel Kayser Massachusetts Institute of Technology, USA
Prof. Ganhui Lan George Washington University, USA
Dr. Jaan Männik University of Tennessee, USA
Prof. Sanbo Qin Florida State University, USA
Dr. Bo Sun Oregon State University, USA
Dr. Bin Tang South University of Science and Technology of China, China

Editorial Board

Prof. Rabiul Ahasan University of Oulu, Finland
Prof. Abass Alavi University of Pennsylvania, USA
Prof. Chris Bystroff Rensselaer Polytechnic Institute, USA
Dr. Luigi Maxmilian Caligiuri University of Calabria, Italy
Prof. Robert H. Chow University of Southern California, USA
Prof. Carmen Domene University of Oxford, UK
Prof. Antonio José da Costa Filho University of São Paulo, Brazil
Prof. Ferdinand Gasparyan Yerevan State University, Armenia
Dr. John Kolega State University of New York, USA
Dr. Pavel Kraikivski Virginia Tech, USA
Dr. Gee A. Lau University of Illinois at Urbana-Champaign, USA
Prof. Yves Mély Louis Pasteur University, France
Dr. Monalisa Mukherjea University of Pennsylvania, USA
Dr. Jerry Opoku-Ansah University of Cape Coast, Ghana
Dr. Xiaodong Pang Florida State University, USA
Prof. Arthur D. Rosen Indiana University, USA
Prof. Brian Matthew Salzberg University of Pennsylvania, USA
Dr. Preet Sharma Midwestern State University, USA
Prof. Jianwei Shuai Xiamen University, China
Prof. Alexander A. Spector Johns Hopkins University, USA
Prof. Munekazu Yamakuchi University of Rochester, USA

Table of Contents

Volume 12 Number 4

October 2022

**NLR's Analogs with Young Blood Cells in Monitoring of Toxicity of Long-Term
Preventing Immunosuppression in the Liver Transplant's Recipients**

A. N. Shoutko, O. A. Gerasimova.....173

Cancer-Specific Resonances

A. Szasz.....185

ISFET Based Immunosensor

F. Gasparyan, L. Gasparyan, V. Simonyan.....223

Can a Molecule Be “Intelligent”? Unexpected Connections between Physics and Biology

G. Paoli.....234

An Hybrid Model for Rectal Tumour Response Prediction during Radiotherapy

A. Sena, G. Laurent, B. Nicolas, V. Dimitris, S. Olivier, C. Thierry, L. Philippe, R. Vincent, R. Pascal.....245

Study on Plant Radiation Signal Transduction for Human Self-Healing

X. Z. Yuan, J. F. Yuan, Q. Bi, K. Z. Song.....265

Open Journal of Biophysics (OJBIPHY)

Journal Information

SUBSCRIPTIONS

The *Open Journal of Biophysics* (Online at Scientific Research Publishing, <https://www.scirp.org/>) is published quarterly by Scientific Research Publishing, Inc., USA.

Subscription rates:

Print: \$79 per issue.

To subscribe, please contact Journals Subscriptions Department, E-mail: sub@scirp.org

SERVICES

Advertisements

Advertisement Sales Department, E-mail: service@scirp.org

Reprints (minimum quantity 100 copies)

Reprints Co-ordinator, Scientific Research Publishing, Inc., USA.

E-mail: sub@scirp.org

COPYRIGHT

Copyright and reuse rights for the front matter of the journal:

Copyright © 2022 by Scientific Research Publishing Inc.

This work is licensed under the Creative Commons Attribution International License (CC BY).

<http://creativecommons.org/licenses/by/4.0/>

Copyright for individual papers of the journal:

Copyright © 2022 by author(s) and Scientific Research Publishing Inc.

Reuse rights for individual papers:

Note: At SCIRP authors can choose between CC BY and CC BY-NC. Please consult each paper for its reuse rights.

Disclaimer of liability

Statements and opinions expressed in the articles and communications are those of the individual contributors and not the statements and opinion of Scientific Research Publishing, Inc. We assume no responsibility or liability for any damage or injury to persons or property arising out of the use of any materials, instructions, methods or ideas contained herein. We expressly disclaim any implied warranties of merchantability or fitness for a particular purpose. If expert assistance is required, the services of a competent professional person should be sought.

PRODUCTION INFORMATION

For manuscripts that have been accepted for publication, please contact:

E-mail: ojbiphy@scirp.org

NLR's Analogs with Young Blood Cells in Monitoring of Toxicity of Long-Term Preventing Immunosuppression in the Liver Transplant's Recipients

Aleksey N. Shoutko, Olga A. Gerasimova

Department of Transplantation, Stem Cells of Russian Research Center of Radiology and Surgical Technologies named after A. M. Granov, Saint-Petersburg, Russia

Email: info@rrcrst

How to cite this paper: Shoutko, A.N. and Gerasimova, O.A. (2022) NLR's Analogs with Young Blood Cells in Monitoring of Toxicity of Long-Term Preventing Immunosuppression in the Liver Transplant's Recipients. *Open Journal of Biophysics*, 12, 173-184.

<https://doi.org/10.4236/ojbiphy.2022.124008>

Received: August 24, 2022

Accepted: September 27, 2022

Published: September 30, 2022

Copyright © 2022 by author(s) and Scientific Research Publishing Inc.

This work is licensed under the Creative Commons Attribution International License (CC BY 4.0).

<http://creativecommons.org/licenses/by/4.0/>



Open Access

Abstract

The blood neutrophils to lymphocytes ratio (NLR) reflects the physiological homeostasis between lymphopoiesis and myelopoiesis, and its elevation serves as a harmful sign in many pathologies, partially, late rejection of allograft. The stem and young lymphoid cells have regenerative-trophic properties, which can affect the relevance of NLR, being opposed to immune properties, associated with bulk lymphocytes. In the present article, we have analyzed for the first time the applicability of NLR's analogs with stem and immature blood cells for monitoring harmful long-term shifting from lymphopoiesis to myelopoiesis in transplant's recipients received conventional immunosuppressive treatment. In opposition to conventional NLR, the ratio of subpopulation of CD31 cells committed to the liver tissue by alfa-fetoprotein (AFP), seems sensitive enough for such monitoring several years after transplantation of the liver from the dead.

Keywords

Liver, Transplantation, Health, Late Period, Monitoring, Stem, Progenitor Cells, NLR

1. Introduction

In the last decade, the neutrophil-to-lymphocyte blood ratio (NLR) has been evaluated as a simple and universal criterion for the severity of various pathological conditions of a person. An increase in the number of neutrophils in the N/L reflects inflammation, while lymphopenia is associated with somatic ex-

haustion (malnutrition syndrome) and hypocellularity of hematopoietic tissue [1]. The NLR competes with the “immunological jungle”, for example, at selecting patients promising for transplantation [2]. NLR measured during 12 months after liver transplantation (LT) predicts overall survival in the next 7 - 9 years and closely correlates with nutrition’s markers [3].

The population of human lymphoid precursors, migrating from the bone marrow to the thymus gland and peripheral blood, can affect the prognostic properties of NLR in a special, non-immune way [4]. Previously, we showed the ability of Thy-1 stage thymocytes (markers: deoxynucleotidyl transferase TdT+, CD133+, CD90+, CD34+, CD31+) to participate in regeneration [5]. Trophic influence, in particular, may answer the question of why a decrease in tissue renewal in the denominator of the ratio leads to a worse prognosis for a transplant, although lymphopenia weakens its immune rejection according to conventional wisdom.

In view of this, an ability of lymphoid progenitors CD133 and young CD31 “regulatory cells” (T reg) to become committed/aimed to the liver tissue presents additional interest [6] [7] [8] [9]. Thus, stem cells and early precursors express properties opposite to the supervisory ones. The contribution of such morphogenic-trophic lymphoid component to the prognostic properties of NLR should be studied at the level of cells in the early stages of the differentiation’s continuum discussed in [10]. We tested this approach/principle for monitoring long-term periods after liver’s transplantation with the aim to justify the questionable limitation of immunosuppressive treatment in it. Thus, the report is devoted to the study of dynamics of N/L with cells of varying degrees of differentiation/maturity in recipients of the liver from dead donors.

2. Methods

2.1. Patients

We report 22 liver transplant recipients cured and investigated in the department of transplantation and stem cells of the Russian Center for Radiology and Surgical Technologies named after A. M. Granov (FSBI RNCRSH, Saint-Petersburg, RF). They were regularly examined during the entire follow-up period, performing clinical and biochemical blood analysis, abdominal ultrasound with elastometry, monitoring of the concentration of tacrolimus in the blood, and maintaining its concentration at the level of 3 - 5 ng/ml. Based on the clinical laboratory data, the average LNR calculated 1, 3, 5 and 10 years after liver transplantation (LT) were not statistically different.

2.2. Blood Samples for Flow Cytometry

Blood samples 7 - 8 ml obtained at various times after surgery and were used on the day of receipt, without storage. The viability of mononuclear cells (MNC) from the entire interphase zone of the Ficoll density gradient controlled using a trypan blue exclusion test. Before cytometric phenotyping, cells were stained ac-

ording to standard procedures to detect forms in the synthetic (S) and mitotic phases (M) of cell cycle [11] with Hoechst 33342 reagent (bisbenzimidazole fluorochrome; Sigma-Aldrich, St. Louis, Missouri, USA). CD133+, CD31+ cells, CD133+ AFP+, and CD31+ AFP+ double positive cells were stained using standard Miltenyi Biotec protocol for CD133/2 antibodies (Ab) conjugated with allophycocyanin (APC), BD Bioscience Pharmingen protocol for CD31 Ab with conjugated with fluorescein isothiocyanate (FITC), and R&D Systems protocol for α -fetoprotein (AFP) Ab conjugated with phycoerythrin (PE).

2.3. Flow Cytometry

The percentage of positive cells was calculated by subtracting the value for antibodies of the corresponding control isotype. At least 500,000 total events were recorded twice to detect CD133+ cells. A dot graph of Hoechst 33342 radiation in blue (x-axis) and red (y-axis) wavelengths was used to separate the events of (G0 + G1), S, and (G2 + M) phases.

2.4. The Original Data of the Tissues' Content of the Transcripts, Which Are Typical for Different Blood Cells

Primary data on the content of transcripts of cells of various histotypes in human liver tissue and other organs were extracted from the database of free access [12] and were subjected to graph-statistical analysis.

2.5. Statistical Analyses

Individual parameters were evaluated statistically with the calculation of the mean value, standard deviation (SD) and standard error (SE). The average values of M were compared using the t -test and the probability of p . The trends of parameter relationships using mathematical functions automatically generated in Excel are described. The determination of the coefficient R^2 was used as a statistical measure of the correspondence of the regression line to the data entered into the program. Satisfactory values of R^2 were confirmed using Equation (1) for the parameter t :

$$t = R^2 \times (n - 2) / (1 - R^2) \quad (1)$$

3. Results

3.1. General Characters of Patients during Early and Late Period after Surgery

According to **Figure 1**, the shifts of maximum of distribution (triangles) on the time's scale from “-SD” to “+SD” indicate the result of patients' selection by death between early time (0 - 16 months) and late average time (58.8 months; 24 - 106) after LT.

A shift of distribution of lymphocytes to the negative SD in a late period means a worst quality of health in the rest of long-lived persons. Most likely, the dead were those who had a lowered level of lymphocytes in the early period after

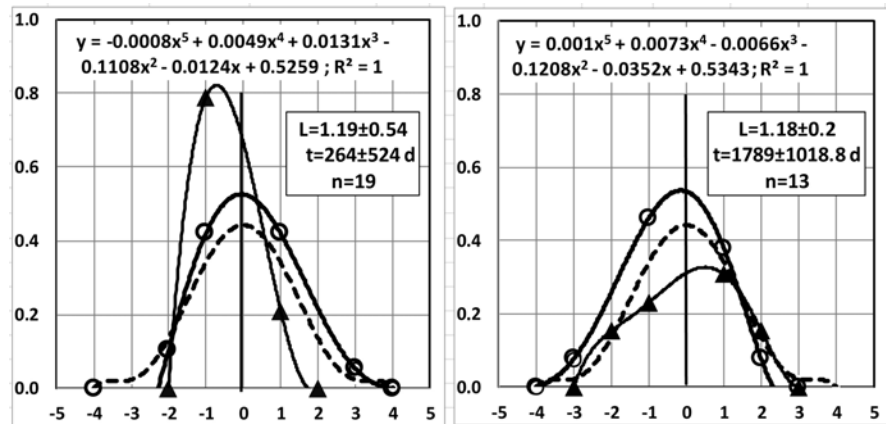


Figure 1. Distribution of individual times (t , triangles) and lymphocytes (L , circles) of recipients in the early and late periods after liver transplantation. The X-axis is the standard errors (SD) for t and L parameters. The Y-axis the distribution of SD for t (thin lines) and L (thick lines) parameters. The dotted line is a normal distribution as a referent.

LT. Meanwhile, the rest of alive with elevated lymphocytes (left circles at -2 SD and $+3$ SD) acquired steadily a lymphopenia in the late period (right circles at -3 SD and $+2$ SD). The equality of low lymphocyte levels in early and late groups (1.18×10^9 and 1.19×10^9 per l) is a result of described redistribution of patients between average 9 and 59 months after LT.

The percentage of MNC in S-phase of the cycle increases with time after LT, meanwhile the percentage of mitotic cells (M) decreases (**Figure 2**).

3.2. Post-Operative Kinetics' Characters of the NLR's Analogs

1) To make a choice of a cell markers (m), which most interesting for investigation NLR at the lower level of cell differentiation, the original marker's transcripts " m " in the normal liver tissue (L_t) were extracted from database [12] and transformed into ratio $r = m_{L_t}/m_{BM}$, where (BM) is a normal bone marrow's tissue as a referent one. The range of such normalized (relatively) content " r " for each cell's markers let to compare them quantitatively inside an organ and between organs. The comparison of calculated " r " is shown in **Figure 3**.

If placenta (P) contains the substances provided the regeneration at large, then the markers of myeloid cells CD33, T-lymphocytes CD2, CD3, CD7, and B-lymphocytes CD19, CD27 seem less important for tissue's renewing in comparing with Thy-1, CD31, CD133, CD34, CD25, PD-1L, and DNTTIP1 ($p < 0.01$). A similar conclusion is actually for liver tissue: Thy-1, CD25, CD34 and PD-1L CD31, CD133, DNTTIP1, and CD2. Their relative content is ≥ 0.4 of that bone marrow ($p = 0.005$). The domination in liver and placenta of unmaturing cells' markers shows the lack of understanding of the interplay between hematopoietic stem cells (HSCs) and the immune system in a liver pathology and in other pathologies as well. The morphogenic-trophic properties of unmaturing lymphocytes oppose to function of security and immune surveillance associated with matured lymphoid cells [13]. Thy-1 (CD90) is a lymphoid stem cell marker,

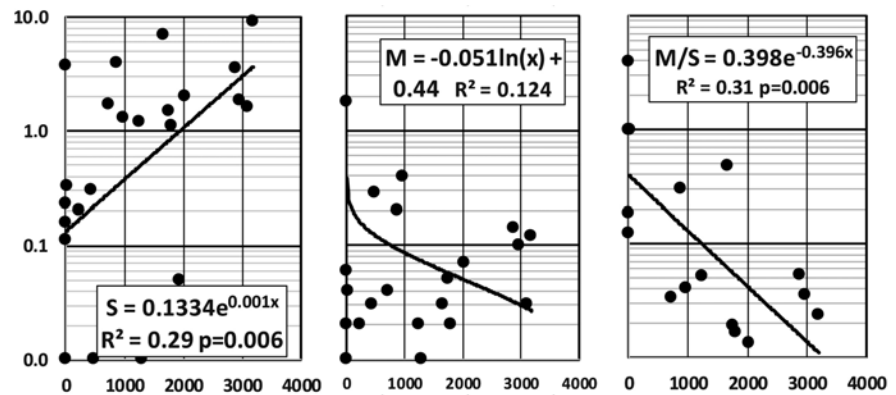


Figure 2. Proliferative activity of MNC by time (days) after LT. The approximations of the data in **Figure 2** show an exponential loss of cells reproduction. Thus, there is evidence for a reliable contribution of bulk lymphocytes in the increment of NLR during the post-operating time.

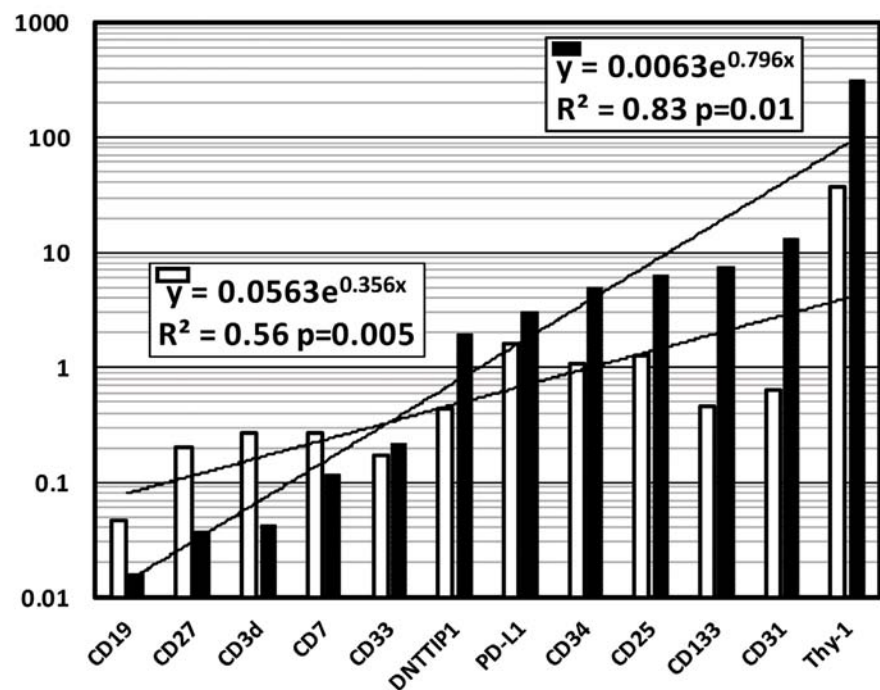


Figure 3. Distribution of relative protein markers (r) for normal liver (m_{L^t}/m_{BM^t} , white) and normal placenta (m_p/m_{BM^p} , black).

being a liver stem cell marker as well [14].

Double-positive CD34 and CD133 stem cells give rise both the early endothelial progenitors and stem cells lymphoid lineage with marker terminal deoxynucleotidyl transferase (TdT), meanwhile CD34 stem cells produce mostly erythro-myeloid progenitors [15] [16] [17] [18]. CD34 stem cells produce mostly erythro-myeloid progenitors [15] [16] [17] [18]. CD31 marker of T-reg and endothelial progenitors [19], and CD25 marker of T-reg lymphocytes [16] coexpress both with CD34 stem cells, and each other [6] [10] [20] [21]. Programmed death-ligand 1 (PD-L1, CD274) plays a major role in suppressing the immune system in certain cases, such as pregnancy, tissue transplantation, autoimmune

diseases, hepatitis, etc. [12]. PD-L1 expression on circulating CD34 hematopoietic stem cells closely correlated with apoptosis of Tcells [22]. Apoptosis followed by delivering of TdT in intercellular media [5]. Deoxynucleotidyl transferase terminal interacting protein (DNTTIP1), enhances the activity of terminal deoxynucleotidyl transferase TdT and vasoreparative properties of CD34 cells [12] [23].

This short overview leads us to investigate the prognostic value of NLR during the late period after LT in terms of CD133 and CD31 blood cells. The marker alpha-fetoprotein AFP used also, basing on our previous experience with it [7].

2) The average blood's content of neutrophils, lymphocytes, and subpopulations CD133, CD133 AFP, CD31, CD31 AFP in them presented in **Table 1** for the average early and late periods after LT.

According to **Table 1**, a double positive protein CD31AFP only gives a better result than conventional LNR with white blood cells (WBC). $LNR_{CD31AFP}$ results from the arithmetic division of the percentage of these subpopulations in granulocytes and lymphocytes fractions selected on the flow cytometry plot (side scattering vs. forward scattering). According to **Table 1**, the deviation of the $LNR_{CD31AFP}$ is higher (21.7-folds vs. 2.6 folds) and better statistically ($p = 0.003$ vs. $p = 0.04$) in comparing with conventional NLR with white blood cells.

Kinetic features of conventional NLR, NLR's for CD133, CD133AFP, and NLR for CD31, CD31AFP shows **Figure 4**.

Figure 4 shows unsuitability of conventional WBC's NLR for monitoring its late dynamic. The early abrupt fall of the NLR_{CD31} and $NLR_{CD31AFP}$ during 16 months after LT, followed by their slow rise up to 106 months. The most reliable long-term raise with doubling period 1.46 years found for $NLR_{CD31AFP}$ ($p = 0.015$).

Table 1. Average characters of NLR for blood cells at different level of their maturation in early and late period after LT.

Conditions	Conventional WBC	CD 133	CD133AFP	CD31	CD31AFP	Time after operation, days
N, % early	5.27 ± 0.83	0.72 ± 0.145	0.308 ± 0.096	59.04 ± 6.36	57.33 ± 6.44	$89 \pm 38^*$ 29.7 ± 9.9
N, % late	3.1 ± 0.42	0.257 ± 0.043	0.527 ± 0.428	12.83 ± 2.01	10.72 ± 2.1	$1891 \pm 227^*$ 1937 ± 261
<i>p</i>	0.04	0.008	0.62	<0.001	<0.001	<0.001
NLR early	6.8 ± 1.83	13.85 ± 3.78	48.9 ± 22.57	10.9 ± 4.97	229.86 ± 60.65	$89 \pm 38^*$ 29.7 ± 9.9
NLR late	2.6 ± 0.39	7.97 ± 2.57	44.81 ± 11.74	2.89 ± 0.79	10.58 ± 3.44	$1891 \pm 227^*$ 1937 ± 261
<i>p</i>	0.04	0.21	0.53	0.13	0.003	<0.001

(*) Average time relates to conventional data received with WBC.

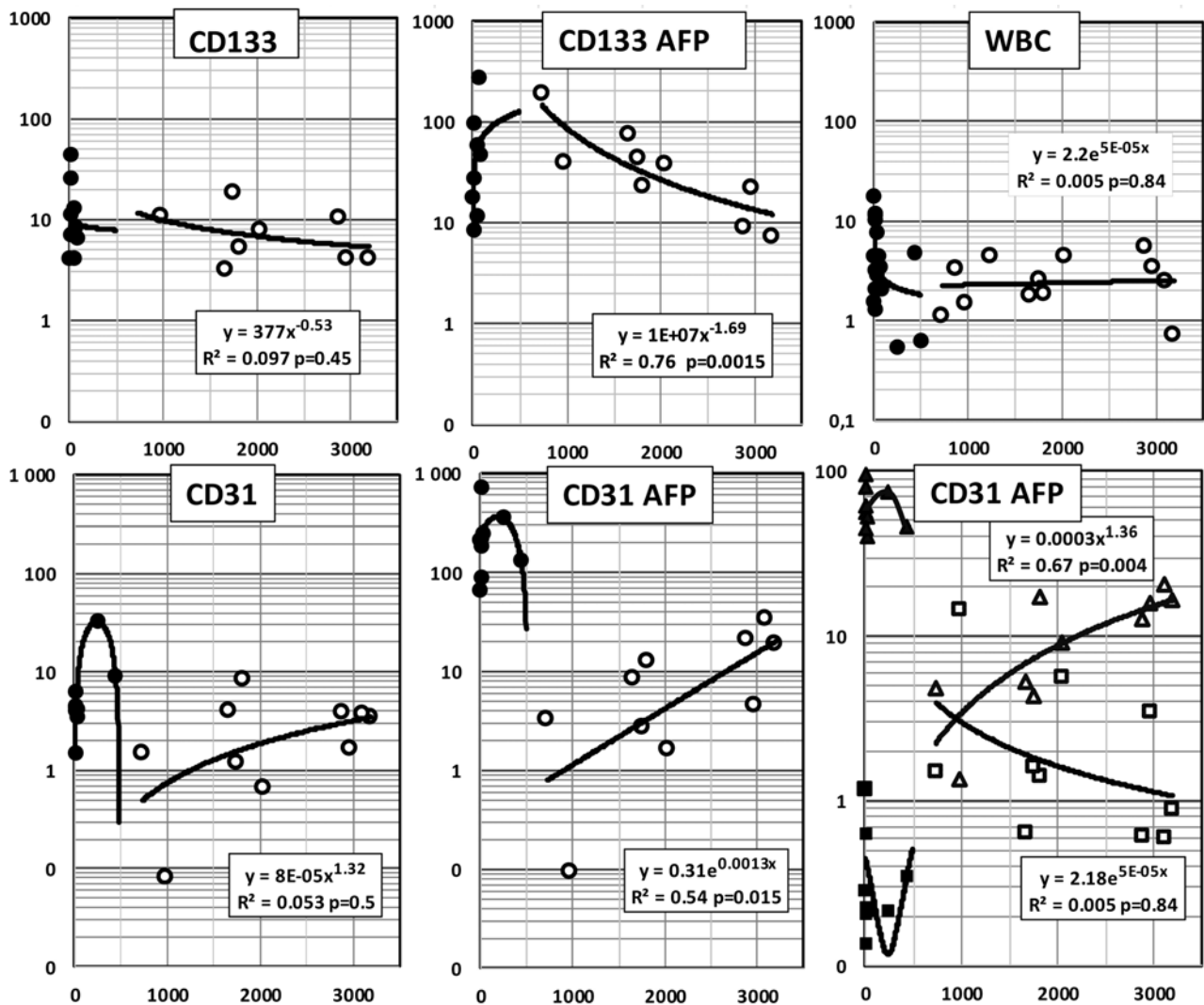


Figure 4. Long-term kinetic of the markers in the blood after LT. The X-axis is the time elapsed after the operation, days. Black symbols show early period; white symbols show late period after transplantation. The Y-axis is the value of the NLR (circles) for different populations shown in the small upper boxes. Triangles-granulocytes, %; squares-lymphocytes, %.

In parallel, calculating the doubling period of a numerator (granulocytes CD31AFP) was ≈ 2.37 years and the period of twofold reduction of the denominator (lymphocytes CD31AFP) was ≈ 3.79 years.

3.3. Discussion

The steady lowering of lymphopoiesis according to S and M/S parameters accompanied followed by low sensitivity of conventional NLR with WBC (Figure 4) led us to investigate the ratio with small subpopulations of un成熟的 cells. According to Figure 4, period 1.2 years after LT seems optimal for selection of recipients that are most resistant to a rejection. During selection the survival can reduce to 73 percentage [24]. In result, most interesting AFP-positive CD31 subpopulation have highest CD133AFP lymphocytes and lowest both CD31AFP granulocytes and $NLR_{CD31AFP}$ at 1.9 years after LT (Figure 4). In relation to liver

tissue, such a shift may indicate the prevailing of capillarization over endothelial fenestration, fraught with portal hypertension [25]. Nevertheless, the main benefit of cytotoxic treatment appears to this time, *i.e.* during the early period shown by black symbols. During the next 7 years, the patients' survival decreases slowly, approximately 2.1% - 2.3% per year [26] [27], and $NLR_{CD31AFP}$ is getting worse steadily, increasing from 1 to 20 (Figure 4). The increase of $NLR_{CD31AFP}$ is, obviously, a more sensitive indicator than conventional NLR with WBC. CD31 lymphocytes, AFP-committed to the liver tissue, belong to immature Treg, and their slow depletion becomes toxic for recipients' alive. Thus, the $NLR_{CD31AFP}$ can be a potential measure of the harm to the health of a recipient after 1.4 - 1.9 years, with doubling time 3.79 years (Table 1).

There is a parallel between the prognostic advantage of NLR test with young blood cells and domination of immature lymphocytes' protein markers in the liver tissue (Figure 3). An increased number of subpopulations of "T-regulatory cell" (T-reg) in both the blood and in the liver transplant do not support the generally accepted immune explanation of the role of lymphopoiesis in physiology and pathology of mammals [28], partially, an "operational tolerance", a phenomenon that is believed to occur due to suppression of the immune rejection by Treg. A recent approach to reduce donor-specific alloreactivity to liver transplant, using a regulatory T-cell (Treg) as a specific immunosuppressive subpopulation [29], meets a logic objection. The studies have demonstrated that the number and suppressive activity of Treg increase with age [30]. It is not clear how these changes reconcile with worse results of liver transplantation in the elderly [31], especially, with the facts, that the risk of graft rejection is inversely related to age [32].

A reliable reason for the worse survival of an elderly after LT is their worse health rather than increased Treg as such [33]. Almost all T-reg cells are intermediate maturing cells in the differentiation's range: "hematopoietic stem cells (HSCs)/precursors of T-lymphocytes and mature/senescent T cells". Thus, an increase in "T-reg" means a "shift to the left" of the entire poorly differentiated pool, including an increase in HSCs and lymphoid precursors such as cortical thymocytes Thy, CD25, CD31 and others. Such a shift is accompanied by inevitable lymphopenia with a corresponding effect on the NLR index. This fundamental property of lymphocytopoiesis is ignored by the dominant immunological interpretation of the causes of operational "tolerance", despite the ever-increasing amount of information about the beneficial effect of HSC and early (immature) precursors on the regenerative functions of various organs and tissues in various pathological situations. Such a "feeder, trophic, morphogenic" ability of immature lymphocyte and HSCs can mimic the phenomena described as immune evasion in cancer or operational "tolerance" in organ transplantation, and many other physiological/pathophysiological phenomena that are today in the field of purely immunological interpretations, in particular, suppression of immunity by "regulatory" cell. In the view morphogenic properties of

young lymphocytes, the opposite dynamic lymphoid and myeloid components of CD31AFP cells reflects the interference of symmetric hematopoiesis of white blood cells with asymmetric (normal) one. It stays a maximal during 1.2 years after LT, normalizes to a minimal at 1.9 years, and increases repeatedly toward 8 - 9 years after LT. These referent periods correspond to dying of originally weak recipients, selection of $\approx 70\%$ of the alive /benefit, and getting them slowly to the worst, probably, via secondary decapillarization (**Figure 4**). A normal liver belongs to the group of tissues with the lowest original/natural vascularization in terms of endothelial markers CD31 in tissues, and with the shortest life span in case of their malignization [13].

Thus, the strategy of recipients' care after 1.4 - 1.9 years has to keep under control the achieved lowest $NLR_{CD31AFP}$ by reduction of the immunosuppressing therapy, as it diminishes of CD31AFP' lymphocyte content in the blood.

4. Conclusion

In opposition to conventional NLR, the ratio of subpopulation of CD31 cells committed to the liver tissue by AFP, seems acceptable for monitoring of harmful long-term shifting from lymphopoiesis to myelopoiesis in a transplant's recipients received conventional immunosuppressive treatment.

Acknowledgements

We acknowledge financial support from Ministry of Health, Russian Federation.

Conflicts of Interest

The authors declare no conflicts of interest regarding the publication of this paper.

References

- [1] Fock, R.A., Blatt, S.L., Beutler, B., Pereira, J., Tsujita, M., de Barros, F.E.V. and Borelli, P. (2010) Study of Lymphocyte Subpopulations in Bone Marrow in a Model of Protein-Energy Malnutrition. *Nutrition*, **26**, 1021-1028.
<https://doi.org/10.1016/j.nut.2009.08.026>
- [2] Angelico, R., Parente, A. and Manzia, T.M. (2017) Using a Weaning Immunosuppression Protocol in Liver Transplantation Recipients with Hepatocellular Carcinoma: A Compromise between the Risk of Recurrence and the Risk of Rejection? *Translational Gastroenterology and Hepatology*, **2**, 74.
<https://doi.org/10.21037/tgh.2017.08.07>
- [3] Pravisani, R., Mocchegiani, F., Isola, M., Lorenzin, D., Adani, G.L., Cherchi, V., De Martino, M., Risaliti, A., Lai, Q., Vivarelli, M. and Baccarani, U. (2021) Postoperative Trends and Prognostic Values of Inflammatory and Nutritional Biomarkers after Liver Transplantation for Hepatocellular Carcinoma. *Cancers*, **13**, 513.
<https://doi.org/10.3390/cancers13030513>
- [4] Lin, B.-Y., Zhou, L., Geng, L., Zheng, Z.-Y., Jia, J.-J., Zhang, J., Yao, J. and Zheng, S.-S. (2015) High Neutrophil-Lymphocyte Ratio Indicates Poor Prognosis for Acute-on-Chronic Liver Failure after Liver Transplantation. *World Journal of Gas-*

- troenterology*, **21**, 3317-3324. <https://doi.org/10.3748/wjg.v21.i11.3317>
- [5] Shoutko, A.N. (2021) The Possible Involvement of Apoptotic Decay of Terminal Deoxynucleotidyl Transferase-Positive Lymphocytes in the Reutilization of the Extracellular DNA Fragments by Surrounding Living Cells. *Open Journal of Biophysics*, **11**, 371-382. <https://doi.org/10.4236/ojbiphy.2021.114014>
- [6] Huang, L., Zheng, Y., Yuan, X., Ma, Y., Xie, G., Wang, W., Chen, H. and Shen, L. (2017) Decreased Frequencies and Impaired Functions of the CD31⁺ Subpopulation in T_{reg} Cells Associated with Decreased FoxP3 Expression and Enhanced T_{reg} Cell Defects in Patients with Coronary Heart Disease. *Clinical & Experimental Immunology*, **187**, 441-454. <https://doi.org/10.1111/cei.12897>
- [7] Shoutko, A.N., Gerasimova, O.A., Fedorov, V.A. and Zherebtsov, F.K. (2019) Non-Invasive Vibration-Stress of the Cirrhotic Liver of Patients Waiting for Transplantation Induces of Circulating CD133⁺ Stem Lymphocytes Committed Phenotypically toward the Liver. *Open Journal of Biophysics*, **9**, 155-168. <http://www.scirp.org/journal/ojbiphy>
<https://doi.org/10.4236/ojbiphy.2019.93012>
- [8] Shoutko, A.N., Gerasimova, O.A. and Mus, V.F. (2020) Lymphocyte Reproductive Activity at Lethal Diseases. In: *Prime Archives in Genetics*, Vide Leaf, Hyderabad, 1-25. <https://doi.org/10.37247/PAG.1.2020.2>
- [9] Shoutko, A.N., Gerasimova, O.A., Marchenko, N.V. and Zherebtsov, F.K. (2021) Induction of Circulating CD133⁺ Stem Cells Committed to Cirrhotic Livers in Waitlisted Patients Annuary. *Russian Journal of Transplantation and Artificial Organs*, **22**, 43-51. <https://doi.org/10.15825/1995-1191-2020-4-43-51>
- [10] Le, J., Ha, V.L., Li, F., Camacho, V., Patel, S., Welner, R.S. and Parekh, C. (2019) Single Cell Transcriptome Mapping of Human Thymopoiesis Reveals a Continuum of Cell States during T-Lineage Specification and Commitment. *Blood*, **134**, 1183. <https://doi.org/10.1182/blood-2019-129886>
- [11] Sales-Pardo, I., Avendaño, A., Martínez-Muñoz, V., García-Escarp, M., Celis, R., Whittle, P., Barquinero, J., Domingo, J.C., Marin, P., Petriz, J., *et al.* (2006) Flow Cytometry of the Side Population: Tips and Tricks. *Cellular Oncology*, **28**, 37-53. <https://www.ncbi.nlm.nih.gov/pubmed/16675880>
<https://doi.org/10.1155/2006/536519>
- [12] The Human Protein Atlas. Sections: Tissue Cell Type. https://www.proteinatlas.org/about/licence#citation_guidelines_for_the_human_protein_atlas
- [13] Shoutko, A.N. (2022) Tissues Protein Microenvironment and Survival by Age at Cancers. *Acta Scientific Cancer Biology*, **6**, Article No. 7. <https://actascientific.com/ASCB/ASCB-06-0380.php>
- [14] Lombard, C.A., Prigent, J. and Sokal, E.M. (2013) Human Liver Progenitor Cells for Liver Repair. *Cell Medicine*, **5**, 1-16. <https://doi.org/10.3727/215517913X666459>
- [15] Gore, S.D., Kastan, M. and Civin, C.I. (1991) Normal Human Bone Marrow Precursors That Express Terminal Deoxynucleotidyl Transferase Include T-Cell Precursors and Possible Lymphoid Stem Cells. *Blood*, **77**, 1681-1690. <https://doi.org/10.1182/blood.V77.8.1681.1681>
- [16] Schwartzberg, S., Mor, A., Luboshits, G., Planer, D., Deutsch, V., Keren, G. and George, J. (2005) Association between Circulating Early Endothelial Progenitors and CD4⁺ CD25⁺ Regulatory T Cells: A Possible Cross-Talk between Immunity and Angiogenesis? *American Journal of Immunology*, **1**, 143-147. <https://doi.org/10.3844/ajisp.2005.143.147>

- [17] Takahashi, M., Matsuoka, Y., Sumide, K., Nakatsuka, R., Fujioka, T., Kohno, H., Sasaki, Y., Matsui, K., Asano, H., Kaneko, K. and Sonoda, Y. (2014) CD133 Is a Positive Marker for a Distinct Class of Primitive Human Cord Blood-Derived CD34-Negative Hematopoietic Stem Cells. *Leukemia*, **28**, 1308-1315. <https://doi.org/10.1038/leu.2013.326>
- [18] Radtke, S., Haworth, K.G. and Kiem, H.-P. (2015) CD133+ CD34+ HSPCs Are Not Significantly Increased in Fetal Liver Compared to Adult or Umbilical Cord HSPCs. *Blood*, **126**, 2369. <https://doi.org/10.1182/blood.V126.23.2369.2369>
- [19] Billaud, M., Donnenberg, V.S., Ellis, B.W., Meyer, E.M., Donnenberg, A.D., Hill, J.C., Richards, T.D., Gleason, T.G. and Phillippi, J.A. (2017) Classification and Functional Characterization of Vasa Vasorum-Associated Perivascular Progenitor Cells in Human Aorta. *Stem Cell Reports*, **9**, 292-303. <https://doi.org/10.1016/j.stemcr.2017.04.028>
- [20] Mackay, L.S., Dodd, S., Dougall, I.G., Tomlinson, W., Lordan, J., Fisher, A.J. and Corris, P.A. (2013) Isolation and Characterisation of Human Pulmonary Microvascular Endothelial Cells from Patients with Severe Emphysema. *Respiratory Research*, **14**, Article No. 23. <https://doi.org/10.1186/1465-9921-14-23>
- [21] Wang, C., Li, Y., Yang, M., Zou, Y., Liu, H., Liang, Z., Yin, Y., Niu, G., Yan, Z. and Zhang, B. (2018) Efficient Differentiation of Bone Marrow Mesenchymal Stem Cells. *European Journal of Vascular and Endovascular Surgery*, **55**, 257-265. <https://doi.org/10.1016/j.ejvs.2017.10.012>
- [22] Abdellatif, H. and Shiha, G. (2018) PD-L1 Expression on Circulating CD34+ Hematopoietic Stem Cells Closely Correlated with T-Cell Apoptosis in Chronic Hepatitis C Infected Patients. *International Journal of Stem Cells*, **11**, 78-86. <https://doi.org/10.15283/ijsc17047>
- [23] Bakhashab, S., Ahmed, F.W., Schulten, H.-J., Bashir, A., Karim, S., Al-Malki, A.L., Gari, M.A., Abuzenadah, A.M., Chaudhary, A.G., Alqahtani M.H., *et al.* (2016) Metformin Improves the Angiogenic Potential of Human CD34+ Cells Co-Incident with Downregulating CXCL10 and TIMP1 Gene Expression and Increasing VEGFA under Hyperglycemia and Hypoxia within a Therapeutic Window for Myocardial Infarction. *Cardiovascular Diabetology*, **15**, 27. <https://doi.org/10.1186/s12933-016-0344-2>
- [24] Aulló, M.T.S., Villacampa, E.S. and Garcia-Gil, A. (2012) Impact of Donor Age on Liver Transplants. *Trends in Transplantation*, **6**, 34-40.
- [25] Drzewiecki, K., Choi, J., Brancale, J., Leney-Greene, M.A., Sari, S., Dalgiç, B., Aksu, A.U., Sahin, G.E., Ozen, A., Baris, S., *et al.* (2021) GIMAP5 Maintains Liver Endothelial Cell Homeostasis and Prevents Portal Hypertension. *Journal of Experimental Medicine*, **218**, e20201745. <https://doi.org/10.1084/jem.20201745>
- [26] Jain, A., Reyes, Kashyap, J., Dodson, R., Demetris, S.F., Ruppert, A.J., Abu-Elmagd, K., Marsh, K., Madariaga, W.J., Mazariegos, G., *et al.* (2000) Long-Term Survival after Liver Transplantation in 4,000 Consecutive Patients at a Single Center. *Annals of Surgery*, **232**, 490-500. <https://doi.org/10.1097/0000658-200010000-00004>
- [27] Lué, A., Solanas, E., Baptista, P., Lorente, S., Araiz, J.J., Garcia-Gil, A. and Serrano, M.T. (2016) How Important Is Donor Age in Liver Transplantation? *World Journal of Gastroenterology*, **22**, 4966-4976. <https://doi.org/10.3748/wjg.v22.i21.4966>
- [28] Goswami, T.K., Singh, M., Dhawan, M., Mitra, S., Bin Emran, T., Rabaan, A.A., Al Mutair, A., Al Alawi, Z., Alhumaid, S. and Dhama, K. (2022) Regulatory T Cells (T_{regs}) and Their Therapeutic Potential against Autoimmune Disorders—Advances and Challenges. *Human Vaccines & Immunotherapeutics*, **18**, Article ID: 2035117.

- <https://doi.org/10.1080/21645515.2022.2035117>
- [29] Cvetkovski, F., Hexham, J.M. and Berglund, E. (2021) Strategies for Liver Transplantation Tolerance. *International Journal of Molecular Sciences*, **22**, 2253. <https://doi.org/10.3390/ijms22052253>
- [30] Gregg, R.C., Smith, M., Clark, F.J., Dunnion, D., Khan, N., Chakraverty, R., Nayak, L. and Moss, P.A. (2005) The Number of Human Peripheral Blood CD4+CD25 High Regulatory T Cells Increases with Age. *Clinical and Experimental Immunology*, **140**, 540-546. <https://doi.org/10.1111/j.1365-2249.2005.02798.x>
- [31] Gil, E., Kim, J.M., Jeon, K., Park, H., Kang, D., Cho, J., Suh, G.Y. and Park, J. (2018) Recipient Age and Mortality after Liver Transplantation: A Population-Based Cohort Study. *Transplantation*, **102**, 2025-2032. <https://doi.org/10.1097/TP.0000000000002246>
- [32] Mikulic, D. and Mrzljak, A. (2020) Liver Transplantation and Aging. *World Journal of Transplantation*, **10**, 256-266. <https://doi.org/10.5500/wjt.v10.i9.256>
- [33] Mousa, O.Y., Nguyen, J.H., Ma, Y., Rawal, B., Musto, K.R., Dougherty, M.K., Shalev, J.A. and Harnois, D.M. (2019) Evolving Role of Liver Transplantation in Elderly Recipients. *Liver Transplantation*, **25**, 1363-1373. <https://doi.org/10.1002/lt.25589>

Cancer-Specific Resonances

Andras Szasz

Department of Biotechnics, Hungarian University of Agriculture and Life Sciences, Godollo, Hungary

Email: Szasz.Andras@gek.szie.hu

How to cite this paper: Szasz, A. (2022) Cancer-Specific Resonances. *Open Journal of Biophysics*, 12, 185-222.
<https://doi.org/10.4236/ojbiph.2022.124009>

Received: July 14, 2022

Accepted: October 15, 2022

Published: October 18, 2022

Copyright © 2022 by author(s) and Scientific Research Publishing Inc. This work is licensed under the Creative Commons Attribution International License (CC BY 4.0).

<http://creativecommons.org/licenses/by/4.0/>



Open Access

Abstract

The research of cancer-specific resonances started with Raymond R. Rife's controversial results. The intensive debate began on the topic, and various interpretations of the results deepened after his death. This theme presently sparks desperate debates with extreme opinions, from the dangerous quackery to the brilliant discovery. A part of medical practices applies the resonance principle in various anticancer therapies and uses a variety of devices. Most medical experts refuse such "resonance therapies" due to their confidence in their quackery. I summarized some present problems and proposed a possible solution. My present article aims to discuss some aspects of the biological resonances, trying to clear some vague details of this subject and give a possible stochastic explanation of some resonances in cancer therapy. However, when considering the stochastic explanations of resonance frequencies, there are as many of these as there are enzymatic processes affecting the biological systems.

Keywords

Rife Frequencies, Pythagorean Mystics, Resonances, Noises, Fluctuations, Stochastic Processes, Enzymatic Resonances

1. Introduction

The resonance embraces a broadcategory of systems, especially reaction on a periodic excitation. Resonance occurs in many interactions: mechanical (e.g. strings, acoustic, tuned vibrations, etc.), electrical (e.g. tuned circuits for selectivity, impedance extremes, etc.), atomic (e.g. Mossbauer effect, nuclear magnetic resonance, electron spin-resonance, etc.) or optical (e.g. laser, spectral lines, etc.) and many of their combined effects. In some cases, the phenomenon of harmony is also related to resonances, for example, musical harmony which is composed of various mechanical resonances, or the homeostatic balance created by a complex set of selected bio-interactions.

The role of bioelectromagnetics in the resonance phenomena has turned into a “battlefield” in science. The medical facts and their interpretations are mixed with quackeries and medically not proven theories [1]. These unsatisfactory proofs make the “healing electro-therapeutics” highly controversial. For example, electro homeopathy (or Mattei cancer cure [2] [3]) proposes different resonant optical “colors” of electricity to treat cancer. Experts described it as “utter idiocy” [4].

Severe medical doubts make this topic an impossible research venture. The broad legal and illegal medical applications draw attention to this attention-grabbing topic despite its great challenge with multiple unclear details. Differentiating the quackeries from scientifically approved facts confuses the discussion. Unfortunately, these concepts have been adopted and misinterpreted by the non-scientific community, resulting in the development of pseudoscientific beliefs. A further complication is that almost all unscientific explanations include well-proven facts within their unproven or false statements. Unfortunately, these concepts have been adopted and misinterpreted by the non-scientific community, resulting in the development of pseudoscientific beliefs. This further contributes to the poor acceptance of the topic by professionals. The judgment of a great scientist, Stephen Hawking, summarized it: “The *greatest enemy of knowledge is not ignorance, it is an illusion of knowledge*” [5]. An example of the misuse of a scientific concept involves mechanical resonance, a condition in which a mechanical system responds with increased amplitude when the frequency of the system’s oscillations matches the system’s natural vibration frequency. A frequency limit and definite boundary conditions are disregarded when the concept is used to describe pseudoscientific theories. Another frequent “shift” uses the well-proven quantum-mechanical effects in the micro-world atoms and molecules to explain macroscopic bodies. Therefore, the use of resonance in oncological applications requires in-depth investigations to filter out the facts from the pseudoscience. The question is: “Who is the fake one now?” [6]. I try to collect many ideas connected to resonance phenomena, point out the dubious parts, and focus on possible developments.

2. The Pythagorean Harmony

The ancient Greek culture developed the first resonance theory. Centered on the mechanical resonances of a tense string, Pythagoras introduced a set of resonances that explained leading musical harmony in European culture. The Pythagorean school developed mystic numerology by observing the connections between the mechanical resonance of the tense string and its environmental matter (musical sound). Pythagoras created an approach to the vibration of string using ratios of integers. His discovery became the basis of some geometric and musical works, establishing the numerological harmony of musical tuning [7].

When one string is exactly half the length of another string, the notes will have different pitches but will still be in harmony. The interval between the two

notes is called an octave. The Pythagorean tuning system, developed by Pythagoras, is based on a frequency ratio of musical intervals of 2:3, or the “perfect fifth” (3/2). In musical Pythagorean tuning, the power function of the ratio of “perfect fifth” $\left(\frac{3}{2}\right)^n$. The structure forms a scale and the 2^{-p} transposes the scale to the fundamental octave [8]. The perfect fifth can be divided further on the same ratio following the $2^n 3^m$ (where n and m are integers) division rates on the string. This way the Pythagorean music makes the sounds based on the length of tense strings in a scale, where the template is the “perfect fifth” which divides the string by 2/3 portion. Hence, the correct set of tense string vibrations has a $\frac{1}{2^p} \left(\frac{3}{2}\right)^n = 3^n 2^{n-p}$ [8] divisions in musical structure.

The subjective human sense enjoys musical harmony, which does not fit properly with the mathematical construction. A dissonance appears in senses, the “Pythagorean comma,” or “wolf fifth”. A critical feature appears here: the “dissonance” of the wolf-fifth, a fundamentally psychological rather than based on mathematical objectivity.

The “magic” $\frac{3}{2}$ also appears in other ancient science. Aristotle, a significant influencer of the European culture of ancient times and the middle ages, observed the same ratio between the volumes of the cylinder and its inner nesting sphere, which is valid for their surfaces. Kepler also applied the musical ratio in the cosmos’ harmony, forming the cosmic monochord of the universe [9]. Kepler’s observation of the planets’ distances follows a musical harmony (music of spheres). The proof of this theory, of course, considers the limited possibilities of the observations in Kepler’s time.

Interestingly this early mysticism has some real roots in nature, mainly due to the standing harmonic waves formed in the tense string with fixed ends showing $n \cdot \frac{\lambda}{2}$, where n is integer and $\frac{\lambda}{2}$ is the half-wavelength of the formed wave. The hypothesis of applying ancient numerical wisdom in modern physics surprisingly supported the other “Pythagorean quantization”. The mathematical apparatus of such modern fields as quantum mechanics [10] and the structure of DNA [11] apply the Pythagorean symmetries. The wave quanta with integers appear in the string theory of the standard cosmologic model [12].

The other Pythagorean discovery is the triplets of the right triangle drive obtaining Sommerfeld’s fine-structure constant and show similarities with the quantum Hall effect. It could be applied in the time-dependent quantum mechanics connected to the time-dependent complex nonlinear Riccati equations [13], and the $\frac{e^2}{c} \left[= \frac{e^2}{4\pi\epsilon_0 c} \right]$ in SI units] least Coulombic action. The generalized Pythagorean theorem appears in many topics in physics [10]. It also appears in the space-time distances in special relativity [14], and could be connected to optical imaging by the reciprocal values [15]. The applied Pythagorean triplets

are well described theoretically [16] [17]. The applicability's main origin covers the fundamental distance-like values in the Cartesian coordinate system or the law of cosines in any coordinates. However, the similarities of the Pythagorean triplets and numerical string theory with the quantum effects and differential equations do not mean the quantum-mechanical application or relevance of Pythagorean theorems. These similarities are formal. The simple deterministic mechanical concept has no fundamental connection with the probability-based quantum ideas.

3. Therapies with Bioelectromagnetic Resonant Frequencies

The mechanical behavior of the electromagnetic phenomenon is nonlinear in space distances, causing many complications for the first modern scientific investigators, Coulomb and Ampere. The electric and magnetic fields introduced by Maxwell [18] solved this problem by linearizing the forces depending only on the fields and the resting or moving electric charges. These new constructions could only be detected in specific materials with charges and currents and were otherwise insensible to the human senses. The concept of the electric and magnetic field was therefore perceived as a “miracle” by many laypeople, and many pseudoscientific beliefs targeted it. The main controversial “battlefield” is bioelectromagnetism, the effect of electromagnetic fields on living objects.

Heated debates have emerged on the effects of environmental factors on health and on the development of malignancies, for example, induced by the energy transfer networks (like powerlines) [19] [20] [21] [22] [23]. However, the explanations proved controversial and often found to be inconsistent [24]. Broad approaches are discussed in the topics of “electrosmog” [25] [26], “magnetic field medicine”, [27], “new biophysical field”, “force-free actions” [28], “scalar-wave effects” [29], and “subtle energies” [30]. These topics have created upheaval in the field of bioelectromagnetics, with strong opposing arguments from physical [31] and mathematical points of view [32] [33]. Most of the measured and medically proven but contradictory results in bioelectromagnetism characterize the complex behavior of the biosystems, which has a “Janus face” feature because it inherently depends on internal and external conditions. The same “electrosmog” radiation could be “healthy” or “unhealthy” depending on the conditions [34].

Most of the bioresonance theories involve electromagnetics and/or quantum-mechanical explanations. Nikola Tesla considered resonances as the most general law of nature [35], which focused attention on this topic. Tesla applied electromagnetic resonance in most of his numerous patents, like the alternative current [36] and wireless communication [37], founding a unique bioelectromagnetic view [38]. Tesla worked out a method for electro-therapeutics, using “ultraviolet rays” [39].

The other influence on the bioresonances has a quantum-mechanical origin. The Aharonov-Bohm effect [40] led to new ideas. This quantum-mechanical in-

interference phenomenon may be applied in the concept of the “field-free” vector-potential with possible biological application [41] [42]. The vector potential deals with the influences of the inherent fluctuations that allow the unmeasurable field-effect in a macroscopic spatiotemporal measurement, the vector-potential acts in macro ranges [43].

The “resonance topic” in cancer therapy started with a revolutionary step of optical microscopy, developed by Raymond Royal Rife [44]. The Rifemicroscope had the ultimate resolution at that time [45]. The microscope was able to observe the cellular morphology and changes in cell culture in natural, time-lapse conditions with as high as 31,000 resolution with low aberration, while the standard laboratory microscopes at that time had only 2000 to 2500 [46].

The great advantage of the microscope was its resolution and the possibility of observing the time-lapse dynamics of living microbes [47]. The Rife microscope does not harm the specimens under observation. The microscope’s ability allowed researchers to study the processes caused by environmental interactions. The time-lapse facility was an extraordinary chance to study living interacting cells by visualization and registering the dynamics of cells alive over a long time [48] [49] [50]. Recording the time-lapse microscopy movies of microbes excited the researchers of the time. Note, the time-lapsing nowadays remained very popular and used in many microscopic solutions, mostly applying modern, extreme high-resolution live-cell imaging without Rife’s microscopy.

Using Tesla’s arc lamp idea [51], Rife constructed arc radiation (“beam ray”) in an argon-filled glassflask, pumping it with various modulated radiofrequency (RF) power [52], and he used its radiation for microbes under his microscope [53]. He observed “resonant frequencies,” where the pathogens will perish [54] [55] [56] [57]. Rife collected these unique frequencies and registered the “mortal oscillatory rate” (MOR) for various pathogenic organisms. The resonance idea spread rapidly among the experts and laypersons, assuming the same “curative effect” in vivo, without proof. The new claim declares the cure of cancer without relevant observations. The rigorous theoretical and clinical studies are nowadays also largely missing. Later Rifemodified the cancer-cure idea, saying that he may devitalize the disease.

After the death of Raymond Rife, a large market developed, using his work to provide false hopes for cancer patients (at this point, the market-related profit-making substantially impacted the field). The new “Rife-machines” do not use plasma radiation. Instead, they apply only minimal current (milliamperes) of various modulated RF carrier frequencies, which promises to kill the cancer cells in the whole body. Most of the devices were utterly deceptive, and while they directly did not harm the patients, those who used these were isolated from the benefits of proven treatments by their firm belief that the Rifemachine helps. More and more publications were available by elapsing time, showing the problems with the original Rife frequencies and its “theory” behind them. The theoretical part was fragile; the experimental results had no explanations, while the

publications did not describe the experimental conditions professionally. The lack of evidence and the presentation of only a selection of favorable cases supposedly treated by Rife resulted in the development of a field of “pseudomedicine” supported by electronics [58] [59]. The fraudulent activities were punished [60] [61]. Such “Rife devices” have figured prominently in several fraud cases in the US, typically centered around the uselessness of the devices contrary to their marketed grandiose claims. In a 1996 case, the marketers of a “Rife device” claiming to cure numerous diseases, including cancer and AIDS, were convicted of felony health fraud [62]. The sentencing judge described them as “target[ing] the most vulnerable people, including those suffering from a terminal disease,” and providing false hope [63]. Rife machines have been blamed for the deaths of cancer patients who might have been cured with conventional therapy [64].

Unfortunately, many questionable methods use the “phenomenon” of generating profit from believers without acceptable scientifically and medically approved evidence. Rife devices are currently classified as a subset of radionics devices generally viewed as pseudomedicine by mainstream experts [65]. No evidence was produced [66], and it was declared quackery [67] [68]. The Rife frequency generator is an electronic device purported to cure cancer by transmitting radio waves. Authorities in the UK and the US studied this device: “there is no evidence to show that the Rife machine does what its supporters say it does” [69].

However, the appearance of the bioelectromagnetic resonance needs clarification despite many unsuccessful experiments and sometimes misleading or even falsified data. The mixture of the facts and the hidden false statements using scientific language makes the debate too complicated. Such patented ideas as Lakhovsky’s radio-cellular-oscillator [70] [71], Rife’s resonant waves [57] [72], Priore’s electromagnetic therapy [73] [74] [75], are unproven in systematic studies, but some positive case reports were published. However, these selected results do not provide enough proof to verify the effect.

On the other hand, the missing proofs do not mean directly that the idea is quackery. Future discoveries may find the missing proofs with new research facilities like Gurwitsch’s morphogenesis-based mitotic wave in mitosis [76] [77] [78] and some enzymatic reactions [79]. Gurwitsch’s pioneering work has a revision integrating the bioelectric interactions [80] [81]. However, presently we have only indirect proofs in this field as well. Not enough sensitive tools exist to measure the supposed effects [82].

The psycho-effects of otherwise safe (maybe ineffective) methods keep many of these therapies alive, providing a placebo for the patient [83]. The placebo treatment does not mean “no treatment” [84]; it could help with belief. This psychological issue is mostly palliative [85]. The missing efficacy becomes harmful because the patient remains without professional medical care, and the disease may become irreversible.

Low-level, non-stationary magnetic fields have been observed [86] and adopted [87] as a nonthermal electromagnetic effect. One of the essential nonthermal

processes is the so-called “window” effects [88], which shows significant calcium influx to the cell at the low-frequency modulation of radiofrequency around 16 Hz frequency “window”, having an optimum frequency and amplitude to interact with cellular membranes [89]. The window effects have some resonance characteristics. The measured frequency dependence varies based on the experimental conditions and could act in a synergistic way with chemical processes [90]. The “window” was measured in multiple power ranges [91]. These experiments were considered to be nonthermal due to the low energy (max5 uW/g energy). The maximum of the active Na⁺ flux was observed between 0.1 - 10 MHz [92], which “window” effect could be well explained by the active transport system model in the membrane [93].

4. Controversial “Quantum Resonance” Based on Pythagorean Harmony

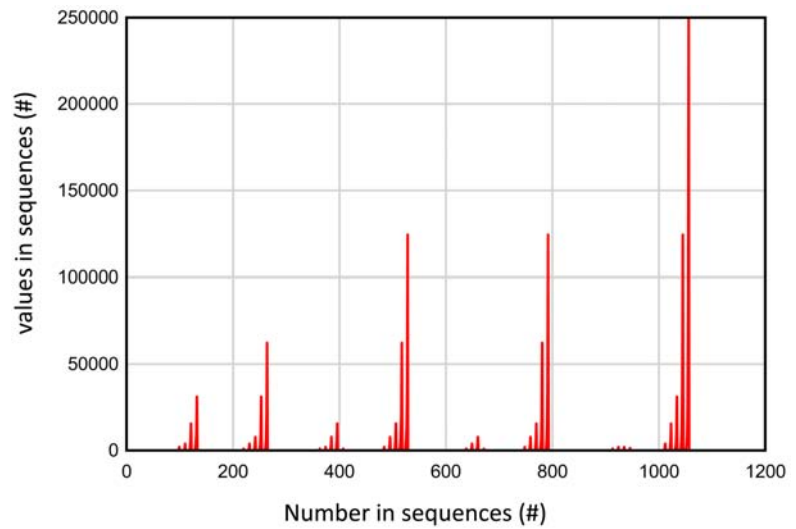
The quantum-mechanical resonances attracted the attention of many researchers. For example, the “orchestrated objective reduction of the quantum state” [94] concentrates on microtubules in the cells; the quantum-field approach of the water [95]. Many publications were devoted to living organisms’ health-sustaining coherent, decoherent frequencies (detrimental) [96]. The idea has a root in the interference of waves. The interference pattern could be constructive and destructive, giving the biological rationale of the wave harmony [97]. These facts prompted the application of the Pythagorean wave harmony on strings to explain the resonance frequencies, including the Rife frequency spectrum. This resulted in a shift from the integer-based ancient set of wavenumbers to the quantum-mechanical energy eigenvalues starting from a reference frequency ($f_{ref} = 1$ Hz, due to practical reason) set of frequencies, defined by the formula called “GM scale” [98]:

$$E_n = hf_{ref} 2^n 3^m (2^p) = \hbar \omega_{ref} 2^{n+p} 3^m \quad (1)$$

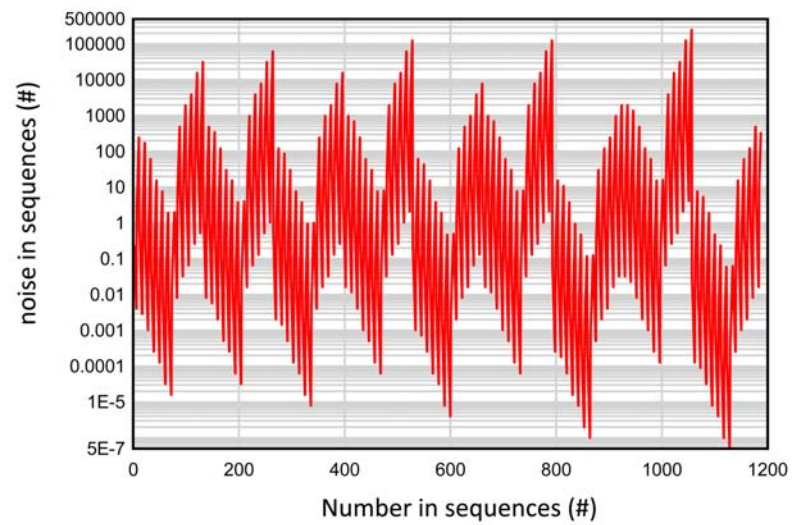
where E_n is the energy values of the discrete coherent electromagnetic waves, h is the Planck constant, and n , m , and p , are selected integers [99]. Analyzing the powerdensity of this generated Pythagorean spectrum, it follows a scaling law of $S(f)$ noise density: $S(f) = f^{-\alpha}$ shown in **Figure 1**. By sorted number-sequences of n , m , and p .

This mathematically correct scaling requests in (1) $n = 0.5$ (wolf sound) too, which is not an integer. The Pythagorean musical structure $\frac{1}{2^p} \left(\frac{3}{2}\right)^n = 3^n 2^{n-p}$ [6] limits the “freedom” of (1), so the spectrum differs from the assumptions of [99].

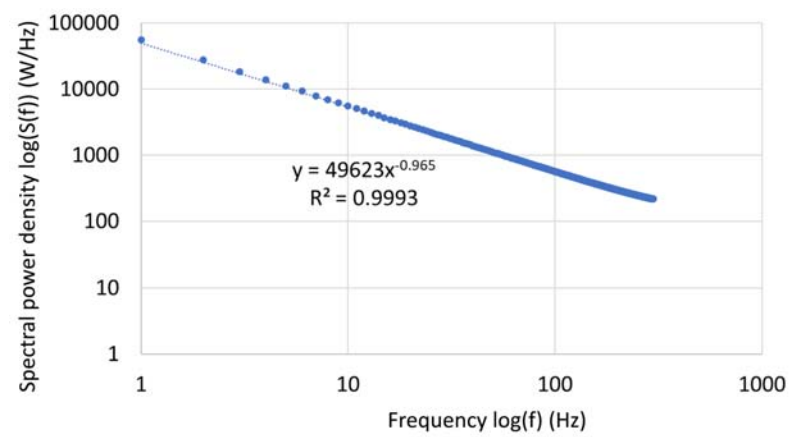
The consequences of the quantum wave in musical harmonic ratio had induced some doubtful research using the “cosmic musical master-code” [100]. The “mastercode” follows the Pythagorean harmony, with an extended anthropomorphic presentation of the human musical sense of harmony. Dubious research explains some fundamental problems in quantum mechanics with the



(a)



(a)



(a)

Figure 1. The frequency spectrum of the Geesink-Meijer “GM scale” (a) The spectrum in frequency; (b) The noise of the spectrum; (c) The $S(f)$ fit with Fourier transformation (FT, $\alpha = 0.965$, Microsoft excel), which practically approaches the pink-noise spectrum [99].

ancient Pythagorean numerology. The descriptions include Bohm's implicate order [101], quantum coherence in living processes [102] [103], and even attempting to explain the origin of life with mineral interactions [104]. The consciousness is described with the help of the generalized Pythagorean musical harmony [105]. The theory also supports such mystique as the afterlife [106].

The theory and its presented proofs have serious challenges:

1) The Pythagorean harmony is valid in a tense string. The waves are formed in fixed boundary conditions, and these determine the waves in a system. What are boundary conditions fixed in this harmony concept? Where are these "strings" which resonate with the Pythagorean scale? How could the tense string waves be formed in the macroscopic cells?

2) The $h \cong 6.6 \times 10^{-34} \text{ J} \cdot \text{s}$, which means subtle energy by (1). The quantum energy is enough to act in a quantum-mechanical object (like an electron in the atoms). However, the proteins are macroscopic (the cells are even more on a macro-scale) and immersed in the environment with thermal fluctuation in body temperature, which drastically exceeds the subtle energy transfer:

$1k_B T \approx 26 \text{ meV} \approx 4.2 \times 10^{-21} \text{ J}$ [107]. One of the lowest binding energy in bio-systems are the hydrogen bonds in various structures, having 6 - 30 kJ/mol ($\approx 2 - 12 k_B T$) [108] [109] [110]; which are 2 - 12 times more than the thermal fluctuation in the living body. How is the energy of "quantum resonance", which is $\approx 10^{13}$ times less than the energy in hydrogen bonds, expected to alter the cancer cells? A question also arises: which signal pathway is chosen and which molecules are involved?

3) The description of (1) uses the 1D string vibrations and the wave-forming on the plane sheets [111]. However, the plane waves (membrane resonances) depend on the shape and thickness of the vibrating sheet (boundary conditions) [112] [113] and are not as simple to interpret as is proposed by the analogy of the tense string vibrations. A detailed and correct description is necessary to explain the proposed effects.

4) This quantum hypothesis continues the Pythagorean number-mystique as a mathematical algorithm for coherent quantum frequencies, used to support the Rife frequencies [114]; and the nonthermal electromagnetic interactions [96]. The Geesink Meijer "GM" scale appears to use similar divisions as the cents. It ranks from 1.0 to 1.898 for "coherent" ("GM-scale") and from 0.974 to 1.837 for "decoherent" "GM spectra", with the same twelve divisions of the "octave" [115]. The normalized frequency spectrum of the "beneficial" vs. "detrimental" signals [96] shows a continuation of the spectrum in an extensive range of frequencies. The slope of the beneficial vs. detrimental plot shows a $\approx 3.4\%$ deviation from the equality of the two opposite effects increasing the doubt about the validity of the hypothesis **Figure 2**.

5) The further dubious consequence of the GM scale is the identical frequency dependence in Hz and GHz regions **Figure 2**. This contradicts the expectations of different mechanisms in these scales. The low frequency is principally active

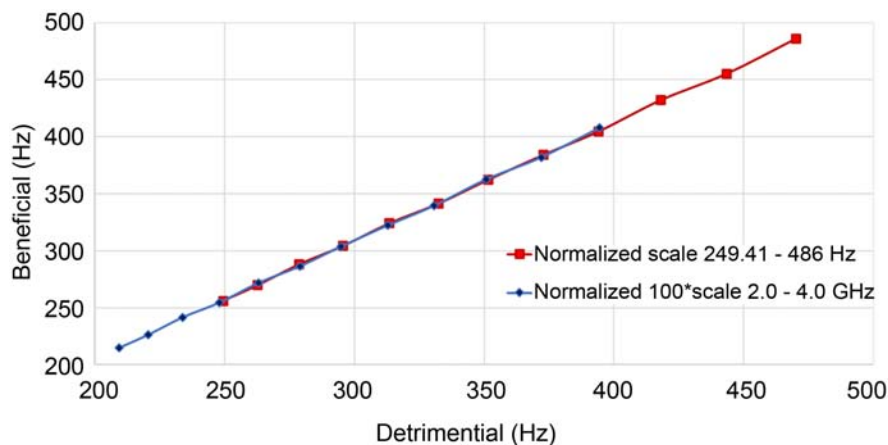


Figure 2. The “beneficial” vs. “detrimental” frequencies of “GM scale” [96]-[101]. A comparison of the GHz and Hz spectra shows complete identical slopes (slope = 1.03, $R^2 = 0.998$).

in the extracellular matrix and the cellular membrane, while the high frequency penetrates the cytosol and changes the molecular processes intracellularly.

6) The fundamental doubt about this hypothesis comes from the harmony itself. The living systems have heterogenic “strings” and “plates” with complex interactions. The existence of these strings and plates resonating in “harmony” is illusory because all the strings and plates have different boundary conditions, so their resonances are far from the same, so their harmony needs much more conditional assumptions than Equation (1) describes. The healthy “harmony” is regulated and controlled by homeostasis, which induces $1/f$ noise calculated by multiple entropy analyses [116].

7) The data contain 219 and 123 separate biomedical studies for healthy homeostatic and cancerous situations, respectively [117]. The essential request of the statistical evaluation is cohort homogeneity which does not exist in the data for the GM-scale. The vast number of observations collect various experimental setups and use various substances, so these do not fit one unified GM-scale. The data do not belong to the same group of experiments, so their interpretation as a cohort is incorrect. We must have data collection and clinical trials according to international standards to surmount the trap of dubious assumptions.

8) According to the above doubts, the Pythagorean quantum coherence is a proofless continuation of the ancient Pythagorean number mysticism. The Pythagorean vibrating strings concept deals with mechanical conditions in a deterministic way. How does it fit the stochastic probability methodology of quantum mechanics? It is not as universal as quantum mechanics and has no such probability-dependent, stochastic phenomena, which are regarded as the corner point of quantum phenomena [118].

5. Doubts on Cancer-Specific “Resonant Harmony”

The health-supporting and detrimental signals from only a few Hz to THz frequencies are included in the massive set of “resonant” frequencies [119], mostly

corresponding with Rife-frequencies results. Decoherence as the hypothetical cause of cancer [120] is also a noteworthy hypothesis. However, there are also numerous open, unanswered questions:

1) Cancer cells are “softer” than their normal host cells, and their membrane tension increases [121]. At the same time, their tumor is “harder” due to the place-demanding proliferation. Cancer elevates the lateral motility of membrane compartments [122], and at the same time, the membrane becomes more rigid in the perpendicular direction [123]. How do these cellular effects act positively or negatively on the resonances of tumor cells?

2) The tumor cells have lower membrane potential than their healthy host cells [124] [125], having shallower potential-well. Consequently, the probability of fixing the wave function inside the well is low (the tunnel effect dominates). How does the strict spectrum form?

3) The extracellular matrix in the cancer cells’ microenvironment is highly disordered [126] [127] because the tumor cells break their networking connections (these are primarily individual, “autonomic” cells). How could resonances modify the harmony between them?

4) The minimal change which we need to modify the cellular structure is the transition of the unfolded state of polypeptides to the α -helix, when the entropy changes (decreases) by $\Delta S_{fold} = -1.38 \times \ln(6^{20}) \times 10^{-23} \text{ J/K} \cong -4.95 \times 10^{-22} \text{ J/K}$ which means the change of the internal energy $\Delta U = T \Delta S_{fold} \cong 1.4 \times 10^{-19} \text{ J}$ [128]. This is considerable energy compared to E_{quant} from (1), where $E_{quant} \cong 10^{-30} \text{ J}$ up to f is in kHz-region. From where does the energy come? Note, the THz frequency or higher (like optical) would be enough to provide the missing energy, but the RF range can not.

5) Cancer cells differ by size and shape from normal cells [129] and from each other [130] and even vary by metastatic potential [131]. How could the resonances with a single frequency modify these objects with various forms and conditions?

6) The beneficial and detrimental frequencies are linearly connected. The general biological frequencies [117] differ from cancerous frequencies in **Figure 3**. An explanation is needed, why are they generally “beneficial” frequencies not beneficial for cancer, and the opposite is that the systemic noncancerous “detrimental” frequencies differ from the detrimental resonances of cancer? Does this mean that the cancerous state is not detrimental?

7) Multiple measurements also show the effects of various parts of the cells in low-frequency regions. These changes are chemical and have nothing to do with such energy described by (1). These effects are induced by the electric field interaction in the classical energy exchanges, such as the Drude-model, frequency dispersions, or charge movements. These exchange energies are much higher than the supposed quantum-mechanical effect in (1). According to our current knowledge, the quantum description of the macro-particles and giant molecules like proteins or DNA is missing. Consequently, the wavefunction and the eigenvalues used in (1) do not describe the macro-objects in such small energies as

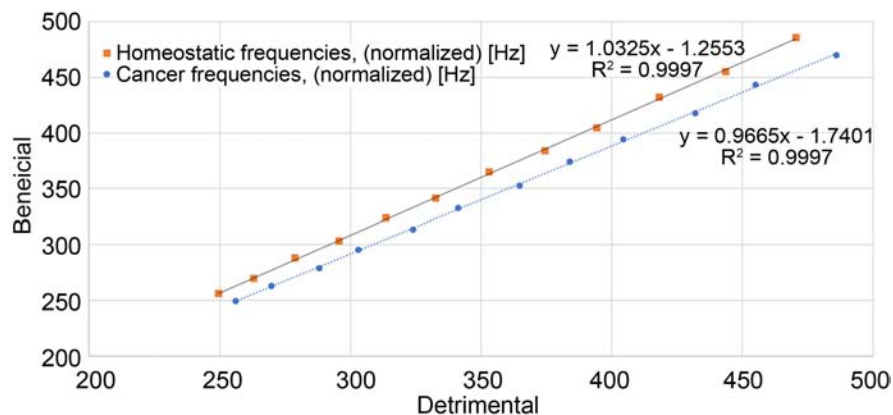


Figure 3. The normalized “beneficial” vs. “detrimental” frequencies (low-frequency spectrum) in cancerous and healthy states. It looks that the “detrimental” frequencies in a healthy state are not parts of the cancerous “detrimental” frequencies, and those frequencies which are “beneficial” in a healthy state are not parts of the beneficial frequencies of the cancer states showing the difference of the “detrimental” categories. A question arises: What do the defined “detrimental” and “beneficial” categories mean?

supposed in (1).

6. The Clinical Renewal of the Rife Concept

The resonant frequencies’ concept was renewed about ten years ago [132]. The “Rife machine”, which uses galvanically coupled current through the body from the electrodes in hands or feet, had been modified for under tongue electrode, providing high RF-frequency (27 MHz) as a carrier and delivering the “resonant frequencies by amplitude modulation of this carrier [133]. The in vitro experiments based on the historical roots [134], including Rife, Laskowski, and others, were used to prove the subtle energy application’s clinical effect [135]. The method could also influence the effect of the cancer stem cells on chemoresistance [136]. A remarkable effect is shown for brain metastases on mammary carcinoma [137] and applied to one of the great challenges of the current oncology approach to hepatocellular carcinoma [138]. The method looks like a ‘shift again’ [139] after the long and complicated hectic changes in resonant frequencies” history.

The protocol of the treatment is simple and ultimately differs from GM-scale. The patient receives the electrode intra-orally, and nothing else is necessary for the process. The applied modulation frequencies are mainly in audio, but in some tumors, it goes up to 100 kHz range [140]. According to the protocol [140] I visually show the spectra for different cancer locations (Figure 4).

The patient receives every individual frequency for 3 s and sorts up to the higher values. Spectrum modulation frequencies are provided. The entire therapy session has 1 h duration, where the scan of frequencies is repeated when all the “prescribed” resonances were given [141] (Figure 5).

Together with the questioned, unknown molecular mechanisms of the method, the technical realization of the treatment has many challenges and doubts.

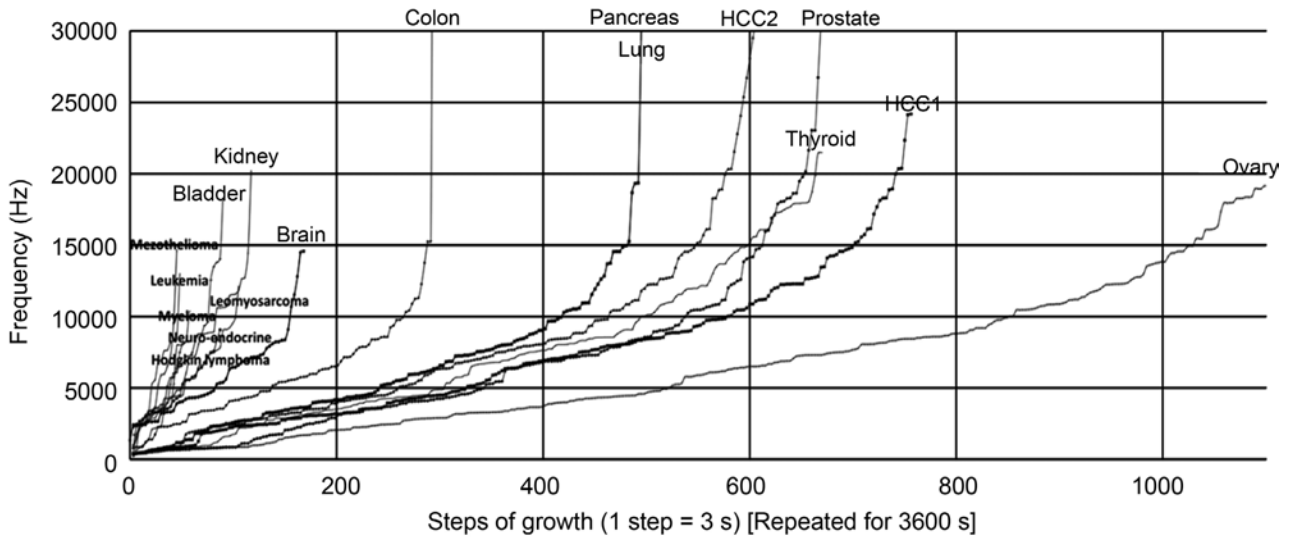


Figure 4. The frequency spectrum vs. time of the treatment in different diseases. The discrete points of the frequencies subsequently increase by 3 s constant state. The 60min duration of the treatment involves repetition of the discrete spectrum until the end of the treatment period.

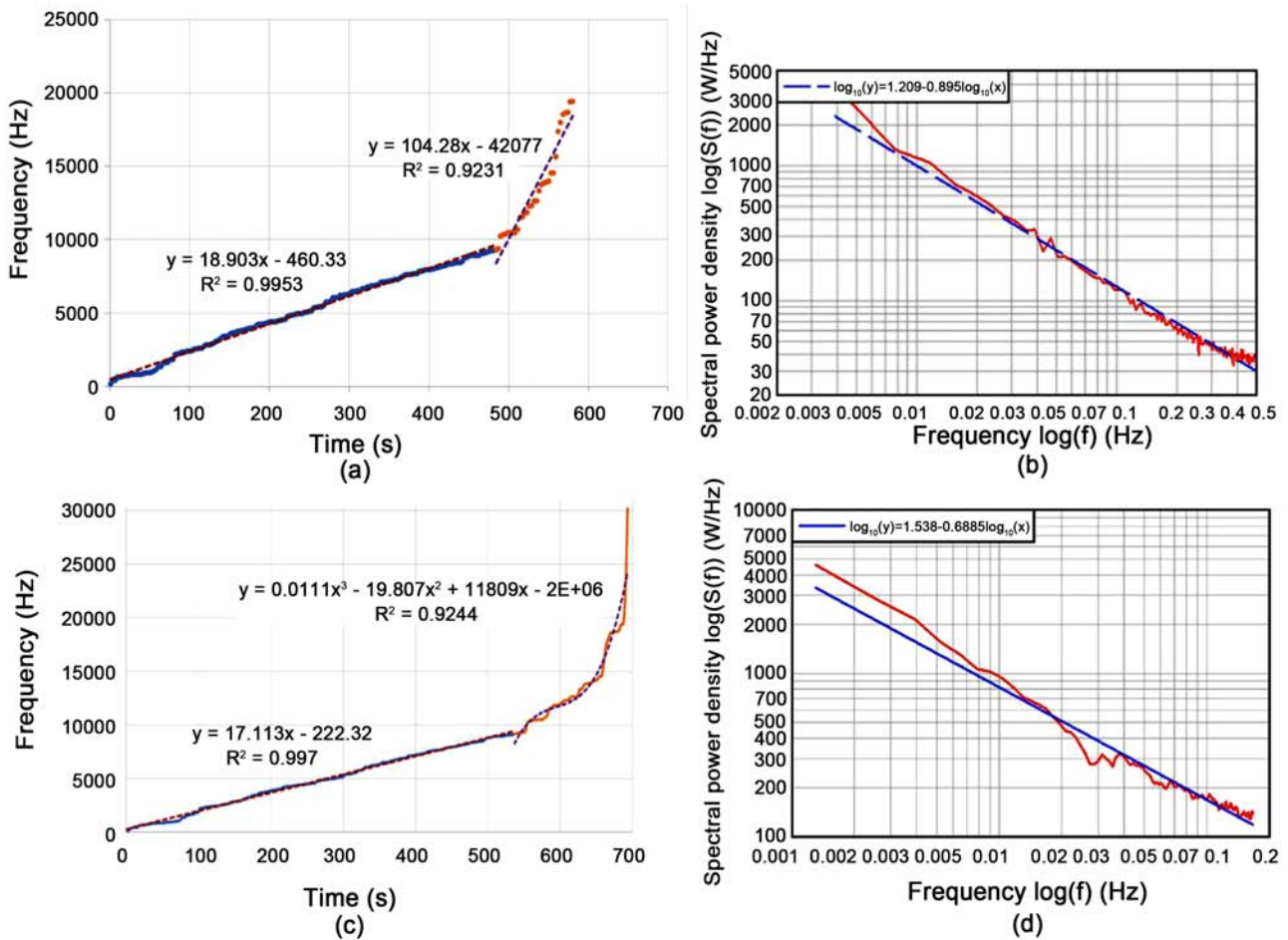


Figure 5. Example of breast treatment frequency applications. (a) the discrete frequencies by time (1 step = 3 s) [142]. Treatment repeats it until 60 min; (b) the spectral power density $S(f)$ fit by FFT ($\alpha = 0.895$, Dplot); (c) Breast treatment in other publication; (d) its spectral density by FFT ($\alpha = 0.6885$, Dplot).

1) Only a single electrode, the intrabuccal spoon-shaped one, exists immersed in a saline environment. This single electrode does not form a definite RF electric circuit. The missing fixed RF circuit occasionally closes capacitively, coupled to the actual, uncontrolled environment of the patient [143].

2) The patient receives uncontrolled minimal (subtle) current intensity (μA) on an uncontrolled path of the current flow. How does it act selectively on the malignant cells throughout the whole body?

3) Notably, the shown SAR is $\approx 5 \text{ W/kg}$ which is shown in the many independent parts of the body [143], implying the homogeneous SAR in the entire system. In the case of a 60 kg patient, it requests tremendous 300 W power homogeneously distributed into the body. From where this extreme power is coming? It is not possible to introduce such high power intrabuccally, and the power supply is via a rechargeable battery.

4) There is no information on how the frequencies were chosen. Was it measured (not published) or is there a principal hypothesis? The frequency's power density has a slope of $\approx 0.6 - 0.8$ on the double logarithmic scale. A publication referring to the treatments of breast cancer, hepatocellular carcinoma (HCC) [142] shows inhibited cancer-cell proliferation by specific modulation frequencies compared to random frequency reference. Frequencies differ by the individuals [140], while the power density fits well to the different diseases: for breast cancer $S_{\text{breast}}(f) \cong 1.533 - 0.8797 \log(f)$; HCC: $S_{\text{HCC}}(f) \cong 1.554 - 0.8790 \log(f)$; and the random frequencies although the method of randomizing the frequencies was not published)

$$S_{\text{random}}(f) \cong 1.598 - 0.8754 \log(f).$$

5) Technical details are missing about the modulation depth, accuracy of the frequencies, and the applied voltage.

6) The patient's impedance is very personal. No information was given about how it was tuned for personal parameters.

7) The *in vitro* and *in vivo* applications have no adequate technical description of the method, and it appears as if these have much higher energies per unit mass than the subtle (nonthermal) energy in human applications ($\approx 1 \text{ W}/(\text{whole-body})$). The cell sizes and shapes differ *in vitro*, *in vivo*, and *ex vivo* conditions [144] and significantly depend on their tumor microenvironment [145] and the signaling processes [146]. How can the resonances be compared?

8) Case reports show the efficacy. However, the reports on the clinical trials which were started 14 years ago [147] [148] are not available on scientific or academic platforms. The design of a new clinical trial is also announced, but no further information is available [149].

Despite the dubious theoretical concepts, the *in-vitro* and *in-vivo* experiments and the clinical data support the resonant phenomena. In the following, I am trying to give a possible stochastic explanation of the observed results.

7. Stochastic Processes

The living systems form a complex dynamic equilibrium that allows adaptation

to the environmental conditions and internal regulative actions on broad scales in space and time [150]. The dynamic living structures perform random stationary stochastic self-organizing processes. Fractal physiology describes the system with interconnected self-similar spatiotemporal composition by fractal structures in space and time [151] [152] [153]. Moreover, the fractal physiology approach has practical medical applications in diagnoses [154] and therapies [155].

The conventional deterministic descriptions are insufficient to explain the observations, and stochastic processes determine the living objects [156]. The deterministic description is valid only in broad averages in space and time. The averages are macroscopic and could mislead microscopic research, which is necessary for resonance phenomena. Understanding the biological dynamism requires stochastic methodology, using probability “decisions” in all steps, and going over transition states that frequently have enzymatic assistance. The often ignored homeostatic balance governs the living processes in all spatiotemporal scales. Involving homeostasis in explanations is mandatory in order to understand the living complexity [157].

Due to the stochastic phenomena, the signals of the diagnostic parameters of the living processes fluctuate around the average of the band of acceptance signal level. The dynamical changes of microstates of the processes vary the fluctuations, regulated by feedback mechanisms. The negative feedback is the easiest way to regulate the desired values because when it stimulates the suppressor, the promoter limits the changes when it increases. The positive feedback triggers the development of a dynamic step, using the suppressor-promoter actions to reach a new equilibrium state. The overlapping signals and their interconnection create noise. The relatively constant noise time averages $\langle D_i \rangle$ of the microscopic diagnostic states D_i and standard deviation (σ_{D_i}) varies according to internal and external conditions. The homeostasis controls the complete spatiotemporal setting, regulates the order of noise structure, and keeps the signal within a tolerance band around the l_{D_i} (Figure 6).

The subject is healthy when the homeostatic control faultlessly keeps the l_{D_i} bands. Fluctuations $f_{D_i} = D_i - \langle D_i \rangle$ carry the details of the microscopic changes. The change of regulative processes drastically varies the f_{D_i} , delivering information about the transformation of the microscopic interactions. The decomposition of the dynamically varying signals to periodic components (Fourier transformation) allows the signals' frequency, amplitude, and phase changes as components of the “noises”. The noise varies when the immune system develops new functions by “learning” to fight against pathogens. The variation could be observed in cancer development, too [158]. Healthy dynamism correlates with metabolic circles and other fundamental living processes. The emitted (measured) fluctuation components characterize the time-set of different interactions and energy exchanges, showing a correlation of the signal with its earlier value at time-lag τ . The time delay describes the similarity of the signal parts when the exact microscopic change happens in the repeated molecular

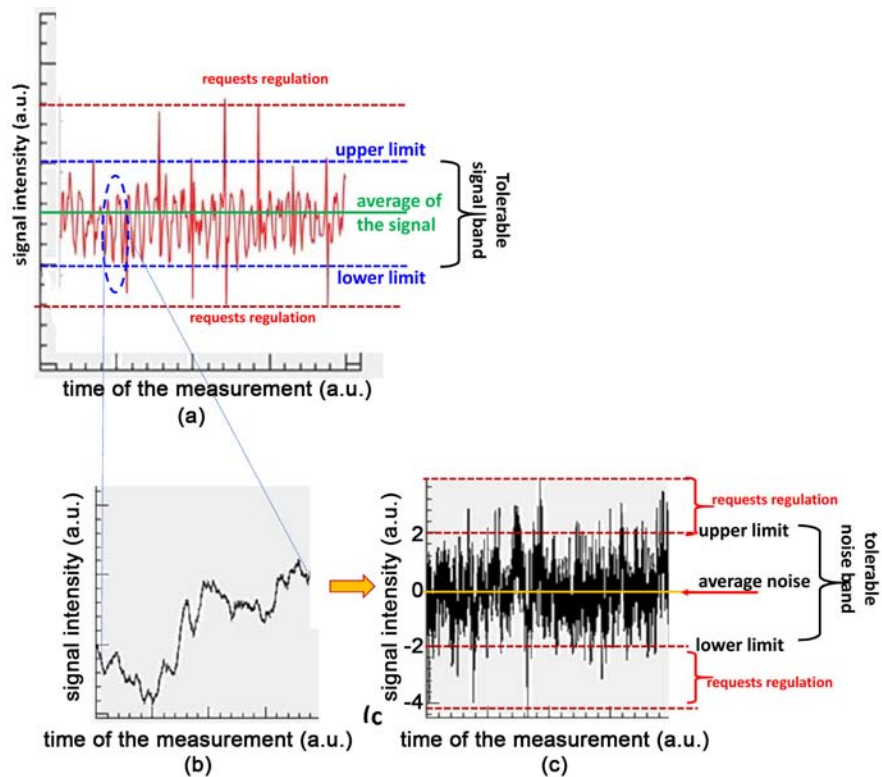


Figure 6. Example of a bio-signal and its noise. (a) the measured signal (b) the enlarged part of the signal, (c) the signal's noise. The usual approach considers the average as the value of a measurement, despite the time dynamics of the signal and the standard deviation being different. The homeostatic control keeps the signal in a tolerable band in equilibrium, and the noise must not exceed the tolerance limit.

signal pathways. The timelag of the autocorrelation function informs the dynamism of the microstates.

The homeostatic balance determines the correlating set of signals involved in the biological changes [159] [160]. The autocorrelation shows the preferences of possible variants of the molecular reactions [161], selection of their timing, and ordering for the desired signal-pathway or enzymatic actions. The frequency-dependent power density spectrum $S(f)$ is a fundamental characterization of the stochastic signals.

The commonly studied simple noise is Gaussian (the amplitudes have normal distribution). The power function of the Gaussian noise is self-similar through many orders of magnitudes showing a simple power function with α

$$S(f) = \frac{A}{f^\alpha} \quad (2)$$

As a consequence of the self-similar, self-organizing processes, the $\alpha = 1$ ($1/f$ noise or pink noise) appears in the timing of healthy life's dynamism [162], [163]. Self-organizing happens in structural and time arrangements [164] and dynamically regulates the processes in the living matter [165]. Halving or doubling the frequency carries an equal amount of noise energy in the $1/f$ noise,

which has some similarities with musical harmony indeed. The self-organized symmetry of the healthy living system transforms the white noise into pink [166], forming the most common signal in biological systems [167].

8. Effect of Low-Frequency, Low-Intensity Intrinsic Excitation

The literature on cellular resonances concentrates on the low-frequency electromagnetic field (LFEMF), which appears in most of the technics of cancer-specific resonance considerations. Numerous reviews [168] [169], and articles report the response of biological matter to LFEMF [170] [171] [172]. The current expectation is that the periodic intrinsic signal of the low-frequency region is biologically active. The earlier model approximations conclude that external excitation with low frequency is not able to make any effects connected to the cellular membrane. The early models assumed that changes in the field strength result from fluctuations of charges on both sides of the cellular membrane, and this fluctuation completely overwhelms the external excitations [173]. The thermal noise fluctuations at the cell membrane exceed any possible LFEMF-induced signals by some orders of magnitudes [173] [174], so thermal noise limits the electromagnetic influences.

Following the method of symmetrical components (zero-mode) of noise [175], a successful model was developed [176]. The noise of electric current mostly follows a directional symmetry between the electrodes. The zero-mode is a noise-sequence of the RF current inducing electrical energy of the cell-membrane capacity and has a uniform potential in spherical symmetry on the membrane, despite the unidirectional current [176]. The low-frequency zero-mode of noise enables the effect of the subtle external excitation in a relatively high thermal noise environment around the cells [177]. The zero-mode noise-sequence excitation produced by an external periodic signal is symmetrical around the cell.

The complete symmetry required in order to induce a pure zero-mode field at a single cell using outer field generators is impossible because most applied external fields are unidirectional. However, there are self-induced and non-direct methods of constructing zero-mode noise components by applying external energy. Dynamic changing of the extracellular matrix (ECM) composition induces ionic currents producing zero-mode noise around the cell. The thermo-diffusion offers another possibility of zero-mode noise. It could be achieved by capacitively coupled electromagnetic field within a specific frequency range [178] [179] [180] provided the RF current is able to penetrate directly into the cytosol.

Only negligible field penetrates the cell in low-frequency RF current (<10 kHz). The ECM absorbs the vast majority of the energy at these frequencies. The deviation of current flow leads to thermal gradients (thermal currents) from the ECM to the inside of the cell [181]. This thermal current also carries ions through, leading to thermo-diffusion, thus creating the symmetric electric cur-

rent, which induces a zero-mode noise in the cell membrane. Both methods generate a centrally symmetric effect by the ionic and/or thermal gradient through the cellular membrane (**Figure 7**); therefore, even small fields with zero-mode components could elicit biological effects.

The isotropic membrane appears as a condition of the symmetrical zero-mode noises. However, all cells have anisotropy on their membranes, especially the unhealthy cells (like malignant cells). Here various membrane segments with different electrical properties exist, allowing additional ionic exchanges. The anisotropy increases the non-zero noise mode, having less possibility of direct excitation with signal amplification of the membrane by ion-diffusion. In these conditions, thermal diffusion and its assistance for ionic exchanges remain the option to produce zero-mode noise.

9. Stochastic Resonance

The resonant behavior of stochastic processes is a noise-guided phenomenon [182]. Adding noise to an external deterministic signal of a nonlinear system produces a stochastic resonant (SR) output. The processes in living objects are inherently nonlinear and have bifurcative and probability-determined (stochastic) decisions of the promoter-suppressor actions at all levels of the organism [183]. The anharmonic factor of the potential well of molecules does not allow deterministic decisions. The applied external signal modulation is intended to go over the energy barrier $\Delta E(x)$ between the targeted initial substrate material (S) and the final product (P). The amplitude A of periodic external signal is small compared to the internal noises of the system, and so the provided formation does not become compelling enough.

Nevertheless, considerable amplification of the weak periodic signal could be

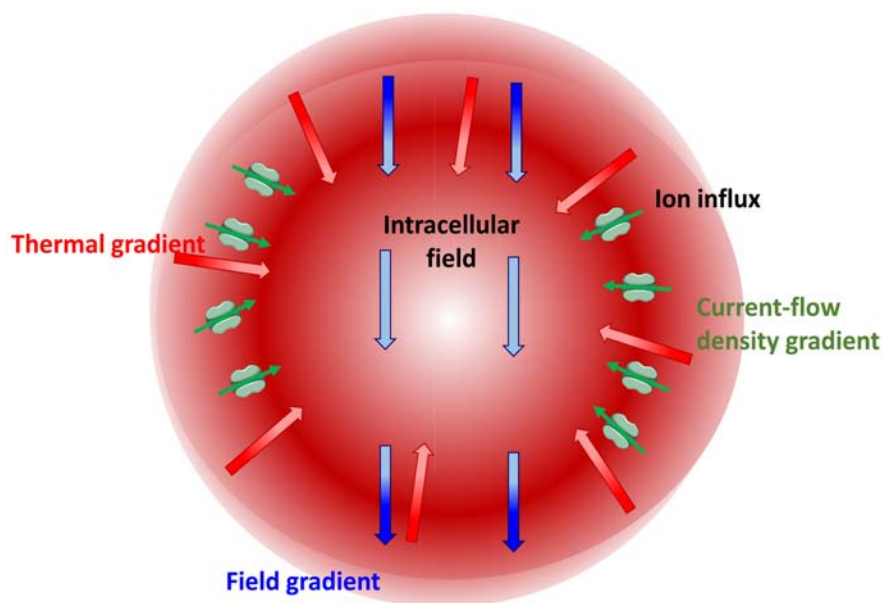


Figure 7. The various gradients at the cell membrane created by the RF-current.

observed by SR, depending on the strength of additional external noise to the intended excitation signal (**Figure 8**). The SR is only possible in nonlinear systems like living matter when the exciting signal is “noisy”. In the models and also in a majority of the practical situations, external or internal Gaussian white noise [184] [185], pink noise [186], Gaussian colored noises [187], or non-Gaussian noises [186] [188] accompany the specific periodic signal.

The signal-to-noise ratio (SNR) amplification has a broad peak in SR conditions, depending on the noise intensity [189] (**Figure 9**).

The optimal noise intensity appears in the maxima of SNR. When the external noise level or the external periodic signal is kept fixed, the SNR has a saturation of increasing frequency or noise intensity, respectively [190]. However, the residence time intervals between consecutive signal peaks have SR peaks depending on the noise intensity or frequency of the external signal [190]. The SR peak

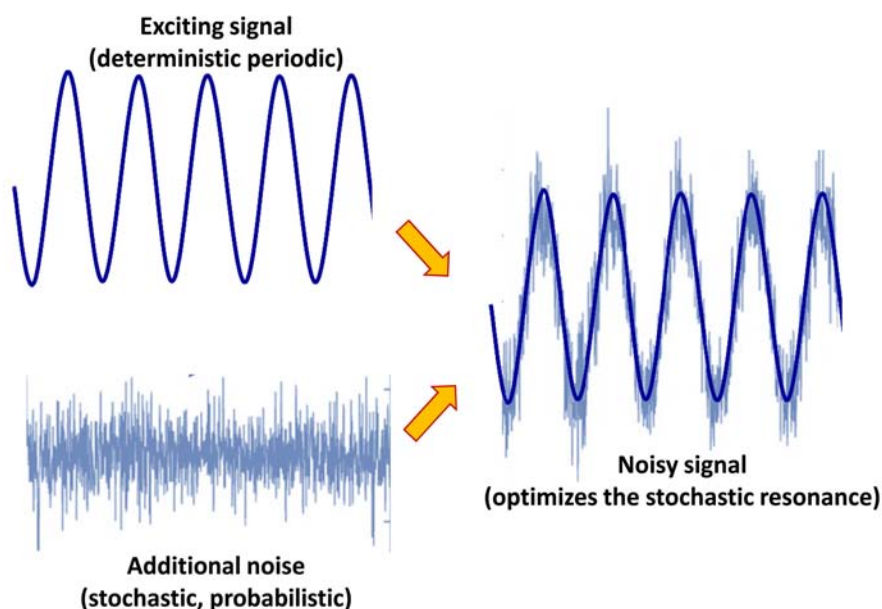


Figure 8. The mixture of the deterministic periodic signal with noise. The resulted “noisy” exciting can induce optimal stochastic resonance.

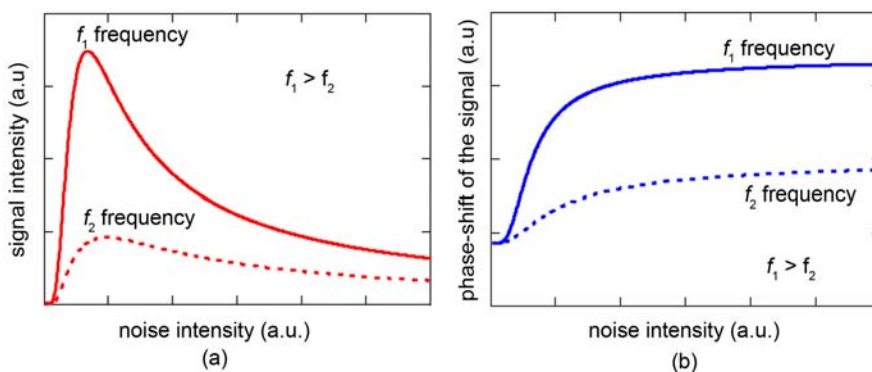


Figure 9. Noise dependence of the parameters of stochastic resonance. (a) Signal intensity. (b) Phase shift.

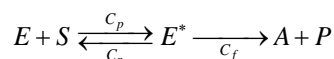
limits the lower and upper levels of SNR, creating a window of the periodic frequency at constant noise. The internal noises adapt to the complex living system by a negative feedback correction of the optimal noise [191] [192]. The optimal noise induces the maximal SNR, dominating all other states. When the noise intensity deviates from the optimal, the signal weakens. The resonant signal obtains its maximum at some noise intensity, which makes the coherence of the multiple resonating units easier, creating feedback driven by the collectivity of the complex system. The optimizing driving force creates collectivity, which surmounts the individual needs of the cells.

The cell waives a part of its energy for collective utilization in exchange for some shared services and enjoys systemic functions connected to its alimentation, optimal survival with the lowest energy consumption, and overall surveillance against pathogens and other invaders. The collectivity works like some kind of democracy [193] within the tissues. The cell became a part of a network exchanging information and materials as well, and in case of damage, the injured tissue has immediate help from its environment. Cancer follows the opposite way [194]. Its state is a “dismantling of multicellularity” [195], and the cellular collectivity disappears [196]. This development is similar to atavism [197]. In this way, cancer development opposes the collective driving force, its “Achillesheel” [198]. While the collectivity emits pink noise [116], the cancer cells deviate in their noise spectrum.

The applied single, noiseless frequency excitation was declared effective in various tumor-specific resonance studies [132] may use the internal noises for SR. However, the internal noise differs between healthy and cancerous emissions. The SR is sensitive to the noises, allowing its tuning to the optimal conditions. Different noise spectra develop a variation of the amplitude maxima of resonant frequencies. The original Rife studies [54] [55] [56] [57], used an argon-gas-filled arc-lamp as the source. It differs from other cancer-specific resonant descriptions because the arc-discharge provides white noise for the carrier frequency and improves a well-formed SR’s probability.

The enzymes execute the molecular biological changes. Most intra and extracellular molecular reactions have a catalytic boost by enzymes to ease the reactions by transition states and the chemical reactions [199]. A simple, early model, the Michaelis-Menten enzyme model [200] (MME), describes the dynamism of the processes where the quantum mechanical rules govern the transition states [201]. The transition changes the cluster configuration and activates the transitional complex [202].

The MME description involves an enzyme (E) starting the formation of the product (P) from a substrate material (S) through a transition state (E^*) with different conversion rates from S to E^* for progressive and reverse C_p , C_r , rates respectively, and finally from E^* to P with C_f .



The first step from the substrate to the transition state is reversible, and the

conditions drive its balance in a negative feedback loop while getting the final product is an unconditional change, the result of the positive feedback process:

The enzymatic processes regenerate the original conformational state of the E enzyme for reuse in a catalytic way. The E^* state has two sub-states (E_1^* and E_2^*) in the reaction: the $E_1^* = (ES)$ complex transforms to P product, via $E_2^* = (EP)$ complex, while the enzyme transforms back to E state at the end of the process. Like all reactions, chemical activity steps are reversible; the progress \leftrightarrow reverse interaction rate balances all steps. The production mechanism must have positive feedback to force P product from the S substrate and shift the equilibrium to a definite direction. The driving force is usually the standard environmental living condition that ignites and controls the process. After finishing the production, the enzyme returns to its initial conformational state and may restart the action. This form of a loop (“catalytic wheel” [203], **Figure 10**), is driven by negative feedback.

The wheel model describes a cyclic catalytic reaction with two conformational states of the process’s speed, described by a steady-state technique [204]. The catalytic wheel decreases the energy barrier (activation energy E_a) between the substrate and product. The E_a has thermal (enthalpy factor) and nonthermal (entropy factor) components, and the change of the activation energy (ΔE_a). The subthreshold signal induces SR resonance which causes modification even in single cells [205], controlling the gating membrane channels and selecting ions, and molecules’ entry to the cytosol [205]. While experimental general Arrhenius

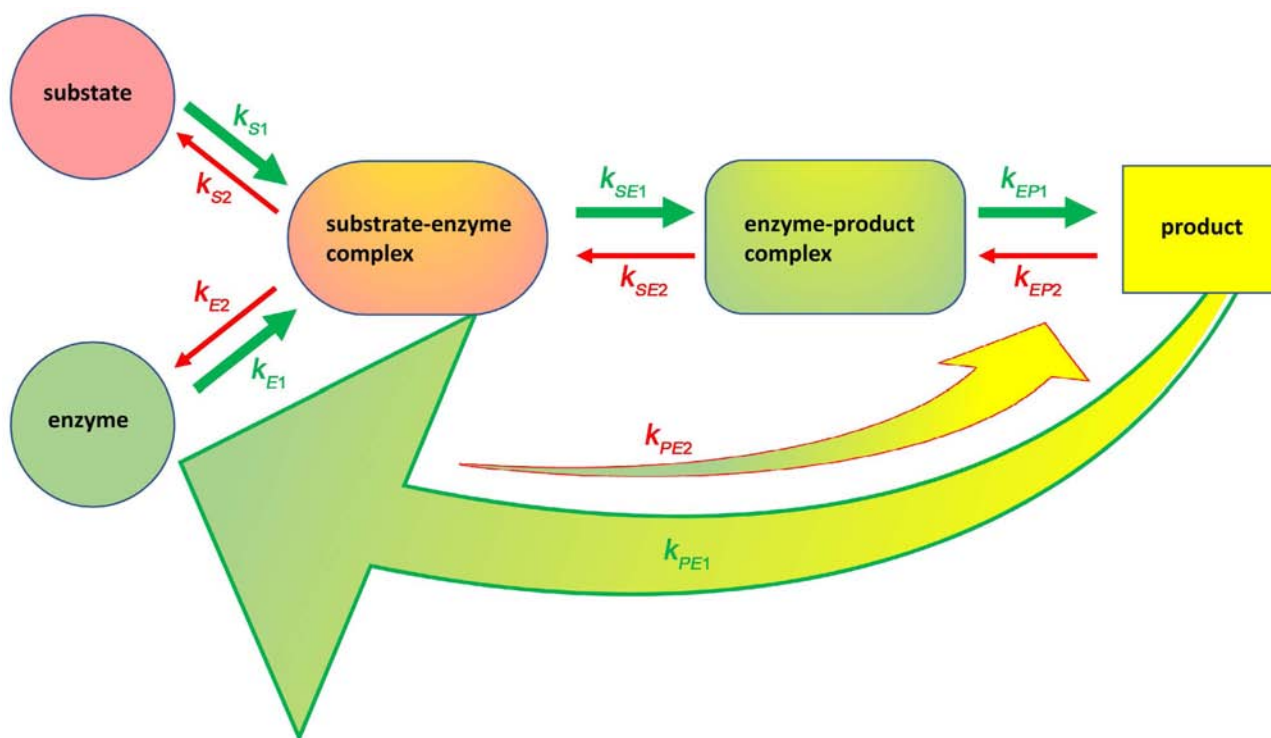


Figure 10. The enzymatic changes during the $S \rightarrow P$ transformation. The well applied ECC conditions drive the relation $k_{S2} < k_{S1}$, $k_{SE2} < k_{SE1}$, $k_{EP2} < k_{EP1}$ and $k_{PE1} < k_{PE2}$, so the “wheel” works in one direction, by the Michaelis-Menten process.

law considers a single step jump over the E_a energy barrier, in real processes, the substrate state never transform into products in a single direct step [206] [207], [208]. In this transition, the thermal and electric effects have similarities, unifying the phenomena in a complex unit [209]. Additionally, a typical quantum-mechanical phenomenon, the tunneling effect through the barrier, could modify the transition [210].

The electric field of various electromagnetic signals could actively ignite, modify or block the enzymatic wheels by electro-conformal coupling (ECC, [211] [212]). ECC uses oscillatory SR stimulation to promote the transition of the substrate to the product [213]. The SR controls the probability of the $S \rightarrow P$ enzymatic process fixing it in the homeostatic dynamic equilibrium [214]. The environmental thermal noise drives the SR providing energy to this process by the Brownian engine [215] [216]. A periodic electric field may convert the accessible energy-producing transports to chemical reactions coupled through enzymatic processes [217]. The ECC rectifies the thermal fluctuations, driving one-directional dynamics [218] [219], representing a “ratchet” like behavior pumping the processes in one direction only, blocking the opposite turn. The thermal fluctuations, together with the electric noises of the incident signal, provide the available free energy [218]. The thermal energy is high: the ATP hydrolysis has $\approx 10^{-16}$ W, while the thermal factor of dynamic molecular scattering provides 10^{-8} W [220]. The Brownian engine processes work with irreversible thermodynamics with an external periodic perturbation [221]. The thermal components of the micro and macro environment of the tumor cells determine the ECC. When the noise is thermal (white), the ECC has an optimal temperature, but in colored noise (like $1/f$ noise) conditions, the temperature dependence is weaker.

A considerable number of enzymes and enzymatic reactions exist in human biology. The cancer metabolic pathways alone have many enzymatic processes [222] [223], which is a small part of the complete number of enzymes involved in various homeostatic bioreactions. The complexity makes the huge adaption of the system to environmental changes possible when the homeostatic network substitutes a missing process with others. The enormous number of enzymatic reactions determines the number of SR resonant frequencies. Due to the noise dependence of SR, the actual resonance sharply depends on the reaction’s environmental temperature and the excitation signal’s noise. Consequently, the same bioreaction may have various exciting signals for effective and optimal SR. Complicates the selection of SR that the excitation could also be effective on other nonlinear bistable structures, like the activation of voltage-gated ion channels.

The electrically generated subthreshold stimuli affect the transition state of molecular reactions in various biological processes [224]. One of the explanations of the Rife resonant frequencies could involve the SR phenomena. However, in this case, the resonant frequencies express a dense spectrum. It has as

many resonances as enzymatic reactions that exist in the target. However, another request is to drive the cancer cell's cell death when we do not expect prompt necrosis. The SR amplification has to be multiple, with steps of the signal pathway involving different enzymatic processes and resonances. The complexity offers multiple signal variants, which could direct the pathway to the different final results.

Consequently, the stable solution needs a set of SR frequencies in an appropriate time set. The networking has chain reactions through the signal pathways. The subsequent reactions in the chain define the order of the necessary enzymatic action, which can be modified by external signals when their autocorrelation supports the reaction sequences. The optimally chosen exciting signal with properly fitting autocorrelation can drive the ordered chain reaction with subsequent SRs [225].

10. Conclusions

The enzymatic stochastic resonance defines specific resonant frequencies [226] [227] on the molecular level. The stochastic resonance (SR) describes the interaction of a deterministic subthreshold signal and a fluctuation (noise) spectrum. The phenomenon inherently depends on temperature. The resonant frequencies of neuronal-like healthy and cancer cell membrane channels differ and are excitable [228]. The SR may explain the Rife frequencies. The response to weak external electric fields by definite modulation frequencies could remain active far below the thermal noise limit and ignites some molecular processes by the stochastic resonance. The number of resonant frequencies acting in the cellular processes is at least as many as enzymatic activities. Multiple conditional factors modify the resonance and the frequency of the peak, producing a vast number of different resonances.

Additionally, the SR depends on the temperature and pH in the cell's micro-environment. Furthermore, the cellular structure (like size, form), state (like age, stress), and dynamic development (like chemotaxis and cellular division) certainly affect the resonance and shift or even block the resonant frequency. The size of a studied group of molecules offers a typical size dependence of resonances, including harmony between the group members [229]. The intercellular interaction changes the resonances and multiplies the observable resonant peaks. The modulation excitation of membrane rafts [230] [231] considers this possibility with a well-defined spectrum of modulation frequencies [226] [232]. The resonant reaction complexity operates in a network of interactive intra- and extracellular functions. The interconnection of the intracellular complex multi-pathway feedback loops and the multicellular interactions does not allow for the division of the resonance into two distinct "detrimental" and "beneficial" categories. The biological complexity does not permit the black-and-white categorizing and does not allow to deterministically determine that some resonances are healthy and some are not. The "beneficial" signal pathways may work "de-

trimentally” among various tumor microenvironment conditions. All the participating molecules of the complex network have a “double-edged sword” quality, having optimal molecular reactions in a narrow range of conditions. The molecular change presents deterministic-like processes only when we form a large average of the considered parameters on the macroscale. The microscale offers only probabilistic considerations. The apparent deterministic Pythagorean harmony of numbers is valid only in macroscopic averages, but the resonance is microscopic. The explanation of molecular resonance processes incorrectly describes the phenomena in a classical deterministic way.

Electromagnetic medicine represents a new modality, using molecular biology for therapy [233], including oncology [234]. The molecular excitation by using resonances [235] has enormous opportunities. Some bioresonances, like cyclotron resonance [236], are well proven and hypothesized for new kinds of vaccination [237]. The antitumoral vaccination forces tumor-specific immune reactions ignited by thermal and nonthermal effects of nonionizing RF radiation. Bioelectromagnetism activates both the innate and adaptive immune system [238], promoting the abscopal effect [239] [240], and becomes a part of the complementary clinical therapies [241] [242]. However, presently our knowledge about bioelectromagnetic resonances is somewhat limited. Rigorous theoretical and experimental investigations with randomized prospective clinical studies are mandatory for the further clearance of the cancer-specific resonant frequencies.

Acknowledgements

This work was supported by the Hungarian National Research Development and Innovation Office PIACI KFI grant: 2019-1.1.1-PIACI-KFI-2019-00011.

Conflicts of Interest

The author declares no conflicts of interest regarding the publication of this paper.

References

- [1] Kempf, E.J. (1906) European Medicine: A Résumé of Medical Progress during the Eighteenth and Nineteenth Centuries. *Journal of the Medical Library Association*, **3**, 231-248.
- [2] Mattei, C.C. (1880) Principles of Electrohomoeopathy. A New Science Discovered by Count Cesar Mattei of Bologna. Printing and Stereotype Offices V.-E. Gauthier and Co., Nice.
- [3] Baylen, J.O. (1969) The Mattei Cancer Cure: A Victorian Nostrum. *Proceedings of the American Philosophical Society*, **113**, 149-176.
- [4] Memorial Sloan-Kettering Cancer Center (2012, May 29) BioResonance Therapy.
- [5] Suresh, S.K. (2018) The Greatest Enemy of Knowledge Is Not Ignorance, It Is the Illusion of Knowledge.
<https://medium.com/@somesk.ks/the-greatest-enemy-of-knowledge-is-not-ignorance-it-is-the-illusion-of-knowledge-5c0dd1dcca7e>

- [6] Hornberger, J. (2019) Who Is the Fake One Now? Questions of Quackery, Worldiness and Legitimacy. *Critical Public Health*, **29**, 484-493. <https://doi.org/10.1080/09581596.2019.1602719>
- [7] Sethares, W.A. (2005) *Tuning, Timbre, Spectrum, Scale*. Springer, Berlin.
- [8] Sikic, Z. (2016) Generalized Pythagorean Comma. *CroArtScia2011*, Zagreb, 4-7 May 2011, 169-174.
- [9] Livio, M. (2003) *The Golden Ratio: The story of Phi, the World's Most Astonishing Number*. Broadway Books, New York City, 145 p.
- [10] Cui, H.Y. (2002) To String Together Six Theorems of Physics by Pythagoras Theorem.
- [11] Darvas, G., Koblyakov, A.A., Petoukhov, S.V. and Stepanian, I.V. (2012) Symmetries in Molecular-Genetic Systems and Musical Harmony. *Symmetry: Culture and Science*, **23**, 343-375.
- [12] Garrett, S.L. (2020) String Theory. In: *Understanding Acoustics*, Springer, Berlin, 133-178. https://doi.org/10.1007/978-3-030-44787-8_3
- [13] Schuch, D. (2010) Pythagorean Quantization, Action(s) and the Arrow of Time. *Journal of Physics: Conference Series*, **237**, Article ID: 012020. <https://doi.org/10.1088/1742-6596/237/1/012020>
- [14] Overduin, J. and Henry, R.C. (2005) Physics and the Pythagorean Theorem.
- [15] Richinick, J. (2008) The Upside-Down Pythagorean Theorem. *The Mathematical Gazette*, **92**, 313-316. <https://doi.org/10.1017/S0025557200183275>
- [16] Kappraff, J. and Adamson, G.W. (2009) Generalized Genomic Matrices. *Silver Means, and Pythagorean Triples, Forma*, **24**, 41-48.
- [17] Overmarch, A., Ntogramatzidis, L. and Venkatraman, S. (2019) A New Approach to Generate All Pythagorean Triples. *AIMS Mathematics*, **4**, 242-253. <https://doi.org/10.3934/math.2019.2.242>
- [18] Maxwell, J.C. (1998) *A Treatise on Electricity and Magnetism*. Clarendon Press, Oxford.
- [19] Benett, W.R. (1994) Cancer and Power Lines. *Physics Today*, **47**, 23-29. <https://doi.org/10.1063/1.881417>
- [20] Portier, C.J. and Wolfe, M.S. (1998) Assessment of Health Effects from Exposure to Power-Line Frequency Electric and Magnetic Fields. NIH Publication 98-3981. National Institute of Environmental Health Sciences, Research Triangle Park.
- [21] Harland, J.D. and Liburdy, R.P. (1997) Environmental Magnetic Fields Inhibit the Antiproliferation Action of Tamoxifen and Melatonin in a Human Breast Cancer Cell Line. *Bioelectromagnetics*, **18**, 555-562. [https://doi.org/10.1002/\(SICI\)1521-186X\(1997\)18:8<555::AID-BEM4>3.0.CO;2-1](https://doi.org/10.1002/(SICI)1521-186X(1997)18:8<555::AID-BEM4>3.0.CO;2-1)
- [22] Ahlbom, A., Day, N., Feychting, M., Roman, E., Skinner, J., *et al.* (2000) A Pooled Analysis of Magnetic Fields and Childhood Leukemia. *British Journal of Cancer*, **83**, 692-698. <https://doi.org/10.1054/bjoc.2000.1376>
- [23] Greenland, S., Sheppard, A.R., Kaune, W.T., *et al.* (2000) A Pooled Analysis of Magnetic Fields, Wire Codes, and Childhood Leukemia. *Epidemiology*, **11**, 624-634. <https://doi.org/10.1097/00001648-200011000-00003>
- [24] Takebe, H., Shiga, T., Kato, M. and Masada, E. (2001) Biological and Health Effects from Exposure to Power-Line Frequency Electromagnetic Fields. IOS Press, Amsterdam.
- [25] Randerson, J. (2007, January 18) Electrosmog in the Clear with Scientists. *The Guardian*.

- <http://www.guardian.co.uk/technology/2007/jan/18/guardianweeklytechnologysecton4>
- [26] Oschman, J. (2000). *Energy Medicine—The Scientific Basis*. Churchill Livingstone, Edinburgh.
- [27] Loja, T., Stehlikova, O., Palko, L., Vrba, K., Rampl, I. and Klabusay, M. (2014) Influence of Pulsed Electromagnetic and Pulsed Vector Magnetic Potential Field on the Growth of Tumor Cells. *Electromagnetic Biology and Medicine*, **33**, 190-197. <https://doi.org/10.3109/15368378.2013.800104>
- [28] Rein, G. and Tiller, W.A. (1996) Anomalous Information Storage in Water: Spectroscopic Evidence for Non-Quantum Informational Transfer. *Proceedings 3rd International Conference New Energy*, Denver, 24-28 April 1996, 365.
- [29] Meyl, K. (2001) Scalar Waves: Theory and Experiments. *Journal of Scientific Exploration*, **15**, 199-205.
- [30] Tiller, W.A. (1999) Subtle Energies. *Science & Medicine*, **6**, 28 p.
- [31] Hall, H. (2005) A Review of Energy Medicine: The Scientific Basis. *Skeptic Magazine*, **11**, 89-93. <http://quackfiles.blogspot.com/2006/01/review-of-energy-medicine-scientific.html>
- [32] Bruhn, G.W. (2000) Commentary on the Chapter “Scalar Waves”, in “Energy Medicine—The Scientific Basis”. <http://www.mathematik.tu-darmstadt.de/~bruhn/Commentary-Oschman.htm>
- [33] Bruhn, G.W. (2001) On the Existence of K. Meyl’s Scalar Waves. *Journal of Scientific Exploration*, **15**, 206-210.
- [34] Saliev, T., Begimbetova, D., Masoud, A.R. and Matkarimov (2019) Biological Effects of Non-Ionizing Electromagnetic Fields—Two Sides of a Coin. *Progress in Biophysics and Molecular Biology*, **141**, 25-36. <https://doi.org/10.1016/j.pbiomolbio.2018.07.009>
- [35] Carlson, W.B. (2013) *Tesla: Inventor of the Electrical Age*. Princeton University Press, Princeton. <https://doi.org/10.1515/9781400846559>
- [36] Tesla, N. (1891) Patent Title: Alternating Electric Current Generator. US447,921.
- [37] Tesla, N. (1914) Patent Title: Apparatus for Transmitting Electrical Energy. US1119732 A.
- [38] Tesla, N. (1905) Art of Transmitting Electrical Energy through the Natural Medium. United States Patent, No. 787,412.
- [39] Tesla, N. (1898) High Frequency Oscillators for ElectroTherapeutic and Other Purposes. *The Electrical Engineer*, **26**, 346-348.
- [40] Aharonov, Y. and Bohm, D. (1959) Significance of Electromagnetic Potentials in Quantum Theory. *Physical Review*, **115**, 485-491. <https://doi.org/10.1103/PhysRev.115.485>
- [41] Szasz, A., Vincze, Gy. anddocs, G. and Szasz, O. (2009) Do Field-Free Electromagnetic Potentials Play a Role in Biology? *Electromagnetic Biology and Medicine*, **28**, 135-147. <https://doi.org/10.1080/15368370802711938>
- [42] Hegyi, G., Vincze, Gy. and Szasz, A. (2007) Axial Vector Interaction with Bio-Systems. *Electromagnetic Biology and Medicine*, **26**, 107-118. <https://doi.org/10.1080/15368370701380835>
- [43] Andocs, G., Vincze, Gy., Szasz, O., Szendro, P. and Szasz, A. (2009) Effect of Curl-Free Potentials on Water. *Electromagnetic Biology and Medicine*, **28**, 166-181. <https://doi.org/10.1080/15368370902724724>

- [44] A Brief History of Dr. Royal Raymond Rife.
<https://www.nationallibertyalliance.org/files/NaturalHealing/Rife/History%20of%20Dr%20Rife.pdf>
- [45] Bird, C. (1976) What Has Become of the Rife Microscope? *New Age Journal*, March 1976, 41-47.
- [46] Seldel, R.E. and Winter, M.E. (1944) The New Microscopes. *Journal of the Franklin Institute*, **237**, 103-130.
- [47] Kendall, A.I. and Rife, R.R. (1931) Observations on Bacillus Typhosus in Its Filterable State: A Preliminary Communication. *California and Western Medicine*, **35**, 409-411.
- [48] Stylianidou, S., Connor, B., Nissen, S.B., Kuwada, N.J. and Wiggins, P.A. (2016) SuperSegger: Robust Image Segmentation, Analysis and Lineage Tracking of Bacterial Cells. *Molecular Microbiology*, **102**, 690-700.
<https://doi.org/10.1111/mmi.13486>
- [49] Merouan, A., Rey, Villamizar, N., Lu, Y.B., Liadi, I., Romain, G., Lu, J., Singh, H., Cooper, L.J.N., Varadarajan, N. and Roysam, B. (2015) Automated Profiling of Individual Cell-Cell Interactions from High-Throughput Time-Lapse Imaging Microscopy in Nanowell Grids (TIMING). *Bioinformatics*, **31**, 3189-3197.
<https://doi.org/10.1093/bioinformatics/btv355>
- [50] Young, J.W., Locke, J.C.W., Altinok, A., Rosenfeld, N., Bacarian, T., Swain, P.S., Mjolsness, E. and Elowitz, M.B. (2011) Measuring Single-Cell Gene Expression Dynamics in Bacteria Using Fluorescence Time-Lapse Microscopy. *Nature Protocols*, **7**, 80-88. <https://doi.org/10.1038/nprot.2011.432>
- [51] Tesla, N. (1885) Electric Arc Lamp. US171,416.
- [52] Scoon, A. (2001) Special Supplement of Everyday Practical Electronics, April 2001. Wimborne Publishing Ltd., Dorset, and Maxfield & Montrose Interactive Inc., Madison. <https://www.rife.de/files/epearticle.pdf>
- [53] Jones, N. (1938) Dread Disease Germs Destroyed by Rays, Claim of S.D. Scientist: Cancer Blow Seen after 18-Year Toil by Rife. *The San Diego Union-Tribune*, 1.
- [54] Line, B. (2017) Rife's Great Discovery: Why "Resonant Frequency" Therapy Is Kept Hidden from Public Awareness. BioMed Publishing Group, South Lake Tahoe.
- [55] Lynes, B. (1997) The Cancer Cure That Worked: 50 Years of Suppression. Marcus Publishing, Canada.
- [56] Allegretti, M. (2018) The Frequencies of Rifing—From the First Frequencies Discovered by Royal Rife to Today: Guide to Selection and Use of Spooky2 Frequencies.
- [57] Silver, N. (2001) The Handbook of Rife Frequency Healing: Holistic Technology for Cancer and Other Diseases. The Center for Frequency Education Publishing, Stone Ridge.
- [58] Energy Medicine—Radionics Rife Machine.
<http://www.skeptdic.com/radionics.html>
- [59] (1994) Questionable Methods of Cancer Management: Electronic Devices. *CA: A Cancer Journal for Clinicians*, **44**, 115-127. <https://doi.org/10.3322/canjclin.44.2.115>
- [60] Barrett, S. (2010) Device Watch—Rife Device Marketer Sentenced to Prison.
<https://quackwatch.org/device/reports/rife/folsom>
- [61] Barrett, S. (2012) Rife Machine Operator Sued. Quackwatch.
<https://www.quackwatch.org/04ConsumerEducation/News/rife.html>

- [62] Farley, D.F. (1996) Unproven Medical Claims Land Men in Prison, Investigators' Reports. FDA Consumer. U.S. Food and Drug Administration.
https://web.archive.org/web/20071214170405/https://www.fda.gov/fdac/departs/796_irs.html
- [63] Kurtzweil, P. (1996) Investigators' Reports. FDA Consumer. U.S. Food and Drug Administration.
https://web.archive.org/web/20071214170405/https://www.fda.gov/fdac/departs/796_irs.html
- [64] Willmsen, C. and Berens, M.J. (2007) Pair Indicted on Fraud Charges in Medical-Device Probe. *The Seattle Times*.
<https://www.seattletimes.com/seattle-news/pair-indicted-on-fraud-charges-in-medical-device-probe>
- [65] Barrett, S. (2009) Rife Device Marketers Convicted. Quackwatch.
- [66] Johnson, J. (2019) Can the Rife Machine Treat Cancer?
<https://www.medicalnewstoday.com/articles/325628.php>
- [67] Hill, B. (2000) Cheating Death. *The Sydney Morning Herald*.
<http://www.healthwatcher.net/Quackerywatch/Cancer/Cancer-news/smh001230rife-aus.html>
- [68] No Authors Listed (1994) Questionable Methods of Cancer Management: Electronic Devices. *CA: A Cancer Journal for Clinicians*, **44**, 115-127.
<https://doi.org/10.3322/canjclin.44.2.115>
- [69] (2013) Rife Machines and Cancer. Cancer Research UK.
- [70] Lakhovsky, G. (1925) Curing Cancer with Ultra Radio Frequencies. *Radio News*, February, 1282-1283.
- [71] Lakhovsky, G. (1988) Secret of Life: Electricity Radiation & Your Body. 4th Revised Edition, Noontide Press, Newport Beach.
- [72] Rife, R.R. (1953) History of the Development of a Successful Treatment for Cancer and Other Virus, Bacteria and Fungi. Rife Virus Microscope Institute, San Diego.
- [73] Bearden, T.E. (1995) Vacuum Engines and Priore's Methodology: The True Science of Energy Medicine. *Explore*, **6**, 66-76.
- [74] Bateman, J.B. (1978) A Biologically Active Combination of Modulated Magnetic and Microwave Fields: The Prioré Machine. Office of Naval Research, London, Report R-5-78.
- [75] Camp, J. (1973) Magic, Myth and Medicine. Priory Press Ltd., Dunstable.
- [76] Gurwitsch, A.G. (1944) A Biological Field Theory. Nauka, Moscow. (In Russian)
- [77] Beloussov, L.V., Opitz, J.M. and Gilbert, S.F. (1997) Life of Alexander G. Gurwitsch and His Relevant Contribution to the Theory of Morphogenetic Fields. *The International Journal of Developmental Biology*, **41**, 771-777.
- [78] Spemann, H. (1938) Embryonic Development and Induction. Yale University Press, New Haven.
- [79] Manning, C.A. and Vanrenen, L. (1989) Bioenergetic Medicines East and West. North Atlantic Books, Berkeley.
- [80] Levin, M. (2012) Morphogenetic Fields in Embryogenesis, Regeneration, and Cancer: Non-Local Control of Complex Patterning. *Biosystems*, **109**, 243-261.
<https://doi.org/10.1016/j.biosystems.2012.04.005>
- [81] Levin, M. (2003) Bioelectromagnetics in Morphogenesis (Review). *Bioelectromagnetics*, **24**, 295-315. <https://doi.org/10.1002/bem.10104>
- [82] Volodiaev, I. and Beloussov, L.V. (2015) Revisiting the Mitogenetic Effect of Ultra-

- Weak Photon Emission. *Frontiers in Physiology*, **6**, Article No. 241. <https://doi.org/10.3389/fphys.2015.00241>
- [83] Thompson, W.G. (2005) *The Placebo Effect and Health, Combining Science and Compassionate Care*. Prometheus Books, New York.
- [84] Gauler, T.C. and Weihrauch, T.R. (1997) *Placebo*. Urban & Schwarzenberg, Munich.
- [85] Hróbjartsson, A. and Gøtzsche, P.C. (2010) Placebo Interventions for All Clinical Conditions. *The Cochrane Database of Systematic Reviews*, **106**, CD003974. <https://doi.org/10.1002/14651858.CD003974.pub3>
- [86] Lin, J.C. (1989) *Electromagnetic Interaction with Biological Systems*. Pergamon Press, New York, London. <https://doi.org/10.1007/978-1-4684-8059-7>
- [87] Bersani, F. (1999) *Electricity and Magnetism in Biology and Medicine*. Kluwer Academic Plenum Publishers, New York, Boston. <https://doi.org/10.1007/978-1-4615-4867-6>
- [88] Marko, M. (2005) “Biological Windows”: A Tribute to WR Adey. *The Environmentalist*, **25**, 67-74. <https://doi.org/10.1007/s10669-005-4268-8>
- [89] Adey, W.R. (1984) Nonlinear, Nonequilibrium Aspects of Electromagnetic Field interactions at Cell Membranes. In: Adey, W.R. and Lawrence, A.F., Eds., *Nonlinear Electrodynamics in Biological Systems*, Plenum Press, New York, London, 3-22. https://doi.org/10.1007/978-1-4613-2789-9_1
- [90] Adey, W.R. (1990) Joint Actions of Environmental Nonionizing Electromagnetic Fields and Chemical Pollution in Cancer Promotion. *Environmental Health Perspectives*, **86**, 297-305. <https://doi.org/10.1289/ehp.9086297>
- [91] Blackman, C.F., Kinney, L.S., House, D.E., *et al.* (1989) Multiple Power-Density Windows and Their Possible Origin. *Bioelectromagnetics*, **10**, 115-128. <https://doi.org/10.1002/bem.2250100202>
- [92] Liu, D.S., Astumian, R.D. and Tsong, T.Y. (1990) Activation of Na⁺ and K⁺ Pumping Modes of (Na,K)-ATPase by an Oscillating Electric Field. *The Journal of Biological Chemistry*, **265**, 7260-7267. [https://doi.org/10.1016/S0021-9258\(19\)39108-2](https://doi.org/10.1016/S0021-9258(19)39108-2)
- [93] Markin, V.S. and Tsong, T.Y. (1991) Frequency and Concentration Windows for the Electric Activation of a Membrane Active Transport System. *Biophysics Journal*, **59**, 1308-1316. [https://doi.org/10.1016/S0006-3495\(91\)82345-1](https://doi.org/10.1016/S0006-3495(91)82345-1)
- [94] Hameroff, S. and Penrose, R. (2014) Consciousness in the Universe: A Review of the “Orch OR” Theory. *Physics of Life Reviews*, **11**, 39-78. <https://doi.org/10.1016/j.plrev.2013.08.002>
- [95] Del Giudice, E. (2011) The Interplay of Biomolecules and Water at the Origin of the Active Behavior of Living Organisms. *Journal of Physics: Conference Series*, **329**, Article ID: 012001. <https://doi.org/10.1088/1742-6596/329/1/012001>
- [96] Geesink, H.J. and Meijer, D.K.F. (2020) An Integral Predictive Model That Reveals a Causal Relation between Exposures to Non-Thermal Electromagnetic Waves and Healthy or Unhealthy Effects. <https://www.researchgate.net/publication/340488204>
- [97] Bowling, D.L. and Purves, D. (2015) A Biological Rationale for Musical Consonance. *PNAS*, **112**, 11155-11160. <https://doi.org/10.1073/pnas.1505768112>
- [98] Geesink, J.H. and Meijer, D.K.F. (2018) A Semi-Harmonic Electromagnetic Frequency Pattern Organizes Non-Local States and Quantum Entanglement in both EPR Studies and Life Systems. *Journal of Modern Physics*, **9**, 898-924. <https://doi.org/10.4236/jmp.2018.95056>

- [99] Geesink, H.J.H. and Meijer, D.K.F. (2016) Quantum Wave Information of Life Revealed: An Algorithm for Electromagnetic Frequencies That Create Stability of Biological Order, with Implications for Brain Function and Consciousness. *Neuro-Quantology*, **14**, 106-125. <https://doi.org/10.14704/nq.2016.14.1.911>
- [100] Meijer, D.K.F., Jerman, I., Melkikh, A.V. and Sbitnev, V.I. (2019) Consciousness in the Universe Is Tuned by a Musical Master Code: A Hydrodynamic Superfluid Quantum Space Guides a Conformal Mental Attribute of Reality. The Hard Problem in Consciousness Studies Revisited. Project: The Information Universe. On the Missing Link in Concepts on the Architecture of Reality.
- [101] Geesink, H.J.H. and Meijer, D.K.F. (2018) Mathematical Structure for Electromagnetic Frequencies That May Reflect Pilot Waves of Bohm's Implicate Order. *Journal of Modern Physics*, **9**, 851-897. <https://doi.org/10.4236/jmp.2018.95055>
- [102] Geesink, H.J. (2020) Proposed Informational Code of Biomolecules and Its Building Blocks-Quantum Coherence versus Decoherence. Project: Quantum Coherence in Animate and Non-Animate Systems.
- [103] Geesink, H.J.H., Jerman, I. and Meijer, D.K.F. (2019) Water: The Cradle of Life in Action, Cellular Architecture Is Guided by Coherent Quantum Frequencies as Revealed in Pure Water. Projects: Existence, Nature and Significance of Biological Field (the Biofield) Quantum Coherence in Animate and Non-Animate Systems.
- [104] Geesink, H., Meijer, D. and Jerman, I. (2020) Clay Minerals-Information Network Linking Quantum Coherence and First Life. Projects: The Origin of Organisms (Life, Living Process) Based on Long Range Long Term Dynamic Interfacial Water Structures Quantum Coherence in Animate and Non-Animate Systems.
- [105] Brueck, R.L. and Meijer, D.K.F. (2020) A New Premise for Quantum Physics, Consciousness and the Fabric of Reality. Project: The Information Universe. On the Missing Link in Concepts on the Architecture of Reality.
- [106] Meijer, D.K.F. (2019) The Anticipation of Afterlife as Based on Current Physics of Information. Project: The Information Universe. On the Missing Link in Concepts on the Architecture of Reality.
- [107] Milo, R. and Phillips, R. (2016) Cell Biology by the Numbers. Garland Science, New York. <https://doi.org/10.1201/9780429258770>
- [108] Donald, T.H. (2001) Biological Thermodynamics. Cambridge University Press, Cambridge, 37.
- [109] Garrett, G. (1995) Biochemistry. Saunders College Publishing, Philadelphia, 16.
- [110] Lodish, *et al.* (2000) Molecular Cell Biology. 4th Edition, W. H. Freeman, New York.
- [111] Geesink, H.J.H. and Meijer, D.K.F. (2020) Electromagnetic Frequency Patterns That Are Crucial for Health and Disease Reveal a Generalized Biophysical Principle: The GM Scale. *Quantum Biosystems*, **8**, 1-16.
- [112] Guo, W. and Feng, Q. (2019) Free Vibration Analysis of Arbitrary-Shaped Plates Based on the Improved Rayleigh-Ritz Method. *Advances in Civil Engineering*, **2019**, Article ID: 7041592. <https://doi.org/10.1155/2019/7041592>
- [113] Senjanivic, I., Tomic, M., Vladimir, N. and Cho, D.S. (2013) Analytical Solutions for Free Vibrations of a Moderately Thick Rectangular Plate. *Mathematical Problems in Engineering*, **2013**, Article ID: 207460. <https://doi.org/10.1155/2013/207460>
- [114] Geesink, H.J.H. and Meijer, D.K.F. (2017) Nature Unites First, Second and Third Harmonics to Organize Coherent Electromagnetic Frequency Patterns That Are Crucial for Health and Disease.

- <https://www.researchgate.net/publication/317003066>
- [115] Sonderkamp, T., Geesink, H.J.H. and Meijer, D.K.F. (2019) Statistical Analysis and Prospective Application of the GM-Scale, a Semi-Harmonic EMF Scale Proposed to Discriminate between “Coherent” and “Decoherent” EM Frequencies on Life Conditions. *Quantum Biosystems*, **12**, 33-51.
- [116] Costa, M., Goldberger, A.L. and Peng, C.K. (2002) Multiscale Entropy Analysis of Complex Physiologic Time Series. *Physical Review Letters*, **89**, 1-5. <https://doi.org/10.1103/PhysRevLett.89.068102>
- [117] Meijer, D.K.F. and Geesink, H.J.H. (2018) Favourable und Unfavourable EMF Frequency Patterns in Cancer: Perspectives for Improved Therapy and Prevention. *Journal of Cancer Therapy*, **9**, 188-230. <https://doi.org/10.4236/jct.2018.93019>
- [118] Pauri, M. (2003) Don't Ask Pythagoras about the Quantum. *Science & Education*, **12**, 467-477. <https://doi.org/10.1023/A:1025330129744>
- [119] Geesink, J.H. and Meijer, D.K.F. (2017) Bio-Soliton Model That Predicts Non-Thermal Electromagnetic Frequency Bands, That either Stabilize or Destabilize Living Cells. *Electromagnetic Biology and Medicine*, **36**, 357-378. <https://doi.org/10.1080/15368378.2017.1389752>
- [120] Geesink, H.J.H. and Meijer, D.K.F. (2017) Cancer Is Promoted by Cellular States of Electromagnetic Decoherence and can Be Corrected by Exposure to Coherent Non-Ionizing Electromagnetic Fields, a Physical Model about Cell-Sustaining and Cell-Decaying Soliton Eigen-Frequencies. https://www.researchgate.net/publication/316058728_Cancer_is_promoted_by_cellular_states_of_electromagnetic_decoherenceandcanbecorrectedbyexposureto coherentntnon-ionizingelectromagneticfields
- [121] Tsujita, K., Satow, R., Asada, S., Nakamura, Y., Arnes, L., Sako, K., Fujita, Y., Fukami, K. and Itoh, T. (2021) Homeostatic Membrane Tension Constrains Cancer Cell Dissemination by Counteracting BAR Protein Assembly. *Nature Communications*, **12**, Article No. 5930. <https://doi.org/10.1038/s41467-021-26156-4>
- [122] Csoboz, B., Balogh, G.E., Kusz, E., Gombos, I., Peter, M., Crul, T., Gungor, B., Haracska, L., Bogdanovics, G., Torok, Z., Horvath, I. and Vigh, L. (2013) Membrane Fluidity Matters: Hyperthermia from the Aspects of Lipids and Membranes. *International Journal of Hyperthermia*, **29**, 491-499. <https://doi.org/10.3109/02656736.2013.808765>
- [123] Galeotti, T., Borrello, S., Minotti, G. and Masotti, L. (1986) Membrane Alterations in Cancer Cells: The Role of Oxy Radicals. *Annals of the New York Academy of Sciences*, **488**, 468-480. <https://doi.org/10.1111/j.1749-6632.1986.tb46579.x>
- [124] Yang, M. and Brackenbury, W.J. (2013) Membrane Potential and Cancer Progression. *Frontiers in Physiology*, **4**, Article No. 185. <https://doi.org/10.3389/fphys.2013.00185>
- [125] Kadir, L.A., Stacey, M. and Barrett, J.R. (2018) Emerging Roles of the Membrane Potential: Action beyond the Action Potential. *Frontiers in Physiology*, **9**, Article No. 1661. <https://doi.org/10.3389/fphys.2018.01661>
- [126] Szentgyorgyi, A. (1968) Bioelectronics, a Study on Cellular Regulations, Defence and Cancer. Academic Press, New York, London.
- [127] Szentgyorgyi, A. (1998) Electronic Biology and Cancer. Marcel Dekker, New York.
- [128] Maroti, P., Berkes, L. and Tolgyesi, F. (1998) Biophysics Problems. Akademiai Kiado, Budapest.
- [129] Shashini, B., Ariyasu, S., Takeda, R., Suzuki, T., Shiina, S., Akimoto, K., *et al.* (2018) Size-Based Differentiation of Cancer and Normal Cells by a Particle Size Analyzer Assisted by a Cell-Recognition PC Software. *Biological and Pharmaceutical Bulletin*,

- 41, 478-503. <https://doi.org/10.1248/bpb.b17-00776>
- [130] Baba, A.I. and Catoi, C. (2007) Chapter 3. Tumor Cell Morphology. In: Buchares, R.O., Ed., *Comparative Oncology*, The Publishing House of the Romanian Academy, Bucharest. <https://www.ncbi.nlm.nih.gov/books/NBK9553/>
- [131] Lyons, S.M., Alizadeh, E., Mannheimer, J., Schuamberg, K., Castle, J., Schroder, B., *et al.* (2016) Changes in Cell Shape Are Correlated with Metastatic Potential in Murine and Human Osteosarcomas. *Biology Open*, **5**, 289-299. <https://doi.org/10.1242/bio.013409>
- [132] Pache, B. (2018) How Tumor-Specific Modulation Frequencies Were Discovered. *The Cancer Letter*, **44**, 24-29.
- [133] Barbault, A., Costa, F.P., Bottger, B., Munden, R.F., Bomholt, F., Kuster, N. and Pasche, B. (2009) Amplitude-Modulated Electromagnetic Fields for the Treatment of Cancer: Discovery of Tumor-Specific Frequencies and Assessment of a Novel Therapeutic Approach. *Journal of Experimental and Clinical Cancer Research*, **28**, 51. <https://doi.org/10.1186/1756-9966-28-51>
- [134] Jaminez, H., Blackman, C., Lesser, G., Debinski, W., Chan, M., Sharma, S., *et al.* (2018) Use of Non-Ionizing Electromagnetic Fields for the Treatment of Cancer. *Frontiers in Bioscience, Landmark*, **23**, 284-297. <https://doi.org/10.2741/4591>
- [135] Zimmerman, J.W., Jimenez, H., Pennison, M.J., Brezovich, I., Morgan, D., Mudry, A., *et al.* (2013) Targeted Treatment of Cancer with Radiofrequency Electromagnetic Fields Amplitude-Modulated at Tumor-Specific Frequencies. *Chinese Journal of Cancer*, **32**, 573-581. <https://doi.org/10.5732/cjc.013.10177>
- [136] Bose, D., Zimmerman, L.J., Pierobonn, M., Petricoin, E., Tozzi, F., Parikh, A., *et al.* (2011) Chemoresistant Colorectal Cancer Cells and Cancer Stem Cells Mediate Growth and Survival of Bystander Cells. *British Journal of Cancer*, **105**, 1759-1767. <https://doi.org/10.1038/bjc.2011.449>
- [137] Sharma, S., Wu, S.Y., Jimenez, H., Xing, F., Zhu, D., Liu, Y., *et al.* (2019) Ca²⁺ and CACNA1H Mediate Targeted Suppression of Breast Cancer Brain Metastasis by A? RF EMF. *EBioMedicine*, **44**, 194-208. <https://doi.org/10.1016/j.ebiom.2019.05.038>
- [138] Zimmerman, J.W., Pennison, M.J., Brezovich, I., Yi, N., Yang, C.T., Ramaker, R., *et al.* (2012) Cancer Cell Proliferation Is Inhibited by Specific Modulation Frequencies. *British Journal of Cancer*, **106**, 307-313. <https://doi.org/10.1038/bjc.2011.523>
- [139] Blackman, C.K. (2012) Treating Cancer with Amplitude-Modulated Electromagnetic Fields: A Potential Paradigm Shift, Again? *British Journal of Cancer*, **106**, 241-242. <https://doi.org/10.1038/bjc.2011.576>
- [140] Pasche, B. and Barbault, A. (2010) Electromagnetic System for Influencing Cellular Functions in a Warm-Blooded Mammalian Subject. Patent Nr. EP 2139557 B1. <https://patents.google.com/patent/EP2139557B1/en>
- [141] Costa, F.P., de Oliveira, A.C., Meirelles, R., Machado, M.C.C., Zanesco, T., Surjan, R., *et al.* (2011) Treatment of Advanced Hepatocellular Carcinoma with Very Low Levels of Amplitude-Modulated Electromagnetic Fields. *British Journal of Cancer*, **105**, 640-648. <https://doi.org/10.1038/bjc.2011.292>
- [142] Zimmermann, J.W., Pennison, M.J., Brezovich, I., Yi, N., Yang, C.T., Ramaker, R., *et al.* (2011) Cancer Cell Proliferation Is Inhibited by Specific Modulation Frequencies. *British Journal of Cancer*, 1-7.
- [143] Jimenez, H., Wang, M., Zimmerman, J.W., Pennison, M.J., Sharma, S., Surratt, T., *et al.* (2019) Tumour-Specific Amplitude-Modulated Radiofrequency Electromagnetic Fields Induce Differentiation of Hepatocellular Carcinoma via Targeting Ca_v3.2 T-Type Voltage-Gated Calcium Channels and Ca²⁺ Influx. *EBioMedicine*, **44**, 209-224. <https://doi.org/10.1016/j.ebiom.2019.05.034>

- [144] Hum, N.R., Sebastian, A., Gilmore, S.F., He, W., Martin, K.A., Hinckley, A., *et al.* (2020) Comparative Molecular Analysis of Cancer Behavior Cultured *in Vitro*, *In Vivo*, and *Ex Vivo*. *Cancers*, **12**, 690. <https://doi.org/10.3390/cancers12030690>
- [145] Fares, J., Fares, M.Y., Khachfe, H.H., *et al.* (2020) Molecular Principles of Metastasis: A Hallmark of Cancer Revisited. *Signal Transduction and Targeted Therapy*, **5**, Article No. 28. <https://doi.org/10.1038/s41392-020-0134-x>
- [146] de Loof, M., de Jong, S. and Kruyt, F.A.E. (2019) Multiple Interactions between Cancer Cells and the Tumor Microenvironment Modulate TRAIL Signaling: Implications for TRAIL Receptor Targeted Therapy. *Frontiers in Immunology*, **10**, Article No. 1530. <https://doi.org/10.3389/fimmu.2019.01530>
- [147] Pasche, B. and Barbault, A. (2007) A Study of Therapeutic Amplitude-Modulated Electromagnetic Fields in Advanced Tumors (THBC001). ClinicalTrials.gov, Identifier: NCT00440570.
- [148] Pasche, B. and Barbault, A. (2007) A Study of Electromagnetic Waves in the Treatment of the Advanced Hepatocarcinoma (THBC002). ClinicalTrials.gov, Identifier: NCT00440934.
- [149] Pasche, B. and Grant, S.C. (2014) Non-Small Cell Lung Cancer and Precision Medicine, a Model for the Incorporation of Genomic Features into Clinical Trial Design. *JAMA*, **311**, 1975-1976. <https://doi.org/10.1001/jama.2014.3742>
- [150] Anteneodo, C. and da Luz, M.G.E. (2010) Complex Dynamics of Life at Different Scales: From Genomic to Global Environmental Issues. *Philosophical Transactions of the Royal Society A*, **368**, 5561-5568. <https://doi.org/10.1098/rsta.2010.0286>
- [151] Deering, W. and West, B.J. (1992) Fractal Physiology. *IEEE Engineering in Medicine and Biology*, **11**, 40-46. <https://doi.org/10.1109/51.139035>
- [152] West, B.J. (1990) Fractal Physiology and Chaos in Medicine. World Scientific, Singapore, London. <https://doi.org/10.1142/1025>
- [153] Bassingthwaighte, J.B., Leibovitch, L.S. and West, B.J. (1994) Fractal Physiology. Oxford Univ. Press, New York, Oxford.
- [154] Goldberger, A.L., Amaral, L.A., Hausdorff, J.M., *et al.* (2002) Fractal Dynamics in Physiology: Alterations with Disease and Aging. *PNAS Colloquium*, **99**, 2466-2472. <https://doi.org/10.1073/pnas.012579499>
- [155] Szasz, A., Szasz, N. and Szasz, O. (2010) Oncothermia—Principles and Practices. Springer Science, Heidelberg. <https://doi.org/10.1007/978-90-481-9498-8>
- [156] Eskov, V.M., Filatova, O.E., Eskov, V.V., *et al.* (2017) The Evolution of the Idea of Homeostasis: Determinism, Stochastics, and Chaos—Self-Organization. *Biophysics*, **62**, 809-820. <https://doi.org/10.1134/S0006350917050074>
- [157] Billman, G.E. (2020) Homeostasis: The Underappreciated and Far Too Often Ignored Central Organizing Principle of Physiology. *Frontiers in Physiology*, **11**, Article No. 200. <https://doi.org/10.3389/fphys.2020.00200>
- [158] Lovelady, D.C., Richmond, T.C., Maggi, A.N., *et al.* (2007) Distinguishing Cancerous from Noncancerous Cells through Analysis of Electrical Noise. *Physical Review E*, **76**, Article ID: 041908. <https://doi.org/10.1103/PhysRevE.76.041908>
- [159] Potoyan, D.A. and Wolynes, P.G. (2014) On the Dephasing of Genetic Oscillators. *PNAS*, **111**, 2391-2396. <https://doi.org/10.1073/pnas.1323433111>
- [160] Ptitsyn, A.A., Zvonic, S. and Gimble, J.M. (2007) Digital Signal Processing Reveals Circadian Baseline Oscillation in Majority of Mammalian Genes. *PLOS Computational Biology*, **3**, e120. <https://doi.org/10.1371/journal.pcbi.0030120>
- [161] Wang, Y., Wang, X., Wohland, T. and Sampath, K. (2016) Extracellular Interactions

- and Ligand Degradation Shape the Nodal Morphogen Gradient. *ELife*, **5**, e13879. <https://doi.org/10.7554/eLife.13879>
- [162] Cramer, F. (1995) Chaos and Order (The Complex Structure of Living Systems). VCH, Weinheim.
- [163] Peng, C.K., Buldyrev, S.V., Hausdorff, J.M., *et al.* (1994) Fractals in Biology and Medicine: From DNA to the Heartbeat. In: Bunde, A. and Havlin, S., Eds., *Fractals in Science*, Springer-Verlag, Berlin, 49-87. https://doi.org/10.1007/978-3-662-11777-4_3
- [164] Bak, P., Tang, C. and Wiesenfeld, K. (1988) Self-Organized Criticality. *Physical Review A*, **38**, 364-374. <https://doi.org/10.1103/PhysRevA.38.364>
- [165] Musha, T. and Sawada, Y. (1994) Physics of the Living State. IOS Press, Amsterdam.
- [166] Szendro, P., Vincze, G. and Szasz, A. (2001) Bio-Response on White-Noise Excitation. *Electromagnetic Biology and Medicine*, **20**, 215-229. <https://doi.org/10.1081/JBC-100104145>
- [167] Szendro, P., Vincze, G. and Szasz, A. (2001) Pink-Noise Behaviour of Biosystems. *European Biophysics Journal*, **30**, 227-231. <https://doi.org/10.1007/s002490100143>
- [168] Ho, M.W., Popp, F.A. and Warnke, U. (1994) Bioelectrodynamics and Biocommunication. World Scientific, Singapore. <https://doi.org/10.1142/2267>
- [169] Bernardi, P. and D'Inzeo, G. (1989). Physical Mechanisms for Electromagnetic Interaction with Biological Systems. In: Lin, J.C., Ed., *Electromagnetic Interaction with Biological Systems*, Plenum Press, New York, 179-214. https://doi.org/10.1007/978-1-4684-8059-7_9
- [170] Markov, M.S. (1994) Biological Effects of Extremely Low Frequency Magnetic Fields. In: Ueno, S., Ed., *Biomagnetic Stimulation*, Plenum Press, New York, 91-104. https://doi.org/10.1007/978-1-4757-9507-3_7
- [171] Bauerus, Koch, C.L.M., Sommarin, M., Persson, B.R.R., Salford, L.G. and Eberhardt, J.L. (2003) Interaction between Weak Low Frequency Magnetic Fields and Cell Membranes. *Bioelectromagnetics*, **24**, 395-402. <https://doi.org/10.1002/bem.10136>
- [172] Blackman, C.F., Benane, S.G. and House, D.E. (2001) The Influence of 1.2 μ T, 60 Hz Magnetic Fields on Melatonin- and Tamoxifeninduced Inhibition of MCF-7 Cell Growth. *Bioelectromagnetics*, **22**, 122-128. [https://doi.org/10.1002/1521-186X\(200102\)22:2<122::AID-BEM1015>3.0.CO;2-V](https://doi.org/10.1002/1521-186X(200102)22:2<122::AID-BEM1015>3.0.CO;2-V)
- [173] Weaver, J.C. and Astumian, R.D. (1990) The Response of Living Cells to Very Weak Electric Fields: The Thermal Noise Limit. *Science*, **247**, 459-462. <https://doi.org/10.1126/science.2300806>
- [174] Adair, R.K. (1991) Constraints on Biological Effects of Weak Extremely-Low Frequency Electromagnetic Fields. *Physical Review A*, **43**, 1039-1048. <https://doi.org/10.1103/PhysRevA.43.1039>
- [175] White, D.C. and Woodson, H.H. (1959) Electromechanical Energy Conversion. John Wiley & Sons, New York.
- [176] Vincze, Gy., Szasz, A. and Szasz, N. (2005) On the Thermal Noise Limit of Cellular Membranes. *Bioelectromagnetics*, **26**, 28-35. <https://doi.org/10.1002/bem.20051>
- [177] Bier, M. (2005) Gauging the Strength of Power Frequency Fields against Membrane Electrical Noise. *Bioelectromagnetics*, **26**, 595-609. <https://doi.org/10.1002/bem.20148>
- [178] Szasz, A. (2019) Thermal and Nonthermal Effects of Radiofrequency on Living State and Applications as an Adjuvant with Radiation Therapy. *Journal of Radiation and*

- Cancer Research*, **10**, 1-17. https://doi.org/10.4103/jrcr.jrcr_25_18
- [179] Ferenczy, G.L. and Szasz, A. (2020) Ch. 3. Technical Challenges and Proposals in Oncological Hyperthermia. In: Szasz, A., Ed., *Challenges and Solutions of Oncological Hyperthermia*, Cambridge Scholars, Newcastle upon Tyne, 72-90.
- [180] Lee, S.Y., Fiorentini, G., Szasz, A.M., Szigeti, Gy., Szasz, A. and Minnaar, C.A. (2020) Quo Vadis Oncological Hyperthermia (2020)? *Frontiers in Oncology*, **10**, Article No. 1690. <https://doi.org/10.3389/fonc.2020.01690>
- [181] Szasz, A., Vincze, Gy., Szasz, O. and Szasz, N. (2003) An Energy Analysis of Extracellular Hyperthermia. *Magneto- and Electro-Biology*, **22**, 103-115. <https://doi.org/10.1081/JBC-120024620>
- [182] Anishchenko, V.S., Neiman, A.B., Moss, F. and Schimansky-Geier, L. (1999) Stochastic Resonance: Noise-Enhanced Order. *Physics-Uspekhi*, **42**, 7-36. <https://doi.org/10.1070/PU1999v042n01ABEH000444>
- [183] Szasz, A. (1991) An Electronically Driven Instability: The Living State. *Physiological Chemistry and Physics and Medical NMR*, **23**, 43-50.
- [184] Gingl, Z., Makra, P. and Vajtai, R. (2001) High Signal-to-Noise Ratio Gain by Stochastic Resonance in a Double Well. *Fluctuation and Noise Letters*, **1**, L181-L188. <https://doi.org/10.1142/S0219477501000408>
- [185] Szendro, P., Vincze, Gy. and Szasz, A. (1999) Response of Bio-Systems on White Noise Excitation. *Hungarian Agricultural Engineering*, **12**, 31-32.
- [186] Szendro, P., Vincze, Gy. and Szasz, A. (1998) Origin of Pink-Noise in Bio-Systems. *Hungarian Agricultural Engineering*, **11**, 42-43.
- [187] Ma, J., Xiao, T., Hou, Z. and Xin, H. (2008) Coherence Resonance Induced by Colored Noise near Hopf Bifurcation. *Chaos*, **18**, Article ID: 043116. <https://doi.org/10.1063/1.3013178>
- [188] Bybiec, B. and Gudowska-Nowak, E. (2013) Resonant Activation Driven by Strongly Non-Gaussian Noises.
- [189] Revelli, J.A., Sanchez, A.D. and Wio, H.S. (2001) Effect of Non Gaussian Noises on the Stochastic Resonance-Like Phenomenon in Gated Traps.
- [190] Rosso, O.A. and Masoller, C. (2009) Detecting and Quantifying Stochastic and Coherence Resonances via Information-Theory Complexity Measurements. *Physical Review E*, **79**, 040106(R). <https://doi.org/10.1103/PhysRevE.79.040106>
- [191] Krauss, P., Metzner, C., Schilling, A., Schütz, C., Tziridis, K., Fabry, B. and Schulze, H. (2017) Adaptive Stochastic Resonance for Unknown and Variable Input Signals. *Scientific Reports*, **7**, Article No. 2450. <https://doi.org/10.1038/s41598-017-02644-w>
- [192] Krauss, P., Tziridis, K., Metzner, C., Schilling, A., Hoppe, U. and Schulze, H. (2016) Stochastic Resonance Controlled Upregulation of Internal Noise after Hearing Loss as a Putative Cause of Tinnitus-Related Neuronal Hyperactivity, Hypothesis and Theory. *Frontiers in Neuroscience*, **10**, Article No. 597. <https://doi.org/10.3389/fnins.2016.00597>
- [193] West, G.B. and Brown, J.H. (2005) The Origin of Allometric Scaling Laws in Biology from Genomes to Ecosystems: Towards a Quantitative Unifying Theory of Biological Structure and Organization. *Journal of Experimental Biology*, **208**, 1575-1592. <https://doi.org/10.1242/jeb.01589>
- [194] Trigoso, A.S., Pearson, R.B., Paenfuss, A.T., et al. (2018) How the Evolution of Multicellularity Set the Stage for Cancer. *British Journal of Cancer*, **118**, 145-152. <https://doi.org/10.1038/bjc.2017.398>
- [195] Alfarouk, K.O., Shayoub, M.E.A., Muddathir, A.K., Elhassan, G.O. and Bashir,

- A.H.H. (2011) Evolution of Tumour Metabolism Might Reflect Carcinogenesis as a Reverse Evolution Process (Dismantling of Multicellularity). *Cancers*, **3**, 3002-3017. <https://doi.org/10.3390/cancers3033002>
- [196] Szentgyorgyi, A. (1978) *The Living State and Cancer*. Marcel Dekker Inc., New York.
- [197] Lineweaver, C.H., Bussey, K.J., Blackburn, A.C. and Davies, P.C.W. (2021) Cancer Progression as a Sequence of Atavistic Reversions. *BioEssays*, **43**, Article ID: 2000305. <https://doi.org/10.1002/bies.202000305>
- [198] Lineweaver, C.H., Davies, P.C.W. and Vincent, M.D. (2014) Targeting Cancer's Weaknesses (Not Its Strengths): Therapeutic Strategies Suggested by the Atavistic Model. *Bioessays*, **36**, 827-835. <https://doi.org/10.1002/bies.201400070>
- [199] Eyring, H. (1935) The Activated Complex in Chemical Reactions. *The Journal of Chemical Physics*, **3**, 107-115. <https://doi.org/10.1063/1.1749604>
- [200] Michaelis, L. and Menten, M.L. (1913) Die Kinetik der Invertinwirkung. *Biochemische Zeitschrift*, **49**, 333-369. <https://doi.org/10.1021/bi201284u>
- [201] Hele, T.J.H. (2014) Quantum Transition-State Theory. Dissertation.
- [202] Evans, M.G. and Polanyi, M. (1935) Some Applications of the Transition State Method to the Calculation of Reaction Velocities, Especially in Solution. *Transactions of the Faraday Society*, **31**, 875-894. <https://doi.org/10.1039/tf9353100875>
- [203] Tsong, T.Y. and Chang, C.H. (2007) A Markovian Engine for a Biological Energy Transducer: The Catalytic Wheel. *BioSystems*, **88**, 323-333. <https://doi.org/10.1016/j.biosystems.2006.08.014>
- [204] Savageau, M.A. (1998) Development of Fractal Kinetic Theory for Enzyme-Catalysed Reactions and Implications for the Design of Biochemical Pathways. *Biosystems*, **47**, 9-36. [https://doi.org/10.1016/S0303-2647\(98\)00020-3](https://doi.org/10.1016/S0303-2647(98)00020-3)
- [205] Bezrukov, S.M. and Vodyanoy, I. (1997) Stochastic Resonance at the Single-Cell Level. *Nature*, **388**, 632-633. <https://doi.org/10.1038/41684>
- [206] Pearce, J.A. (2013) Comparative Analysis of Mathematical Models of Cell Death and Thermal Damage Processes. *International Journal of Hyperthermia*, **29**, 262-280. <https://doi.org/10.3109/02656736.2013.786140>
- [207] Vincze, Gy., Szasz, O. and Szasz, A. (2015) Generalization of the Thermal Dose of Hyperthermia in Oncology. *Open Journal of Biophysics*, **5**, 97-114. <https://doi.org/10.4236/ojbiphy.2015.54009>
- [208] O'Neill, D.P., Peng, T., Stiegler, P., Mayrhauser, U., Koestenbauer, S., Tscheliessnigg, K., *et al.* (2011) A Three-State Mathematical Model of Hyperthermic Cell Death. *Annals of Biomedical Engineering*, **39**, 570-579. <https://doi.org/10.1007/s10439-010-0177-1>
- [209] Vincze, Gy. and Szasz, A. (2018) Similarities of Modulation by Temperature and by Electric Field. *Ojbiphy*, **8**, 95-103. <https://doi.org/10.4236/ojbiphy.2018.83008>
- [210] Thompson, W.H. (1999) Quantum Mechanical Transition State Theory and Tunneling Corrections. *The Journal of Chemical Physics*, **110**, 4221-4228. <https://doi.org/10.1063/1.478304>
- [211] Tsong, T.Y. and Astumian, R.D. (1988) Electroconformational Coupling: How Membrane-Bound ATPase Transduces Energy from Dynamic Electric Fields. *Annual Review of Physiology*, **50**, 273-290. <https://doi.org/10.1146/annurev.ph.50.030188.001421>
- [212] Astumian, R.D. (1994) Electroconformational Coupling of Membrane Proteins. *Annals of the New York Academy of Sciences*, **720**, 136-140. <https://doi.org/10.1111/j.1749-6632.1994.tb30441.x>

- [213] Markin, V.S., Liu, D., Rosenberg, M.D. *et al.* (1992) Resonance Transduction of Low Level Periodic Signals by an Enzyme: An Oscillatory Activation Barrier Model. *Biophysical Journal*, **61**, 1045-1049. [https://doi.org/10.1016/S0006-3495\(92\)81913-6](https://doi.org/10.1016/S0006-3495(92)81913-6)
- [214] McNamara, B. and Wiesenfeld, K. (1989) Theory of Stochastic Resonance. *Physical Review A*, **39**, 4854-4869. <https://doi.org/10.1103/PhysRevA.39.4854>
- [215] Astumian, R.D. (1997) Thermodynamics and Kinetics of a Brownian Motor. *Science*, **276**, 917-922. <https://doi.org/10.1126/science.276.5314.917>
- [216] Astumian, R.D. and Bier, M. (1994) Fluctuation Driven Ratchets: Molecular Motors. *Physical Review Letters*, **72**, 1766-1769. <https://doi.org/10.1103/PhysRevLett.72.1766>
- [217] Chock, P.B., Tsong, T.Y., *et al.* (1987) Can Free Energy Be Transduced from Noise? *Proceedings of the National Academy of Sciences of the United States of America*, **84**, 434-438. <https://doi.org/10.1073/pnas.84.2.434>
- [218] Astumian, R.D. and Derényi, I. (1998) Fluctuation Driven Transport and Models of Molecular Motors and Pumps. *European Biophysics Journal*, **27**, 474-489. <https://doi.org/10.1007/s002490050158>
- [219] Linke, H., Downton, M.T. and Zuckermann, M.J. (2005) Performance Characteristics of Brownian Motors. *Chaos*, **15**, Article ID: 026111. <https://doi.org/10.1063/1.1871432>
- [220] Tinoco, I., Sauer, K., Wang, J.C., *et al.* (2002) *Physical Chemistry. Principles and Applications in Biological Sciences*. 4th Edition, Prentice-Hall Inc., Hoboken.
- [221] Astumian, R.D. and Chock, P.B. (1989) Effects of Oscillations and Energy-Driven Fluctuations on the Dynamics of Enzyme Catalysis and Free-Energy Transduction. *Physical Review A*, **39**, 6416-6435. <https://doi.org/10.1103/PhysRevA.39.6416>
- [222] Babbi, G., Baldazzi, D., Savojardo, C., Luigi, M.P. and Casadio, R. (2020) Highlighting Human Enzymes Active in Different Metabolic Pathways and Diseases: The Case Study of EC 1.2.3.1 and EC 2.3.1.9. *Biomedicines*, **8**, 250. <https://doi.org/10.3390/biomedicines8080250>
- [223] Romero, P., Wagg, J., Green, M.L., Daiser, D., Krummenacker, M. and Karp, P.D. (2005) Computational Prediction of Human Metabolic Pathways from the Complete Human Genome. *Genome Biology*, **6**, R2. <https://doi.org/10.1186/gb-2004-6-1-r2>
- [224] McDonnell, M. and Abbott, D. (2009) What Is Stochastic Resonance? Definitions, Misconceptions, Debates, and Its Relevance to Biology. *PLOS Computational Biology*, **5**, e1000348. <https://doi.org/10.1371/journal.pcbi.1000348>
- [225] Szasz, A. and Szasz, O. (2020) Ch. 17. Time-Fractal Modulation of Modulated Electro-Hyperthermia (mEHT). In: Szasz, A., Ed., *Challenges and Solutions of Oncological Hyperthermia*, Cambridge Scholars, Newcastle upon Tyne, 377-415.
- [226] Szasz, A. (2021) Therapeutic Basis of Electromagnetic Resonances and Signal Modulation. *Open Journal of Biophysics*, **11**, 314-350. <https://doi.org/10.4236/ojbiphy.2021.113011>
- [227] Szasz, A. (2022) Time-Fractal Modulation—Possible Modulation Effects in Human Therapy. *Open Journal of Biophysics*, **12**, 38-87. <https://doi.org/10.4236/ojbiphy.2022.121003>
- [228] Calabro, E. and Magazu, S. (2020) New Perspectives in the Treatment of Tumor Cells by Electromagnetic Radiation at Resonance Frequencies in Cellular Membrane Channels. *The Open Biotechnology Journal*, **13**, 105-110. <https://doi.org/10.2174/187407070190130105>

- [229] Hanggi, P., Schmid, G. and Goychuk, I. (2002) Excitable Membranes: Channel Noise, Synchronization, and Stochastic Resonance. In: Kramer, B., Ed., *Advances in Solid State Physics*, Vol. 42, Springer-Verlag, Berlin, 359-370.
https://doi.org/10.1007/3-540-45618-X_28
- [230] Szasz, O., Szasz, A.M. Minnaar, C. and Szasz, A. (2017) Heating Preciosity—Trends in Modern Oncological Hyperthermia. *Open Journal of Biophysics*, **7**, 116-144.
<https://doi.org/10.4236/ojbiphy.2017.73010>
- [231] Szasz, O. and Szasz, A. (2014) Oncothermia—Nano-Heating Paradigm. *Journal of Cancer Science and Therapy*, **6**, 117-121.
<https://doi.org/10.4172/1948-5956.1000259>
- [232] Szasz, A. (2013) Chapter 4. Electromagnetic Effects in Nanoscale Range. In: Shimizu, T. and Kondo, T., Eds., *Cellular Response to Physical Stress and Therapeutic Applications*, Nova Science Publishers, Inc., Hauppauge, 55-81.
- [233] Foleti, A., Grimaldi, S., Lisi, A., Ledda, M. and Liboff, A.R. (2013) Bioelectromagnetic Medicine: The Role of Resonance Signaling. *Electromagnetic Biology and Medicine*, **32**, 484-499.
- [234] Lucia, U., Grisolia, G., Ponzetto, A., Bergandi, L. and Silvagno, F. (2020) Thermomagnetic Resonance Affects Cancer Growth and Motility. *Royal Society Open Science*, **7**, Article ID: 200299. <https://doi.org/10.1098/rsos.200299>
- [235] Sahu, S., Ghosh, S., Fujita, D. and Bandyopadhyay, A. (2014) Live Visualizations of Single Isolated Tubulin Protein Self-Assembly via Tunneling Current: Effect of Electromagnetic Pumping during Spontaneous Growth of Microtubule. *Scientific Reports*, **4**, Article No. 7303. <https://doi.org/10.1038/srep07303>
- [236] Liboff, A.R. (1997) Electric-Field Ion Cyclotron Resonance. *Bioelectromagnetics*, **18**, 85-87.
[https://doi.org/10.1002/\(SICI\)1521-186X\(1997\)18:1<85::AID-BEM13>3.0.CO;2-P](https://doi.org/10.1002/(SICI)1521-186X(1997)18:1<85::AID-BEM13>3.0.CO;2-P)
- [237] Liboff, A.R. (2012) Electromagnetic Vaccination. *Medical Hypotheses*, **79**, 331-333.
<https://doi.org/10.1016/j.mehy.2012.05.027>
- [238] Krenacs, T., Meggyeshazi, N., Forika, G., *et al.* (2020) Modulated Electro-Hyperthermia-Induced Tumor Damage Mechanisms Revealed in Cancer Models. *International Journal of Molecular Sciences*, **21**, Article No. 6270.
<https://doi.org/10.3390/ijms21176270>
- [239] Chi, M.S., Mehta, M.P., Yang, K.L., *et al.* (2020) Putative Abscopal Effect in Three Patients Treated by Combined Radiotherapy and Modulated Electrohyperthermia. *Frontiers in Oncology*, **10**, Article No. 254. <https://doi.org/10.3389/fonc.2020.00254>
- [240] Minnaar, C.A., Kotzen, J.A., Ayeni, O.A., *et al.* (2020) Potentiation of the Abscopal Effect by Modulated Electro-Hyperthermia in Locally Advanced Cervical Cancer Patients. *Frontiers in Oncology*, **10**, Article No. 376.
<https://doi.org/10.3389/fonc.2020.00376>
- [241] Chi, K.H. (2020) Tumour-Directed Immunotherapy: Clinical Results of Radiotherapy with Modulated Electro-Hyperthermia. In: Szasz, A., Ed., *Challenges and Solutions of Oncological Hyperthermia*, Cambridge Scholars, Newcastle upon Tyne, 206-226.
- [242] Schirmmacher, V., Lorenzen, D., Van, Gool, S.W., *et al.* (2017) A New Strategy of Cancer Immunotherapy Combining Hyperthermia/Oncolytic Virus Pretreatment with Specific Autologous Anti-Tumor Vaccination—A Review. *Austin Oncology Case Reports*, **2**, 1-8. <https://doi.org/10.26420/austinoncolcaserep.1006.2017>

ISFET Based Immunosensor

Ferdinand Gasparyan^{1,2}, Lusine Gasparyan², Vahan Simonyan²

¹Yerevan State University, Yerevan, Armenia

²DNA-HIVE LLC, Rockville, MD, USA

Email: fgaspar@ysu.am

How to cite this paper: Gasparyan, F., Gasparyan, L. and Simonyan, V. (2022) ISFET Based Immunosensor. *Open Journal of Biophysics*, 12, 223-233.
<https://doi.org/10.4236/ojbiphy.2022.124010>

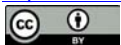
Received: September 17, 2022

Accepted: October 22, 2022

Published: October 25, 2022

Copyright © 2022 by author(s) and Scientific Research Publishing Inc. This work is licensed under the Creative Commons Attribution International License (CC BY 4.0).

<http://creativecommons.org/licenses/by/4.0/>



Open Access

Abstract

A new design of an immunosensor for viral molecules based on the ISFET nanoscale structure has been proposed. Physical processes take place in immunosensor are modeled. The effect of modulation of the surface potential of the interface between a semiconductor depleted layer (channel) and a dielectric during the interaction and immobilization of viral molecules was used. Analytical expression for the source-drain current of ISFET as a function of virus types and concentration is presented and analyzed. Dependency of the source-drain current vs. concentration of viruses is analyzed for the COVID-19 virus.

Keywords

Biosensor, ISFET, Antibody, Virus, Sensitivity

1. Introduction

The threat to global health from viral infections, such as COVID-19, influenza, HIV, hepatitis, Zika, Ebola, etc., has brought into sharp focus the need for rapid, sensitive and selective detection of viruses as well as post-infection antibodies. To solve this problem, devices based on field-effect transistors (FETs) are widely used. In the field of chemical and bio-sensorics, ion-selective field-effect transistors (ISFETs) are used. Invented in 1970 by Piet Bergveld, the ISFET was the first FET based biosensor (BioFET) [1]. The ISFET has now become the basic building block of modern sensor technology [2]. In recent years there has been great progress in applying FET-type biosensors for highly sensitive biological detection. Among them, the ISFET and its latest architectures are the most intriguing approaches in electrical biosensor technology [3].

The electrical sensitivity of the ISFET is totally controlled by the properties of electrolyte, oxide, semiconductor and oxide-electrolyte interface state. Much at-

tention is being paid to the development of semiconductor-based biosensors due to the many advantages they offer, including high sensitivity, faster response times, miniaturization, and low cost manufacturing for rapid biospecific analysis with reusable features. Many devices have been developed for monitoring biological processes, such as nucleic acid hybridization, protein-protein interaction, antigen-antibody bonds, DNA-gold electrode nucleotide bonds, substrate-enzyme reactions, etc.

The Immunologically sensitive FETs (ImFETs) represent the amalgamation of the technologies of solid-state electronics and immunodiagnosics. The immunosensors are fabricated by immobilizing immunoagent, preferably, antibody on the gate region of an ISFET. The unique ISFET transduction mechanism could, in principle, be made possible for detection of a wide array of analytes, ranging from small biomolecules to bacteria. There have been several studies describing the application of ISFET as the ImFET [4]. ImFETs have been developed for the detection and quantification of β -bungarotoxin (β -BuTx) [5], the 85 B antigen complex (Ag85B) [6], and for the detection of the TNF- α protein [7]. Also known biosensors based on nanostructures [8] [9] [10] [11] an extended gate FET (EGFET) [12] [13], and organic electrochemical transistors (OECTs) [14].

Some electrophysical properties of BioFET sensors have also been studied in detail by us [15] [16].

A detailed analysis of the experimental and theoretical works devoted to the study of the various types of ISFET-based immunosensors showed:

- ✓ There are no detailed analytical studies of electrophysical and kinetic processes occurring in the solid part (semiconductor, insulator/oxide), aqueous solution and interfaces (electrolyte-insulator, insulator-semiconductor) of ISFET-based biosensors of various architectures. Accordingly, no specific analytical formulas are proposed that describe the dependence of the signal current on the electrical and geometric parameters of the semiconductor, the oxide layer (layers), the number of foreign particles and molecules in aqueous solution and the state of the interfaces.
- ✓ There are no analytical dependences on the type, charge state, size and concentration of analytes or viruses in aqueous solution.

The purpose of this article is to theoretically model and analyze the physical processes occurring in ISFET-based immunosensors, determine the dependence of the source-drain current on the type and concentration of the unknown viruses in an aqueous solution, analyze the sensitivity of such sensors to the presence of various viruses, propose new solutions, new opportunities and expand areas of application of ISFET-based immunosensors.

2. Physical Processes in the ISFET Based Immunosensors

To study the source-drain current (as an information signal) of the ISFET immunosensor and its sensitivity to the presence of foreign molecules and various viruses in an aqueous solution, it is necessary to consider the physical processes

occurring, in particular, at the interface between the gate insulator of the ISFET and the aqueous solution. It is clear that it is on this interface that antibodies and the corresponding virus molecules associated with them will be immobilized. The main design and physical processes taking place in the ISFET immunosensor for molecules and viruses detection are sketched in **Figure 1**. It is presented a schematic representation of proposed ISFET-based immunosensor (a), one separate sensitive “line” (array) in the form of ISFET line, distribution of the applied gatepotential V_g over the layered structure (b), and energetic band diagram picture of the electrolyte-insulator-semiconductor (EIS) structure (c). Particularly silicon based structures and silicon dioxide as a insulator will be discussed. In **Figure 1** RE is the reference electrode, V_g is the applied gate voltage, φ_{Si} , φ_{ch} , φ_{ox} , φ_{Ab} , φ_V and φ_{dl} are potentials on the silicon substrate, current channel (semiconductor depletion layer), oxide layer, antibody layer, virus molecules layer and double layer¹, correspondingly.

The balance equation for the potentials according to **Figure 1** can be represented as:

$$V_g = \varphi_{Si} + \varphi_{ch} + \varphi_{ox} + \varphi_{cl}. \quad (1)$$

To estimate these potentials as well as the threshold voltage, V_{th} , and flat-band voltage, V_{FB} , we can use the following relations [17] [18] [19] [20] [21]:

$$\begin{aligned} V_{th} &= V_{FB} + 2\varphi_F + \varphi_{ch}, V_{FB} = \varphi_{bs} - \varphi_{ch} + \varphi_{cl} + \varphi_{ox} - \frac{\Phi_{Si} - \Phi_{ox}}{e}, \\ \varphi_{cl} &= \varphi_{dl} + \varphi_{Ab} + \varphi_V, \varphi_{bs} \approx 0, \varphi_{Si} \approx 0, \varphi_F = 2\varphi_T \ln \frac{N_A}{n_i}, \\ \varphi_{ch} &= \sqrt{\frac{4e\varepsilon_0\varepsilon_{Si}N_A\varphi_T}{C_{ox}^2}}, \varphi_T = \frac{k_B T}{e}, \varphi_{dl} = 2\varphi_T \left(\frac{\varepsilon_w}{\varepsilon_r} \frac{N_{sol}}{K_{AK}^+ + H_s^+} \right), \\ \varphi_{ox} &= \frac{Q_{ox}}{C_{ox}} = \frac{eN_t d_{ox}}{\varepsilon\varepsilon_{ox}}, \varphi_{Ab} = \frac{eN_{Ab} d_{Ab}}{\varepsilon_0\varepsilon_{Ab}}, \varphi_V = \frac{eN_V d_V}{\varepsilon_0\varepsilon_V}. \end{aligned} \quad (2)$$

In the above expressions e is the elementary charge, k_B is the Boltzmann's constant, T is the absolute temperature, φ_T is the thermal voltage, φ_F is the Fermi potential, φ_{bs} and φ_{Si} are the electric potentials of the bulk solution and the bulk silicon substrate (they usually have very low values, and in what follows we take them as zero), φ_{dl} , φ_{Ab} and φ_V are the potential drop on the double layer, layers of antibody and virus molecules, correspondingly, Φ_{Si} and Φ_{ox} are the work functions of silicon and silicon dioxide (SiO_2), Q_{ox} is the oxide layer charge per unit area, C_{ox} is the capacitances of the oxide layer per unit area, ε_0 , ε_{Si} , ε_{ox} , ε_w , ε_r , ε_{Ab} and ε_V are the dielectric permittivity

¹A double layer is a structure that appears on the surface of a SiO_2 when it is exposed to an aqueous solution. The double layer refers to two parallel layers of charge surrounding the SiO_2 . The first layer, the surface charge (either positive or negative), consists of ions adsorbed onto the SiO_2 due to chemical interactions. The second layer is composed of ions attracted to the surface charge via the Coulomb force, electrically screening the first layer. This second layer is loosely associated with the SiO_2 . It is made of free ions that move in the aqueous solution under the influence of electric attraction and thermal motion rather than being firmly anchored. It is thus called the “diffuse layer”.

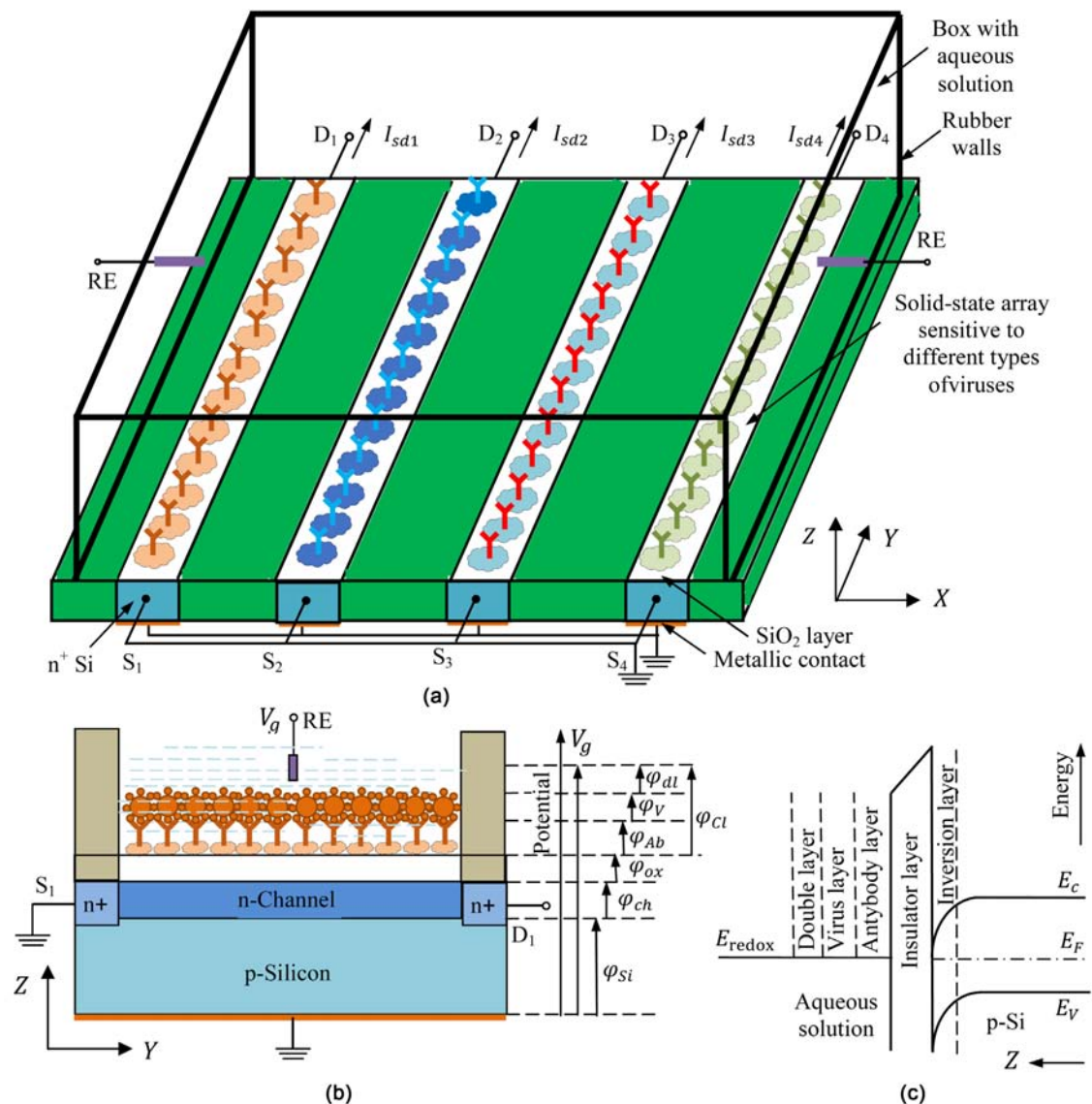


Figure 1. (a) Schematic picture of proposed ISFET based immunosensor for identification and characterization of 4 different viruses and the coordinate system to use. (b) One separate sensitive line (array) and distribution of the applied gate voltage V_g . (c) Energetic band diagram picture of the structure under study. S_1 - S_4 and D_1 - D_4 are source and drain electrodes, correspondingly, I_{sd1} - I_{sd4} are source-drain currents from 4 separate arrays, correspondingly, E_c , E_v and E_F are conduction, valence and Fermi equilibrium energy levels, correspondingly.

of free space, Si, SiO₂, water, electrolyte, antibody and viruses, respectively, N_A is the doping acceptor concentration in p-Si substrate, n_i is the intrinsic carrier concentration in bulk Si, K_{AK}^+ is the molar concentration of the cations in the aqueous solution, H_s^+ is the molar concentration of the hydrogen ions at the oxide surface, N_{sol} is the molar concentration of the aqueous solution, N_t , N_{Ab} and N_v are the concentrations of free electronic bonds (traps), antibody and virus molecules on a unit surface area of the oxide layer, correspondingly, d_{ox} , d_{Ab} and d_v are thicknesses of the oxide and antibody layers, and virus diameter, correspondingly. The redox potential E_{redox} is a measure of the ease with which a molecule accepts electrons, and the double layer in solution con-

sists of Inner Helmholtz layer (IHL), Outer Helmholtz layer (OHL) and Gouy-Chapman layer (GCL) [22].

The main physical processes occur in the conductive inversion channel. Therefore, for further calculations, it is necessary to determine the surface potential of the interface between the semiconductor depletion layer (channel) and insulator φ_{ch} . It can be calculated using the method proposed in [23]. For the channel surface potential we have following expression:

$$\varphi_{ch} = \varphi_T \ln \left(\frac{\eta C_{ox} \varphi_T N_A}{e t n_i^2} \right) + \varphi_T \ln \left\{ \ln \left[1 + \frac{1}{2} \exp \left(\frac{V_g - V_{th}}{\eta \varphi_T} \right) \right] \right\}. \quad (3)$$

Here

$$\eta = 1 + \frac{C_d}{C_{ox}} \approx 1 + \sqrt{\frac{q \varepsilon_0 \varepsilon_{si} N_A}{2 \varphi_T C_{ox}^2}}$$

is the factor of the field-effect transistor non-ideality (C_d is the capacitance of the silicon depletion layer per unit area, **Figure 1**).

3. Source-Drain Current

We consider the case of an inversion n-channel liquid-gated FET (**Figure 1(c)**). It is clear that the majority of processes in the structure are therefore determined by the electrons. The channel source-drain current consists of drift and diffusion components. It is well known that the diffusion component is dominant in the sub-threshold mode and the drift component is dominant in the over-threshold region. The channel source-drain current in Y direction $I_{sd}(y)$ can be calculated using the method of calculating the source-drain current proposed in [23]. For simplicity assuming $\eta \approx 1$ and taking account that oxide layer capacitance for unit area

$$C_{ox} = \frac{\varepsilon_0 \varepsilon_{ox}}{d_{ox}}, \quad (4)$$

and applying the results of [23] to our case, the current can be represented as follows:

$$I_{sd}(V_{ds}) \approx q w n_0 V_{sd} \frac{t}{l} \left[\mu_0 - \theta(V_g + V_{th}) \right] \left\{ 1 + \frac{l_s}{t} \left[\frac{e t^2 n_i^2}{\varepsilon_0 \varepsilon_{ox} \varphi_T N_A} + \ln \left(\frac{\varphi_T \varepsilon_0 \varepsilon_{ox} N_A}{q t^2 n_i^2} \right) \right] \right. \\ \left. + \ln \left[\ln \left(1 + \frac{1}{2} \exp \left(\frac{V_g + V_{th}}{\varphi_T} \right) \right) \right] \right\} \left(1 - e^{-t/l_s} \right) \quad (5)$$

Here

$$l_s = \frac{L_D}{1 + p_0/n_0}, \quad L_D = \sqrt{\frac{\varepsilon_0 \varepsilon_{si} \varphi_T}{q n_0}}, \quad (6)$$

V_{sd} is the source-drain voltage, w , l and t are the inversion channel width, length and thickness, correspondingly, L_D is the Debye screening length, n_0 and p_0 are the concentrations of the equilibrium electrons and holes. The

electron's mobility dependence on the transversal electric field (Y direction) at the applied gate voltage was taken into account using the following empiric equation [24]:

$$\left(\mu_{ef}\right)_x = \mu_0 - \theta(V_{th} + V_g), \quad (7)$$

where μ_0 is the low-field magnitude of the mobility, θ is the coefficient taken as $28 \text{ cm}^2/(\text{Vs})$ [24] [25].

The electrical field in the inversion layer of the semiconductor caused by the applied gate voltage changes the transport behavior of the charge carriers and results in more frequent scattering events than in the absence of the gate voltage. Since the modeling and the measurements are performed for low drain biases in linear mode, the effect of the electron velocity saturation on the drain current can be neglected.

The dependence of the source-drain current of the transistor on the types, geometric dimensions and concentration of viruses can be determined through expressions φ_{Ab} and φ_V .

For simplicity, in numerical calculations we will assume that the concentrations of immobilized antibodies and viruses in the aqueous solution are the same ($N_{Ab} = N_V$). Then dependency of source-drain current from virus types, sizes and concentration will be determined by the ε_V , d_V and N_V .

Numerical Simulation and Discussion for the Case of Covid-19 Virus

For the numerical analysis, below we used the parameters of the Covid-19 virus. To date, research has shown that the viruses that have been identified and isolated can range in diameter size from 20 nm to as large as 500 nm. Aside from spherical virus particles like SARS-CoV-2, whose diameters provide information on their sizes, the length of rod- or filament-shaped viruses can measure to as long as 1000 nm [26]. Measured value of dielectric constant varies from 35 - 65 in the frequency range up to 12 GHz [27], For SARS-CoV-2 the average dielectric constant on the protein-water interface is about 20 - 30 [28], the average size of the spike protein is 10 to 20 nm, and the feature height of particles after BSA (Bovine Serum Albumin) blocking is $4.59 \pm 1.75 \text{ nm}$ [28]. The height of protein particles is increased to $8.17 \pm 1.77 \text{ nm}$, verifying the binding of antibody with antigen. The height of antigen and antibody complex is around 6.3 nm.

Some known electrophysical parameters of the silicon substrate, silicon dioxide and aqueous solution we use from [20] [23]. They are:

$$\begin{aligned} w &= 0.5 \text{ cm}; t = 5 \times 10^{-3} \text{ cm}; l = 1 \text{ cm}; d_{Ab} = 2 \times 10^{-5} \text{ cm}; d_V = 3 \times 10^{-5} \text{ cm}; \\ d_{ox} &= 4 \times 10^{-6} \text{ cm}; \mu_0 = 1400 \text{ cm}^2/\text{V} \cdot \text{s}; \theta = 28 \text{ cm}^2/\text{V} \cdot \text{s}; \varphi_T = 0.026 \text{ V}; \\ \Phi_{Si} &= 4.8 \text{ eV}; \Phi_{ox} = 5 \text{ eV}; N_A = 10^{15} \text{ cm}^{-3}; n_0 = 10^{15} \text{ cm}^{-3}; p_0 = 2.25 \times 10^5 \text{ cm}^{-3}; \\ n_i &= 1.5 \times 10^{10} \text{ cm}^{-3}; N_t = 10^{11} \text{ cm}^{-2}; N_{sol} = 0.015 \text{ mol/l}; K_{AK}^+ = 0.001 \text{ mol/l}; \\ H_s^+ &= 0.005 \text{ mol/l}; N_{Ab} = 10^7; \varepsilon_0 = 8.85 \times 10^{-14} \text{ F/cm}; \varepsilon_w = 80; \varepsilon_r = 78; \\ \varepsilon_{Ab} &= 50; \varepsilon_V = 25; \varepsilon_{ox} = 3.8; \varepsilon_{Si} = 11.7. \end{aligned}$$

In **Figure 2** presented dependencies $I_{sd}(V_{sd})$ for the several values of virus concentration at the $V_g = 1\text{ V}$. The source-drain current increases linearly with the source-drain voltage and with increasing virus concentration (**Figure 2**). At a relatively low concentration of viruses, the source-drain current practically do not change. At concentrations of the order of $N_V \propto 10^3 \div 10^4\text{ cm}^{-2}$, I_{sd} changes slowly (see **Figure 3**) and increases more rapidly as the concentration rises above 10^5 cm^{-2} . It is clear that there is some threshold value of the virus molecules concentration in order of $10^2 \div 10^3\text{ cm}^{-2}$.

The sensitivity S of the source-drain current vs. virus molecules concentration slowly increase beginning of the threshold concentration and can determine as follows:

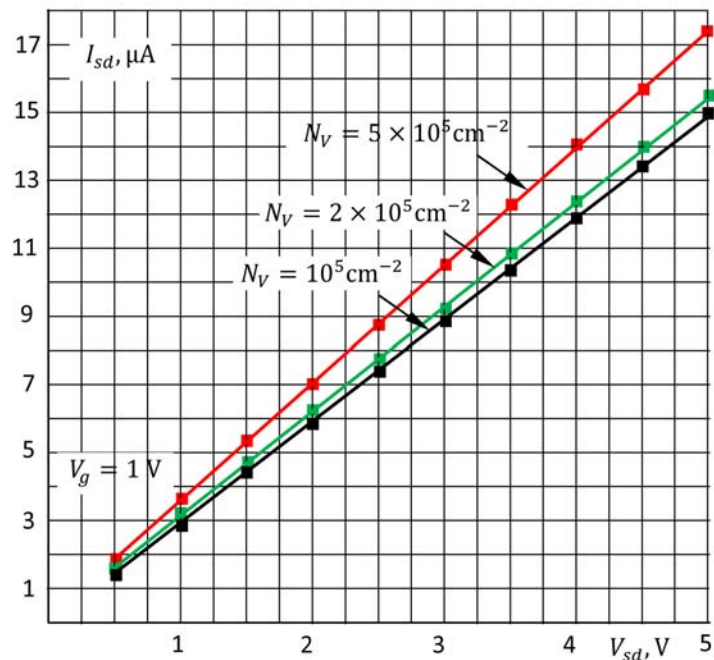


Figure 2. Dependency of source-drain current vs. source-drain voltage at the $V_g = 1\text{ V}$.

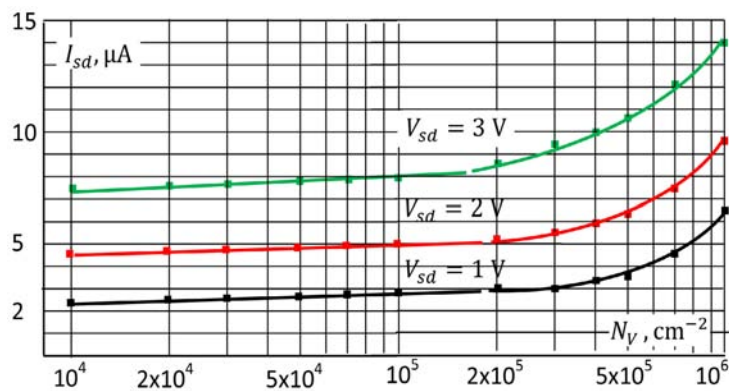


Figure 3. Dependency of source-drain current vs. virus molecules concentration N_V at the $V_g = 1\text{ V}$.

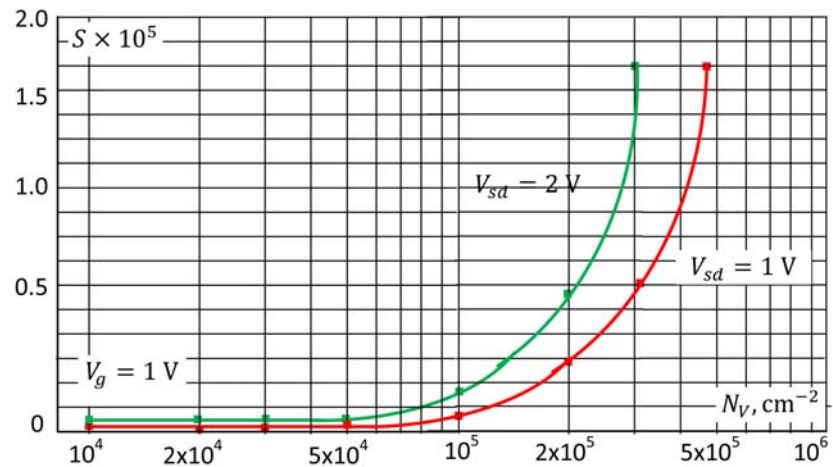


Figure 4. Dependency of current sensitivity vs. virus molecules concentration N_V at the $V_g = 1 \text{ V}$.

$$S = \frac{\Delta I_{sd}}{\Delta N_V}$$

Here ΔI_{ds} and ΔN_V are the elementary increments in the source-drain current and virus molecules concentration, accordingly.

Dependency of current sensitivity vs. virus molecules quantity N_V presented in **Figure 4**.

For repeated use of the proposed construction, it is necessary to purify antibodies from viruses bound to them. Affinity chromatography is an efficient antibody, antigen and protein separation method based on the interaction between specific immobilized ligands and target antibody, antigen, and so on. Populations of available ligands can be used to separate antibodies or their Fab fragments. The detail of repeated use presented in [29] [30].

4. Conclusions

Based on the theoretical modeling of the operation of the ISFET immunosensor and the obtained dependencies for the COVID-19 virus, the following important conclusions can be drawn:

1) Unknown virus detection

With known or given values of gate and source-drain (V_g and V_{sd}) voltages by the change of magnitude of the measured source-drain current I_{sd} , it is possible to detect the presence of foreign unknown molecules and viruses in the aqueous solution.

2) Unknown virus identification

With known or given values of gate and source-drain (V_g and V_{sd}) voltages by the magnitude of the measured source-drain current I_{sd} , it is possible to determine the type of unknown viruses.

3) Unknown virus concentration definition

With known or given gate and source-drain (V_g and V_{sd}) voltages by the

magnitude of the measured source-drain current I_{sd} , it is possible to determine the concentration of unknown viruses in the range $10^4 - 10^6 \text{ cm}^{-2}$.

4) Detection sensitivity for unknown virus

By selecting the gate and source-drain (V_g and V_{sd}) voltages the sensitivity of the ISFET immunosensor can be adjusted to detect unknown viruses.

Author Contribution Information

All authors participated in the statement of the problem and discussion of the results. L. Gasparyan, and F. Gasparyan conducted literature review. F. Gasparyan and V. Simonyan made calculations and participated in the writing of the text of the article.

Conflicts of Interest

The authors declare no conflicts of interest regarding the publication of this paper.

References

- [1] Bergveld, P. (1970) Development of an Ion-Sensitive Solid-State Device for Neurophysiological Measurements. *IEEE Transactions on Biomedical Engineering*, **BME-17**, 70-71. <https://doi.org/10.1109/TBME.1970.4502688>
- [2] Bergveld, P. (1986) The Development and Application of FET-Based Biosensors. *Biosensors*, **2**, 15-33. [https://doi.org/10.1016/0265-928X\(86\)85010-6](https://doi.org/10.1016/0265-928X(86)85010-6)
- [3] Lee, C.-S., Kim, S.K. and Kim, M. (2009) Ion-Sensitive Field-Effect Transistor for Biological Sensing. *Sensors*, **9**, 7111-7131. <https://doi.org/10.3390/s90907111>
- [4] Zachariah, E.S., Gopalakrishnakone, P. and Neuzil, P. (2006) Immunologically Sensitive Field-Effect Transistors. In: Webster, J.G., Ed., *Encyclopedia of Medical Devices and Instrumentation*, John Wiley & Sons, Inc., Hoboken, 98-110. <https://doi.org/10.1002/0471732877.emd141>
- [5] Selvanayagam, Z.E., Neuzil, P., Gopalakrishnakone, P., Sridhar, U., Singh, M. and Ho, L.C. (2002) An ISFET-Based Immunosensor for the Detection of β -Bungarotoxin. *Biosensors and Bioelectronics*, **17**, 821-82. [https://doi.org/10.1016/S0956-5663\(02\)00075-1](https://doi.org/10.1016/S0956-5663(02)00075-1)
- [6] Saengdee, P., Chaisiratanakul, W., Bunjongpru, W., et al. (2016) A Silicon Nitride ISFET Based Immunosensor for Ag85B Detection of Tuberculosis. *The Analyst*, **141**, 5767-5775. <https://doi.org/10.1039/C6AN00568C>
- [7] Vozgirdaite, D., Halima, H.B., Bellagambi, F.G., et al. (2021) Development of an ImmunoFET for Analysis of Tumour Necrosis Factor- α in Artificial Saliva: Application for Heart Failure Monitoring. *Chemosensors*, **9**, Article No. 26. <https://doi.org/10.3390/chemosensors9020026>
- [8] Hosseini, M., Fathollahzadeh, M., Kolahdouz, M., Rostamian, A., Mahmoodian, M., Samaeian, A. and Radamson, H.H. (2018) ISFET Immunosensor Improvement Using Amine-Modified Polystyrene Nanobeads. *Journal of Solid State Electrochemistry*, **22**, 3161-3169. <https://doi.org/10.1007/s10008-018-4025-9>
- [9] Liu, X., Lin, P., Yan, X., et al. (2013) Enzyme-Coated Single ZnO Nanowire FET. *Sensors and Actuators B: Chemical*, **176**, 22-27. <https://doi.org/10.1016/j.snb.2012.08.043>

- [10] Fathollahzadeh, M., Hosseini, M., Norouzi, M., et al. (2018) Immobilization of Glucose Oxidase on ZnO Nanorods Decorated Electrolyte-Gated Field Effect Transistor for Glucose Detection. *Journal of Solid State Electrochemistry*, **22**, 61-67. <https://doi.org/10.1007/s10008-017-3716-y>
- [11] Anvarifard, M.K., Ramezani, Z. and Amiri, I.S. (2020) Label-Free Detection of DNA by a Dielectric Modulated Armchair-Graphene Nanoribbon FET Based Biosensor in a Dual-Nanogap Setup. *Materials Science and Engineering: C*, **117**, Article ID: 111293. <https://doi.org/10.1016/j.msec.2020.111293>
- [12] Pullano, S.A., Critello, C.D., Mahbub, I., Tasneem, N.T., Shamsir, S., Islam, S.K., Greco, M. and Fiorillo, A.S. (2018) EGFET-Based Sensors for Bioanalytical Applications: A Review. *Sensors*, **18**, Article No. 4042. <https://doi.org/10.3390/s18114042>
- [13] Kamahori, M., Ishige, Y. and Shimoda, M. (2008) Enzyme Immunoassay Using a Reusable Extended-Gate Field-Effect-Transistor Sensor with a Ferrocenylalkanethiol-Modified Gold Electrode. *Analytical Sciences*, **24**, 1073-1079. <https://doi.org/10.2116/analsci.24.1073>
- [14] Marquez, A.V., McEvoy, N. and Pakdel, A. (2020) Organic Electrochemical Transistors (OECTs) toward Flexible and Wearable Bioelectronics. *Molecules*, **25**, Article No. 5288. <https://doi.org/10.3390/molecules25225288>
- [15] Gasparyan, L., Mazo, I., Simonyanand, V. and Gasparyan, F. (2020) Noises and Signal-to-Noise Ratio of Nanosize EIS and ISFET Biosensors. *Open Journal of Biophysics*, **10**, 1-12. <https://doi.org/10.4236/ojbiphy.2020.101001>
<https://www.scirp.org/journal/ojbiphy>
- [16] Gasparyan, L., Gasparyan, F. and Simonyan, V. (2021) Internal Electrical Noises of BioFET Sensors Based on Various Architectures. *Open Journal of Biophysics*, **11**, 177-204. <https://doi.org/10.4236/ojbiphy.2021.112006>
- [17] Gasparyan, F.V., Poghossian, A., Vitusevich, S.A., Petrychuk, M.V., Sydoruk, V.A., Siqueira, J.R., Oliveira, O.N., Offenhäusser, A. and Schöning, M.J. (2011) Low-Frequency Noise in Field-Effect Devices Functionalized with Dendrimer/Carbon-Nanotube Multilayers. *IEEE Sensors Journal*, **11**, 142-149. <https://doi.org/10.1109/JSEN.2010.2052355>
- [18] Janicki, M., Daniel, M., Szermer, M. and Napieralski, A. (2004) Ion Sensitive Field Effect Transistor Modeling for Multidomain Simulation Purposes. *Microelectronics Journal*, **35**, 831-840. <https://doi.org/10.1016/j.mejo.2004.06.015>
- [19] Hassibi, A., Navid, R., Dutton, R.W. and Lee, T.H. (2004) Comprehensive Study of Noise Processes in Electrode Electrolyte Interfaces. *Journal of Applied Physics*, **96**, 1074-1082. <https://doi.org/10.1063/1.1755429>
- [20] Sze, S.M. and Ng, K.K. (2006) *Physics of Semiconductor Devices*. 3rd Edition, John Wiley & Sons, Hoboken. <https://doi.org/10.1002/0470068329>
- [21] Ytterdal, T., Cheng, Y. and Fjeldly, T.A. (2003) *Device Modeling for Analog and RF CMOS Circuit Design*. John Wiley & Sons, Hoboken. <https://doi.org/10.1002/0470863803>
- [22] Nakamura, M., Sato, N., Hoshi, N. and Sakata, O. (2011) Outer Helmholtz Plane of the Electrical Double Layer Formed at the Solid Electrode-Liquide Interface. *ChemPhysChem*, **12**, 1430-1434. <https://doi.org/10.1002/cphc.201100011>
- [23] Pud, S., Gasparyan, F., Petrychuk, M., Li, J., Offenhausser, A. and Vitusevich, S.A. (2014) Single Trap Dynamics in Electrolyte-Gated Si-Nanowire Field Effect Transistors. *Journal of Applied Physics*, **115**, Article ID: 233705. <https://doi.org/10.1063/1.4883757>

- [24] Park, C., Lee, C., Lee, K., Moon, B.-J., Byun, Y.H. and Shur, M. (1991) A Unified Current-Voltage Model for Long-Channel nMOSFETs. *IEEE Transactions on Electron Devices*, **38**, 399-406. <https://doi.org/10.1109/16.69923>
- [25] Goldenblat, G.S. and Huang, C.-L. (1989) Engineering Model For Inversion Channel Mobility for 60-300 K Temperature Range. *Electronics Letters*, **25**, 634-636. <https://doi.org/10.1049/el:19890430>
- [26] Cuffari, B. (2021) The Size of SARS-CoV-2 and Its Implications. <https://www.news-medical.net/health/The-Size-of-SARS-CoV-2-Compared-to-Other-Things.aspx>
- [27] Abdulkarim, Y.I., Awl, H.N., Muhammadsharif, F.F., Sidiq, K.R., Saeed, S.R., Karaaslan, M., Huang, S., Luo, H. and Deng, L. (2009) Design and Study of a Coronavirus-Shaped Metamaterial Sensor Stimulated by Electromagnetic Waves for Rapid Diagnosis of Covid-19. arXiv:2009.08862.
- [28] Liu, H., Yang, A., Song, J., *et al.* (2021) Ultrafast, Sensitive, and Portable Detection of COVID-19 IgG Using Flexible Organic Electrochemical Transistors. *Science Advances*, **7**, eabg8387. <https://doi.org/10.1126/sciadv.abg8387>
- [29] Sheng, S. and Kong, F. (2012) Separation of Antigens and Antibodies by Immunoaffinity Chromatography. *Pharmaceutical Biology*, **50**, 1038-1044. <https://doi.org/10.3109/13880209.2011.653493>
- [30] Ayyar, B.V., Arora, S., Murphy, C. and O’Kennedy, R. (2012) Affinity Chromatography as a Tool for Antibody Purification. *Methods*, **56**, 116-129. <https://doi.org/10.1016/j.ymeth.2011.10.007>

Can a Molecule Be “Intelligent”? Unexpected Connections between Physics and Biology

Guido Paoli

Valsé Pantellini Foundation for Research and Studies on Degenerative Diseases-Italian Branch, Florence, Italy

Email: guido@valsepantellini.org

How to cite this paper: Paoli, G. (2022) Can a Molecule Be “Intelligent”? Unexpected Connections between Physics and Biology. *Open Journal of Biophysics*, 12, 234-244.

<https://doi.org/10.4236/ojbiphy.2022.124011>

Received: September 19, 2022

Accepted: October 23, 2022

Published: October 26, 2022

Copyright © 2022 by author(s) and Scientific Research Publishing Inc. This work is licensed under the Creative Commons Attribution International License (CC BY 4.0).

<http://creativecommons.org/licenses/by/4.0/>



Open Access

Abstract

It is important to look at the behaviour of a living system from the point of view of the biophysical paradigm. In fact, the chemical reactions, which allow us to understand how metabolic processes take place, are short-range and they are activated at a distance of one atomic or molecular diameter. 100,000 reactions/sec. take place in a cell, perfectly balanced in space and time, *i.e.* these happen at the right time and in the right place. So, it is chemically inexplicable how this can be possible, because it is absolutely necessary that molecules recognize each other at distances greater than a molecular diameter. The biophysical paradigm, through coherent resonance mechanisms, tries to explain how molecules can recognize each other “from afar”. It is a matter of beginning to understand that, probably, the same atoms and molecules are endowed with a kind of “intrinsic intelligence” that guides them in their interactions, and the key to understanding can only be of physical type. We can also hypothesize that a cellular information mechanism based on endogenous electromagnetic fields exists. In this way, DNA could play a role of in-out antenna, due to its double helix shape (resonant LC circuit). This paper speaks about these unexpected, but not too many, connections between Physics and Biology.

Keywords

Resonance, Information, Biophoton, DNA Antenna

1. Introduction

The purpose of science is to come to a plausible, objective description of reality and the laws that control the observed phenomena (possibly with “predictive character”), starting from the yet unknown. Dealing with science means asking nature questions and trying to understand the answers, not believing in having

the answers already to questions that have not yet been raised. It means having doubts, accepting that one's own ideas might be wrong or imprecise, and accepting that what we believe we know today might be questioned tomorrow. As Nobel Prize winner Francis Crick said: "*The real ability of science lies in the ideas and new hypotheses, regardless of whether they turn out to be right or wrong.*"

Medical Science and Biology have systematically and with almost absolute confidence been based on the biochemical paradigm in which it is, indeed, Chemistry that commands the reactions and metabolic processes occurring in living systems, and in the human one in particular. Although it undoubtedly allowed to obtain very important and decisive therapeutic successes for people's health, it is this confidence that leaves room for very critical questions related to understanding how the biological system (and its constituent parts) proceeds and how it has the ability to self-regulate and self-organize, as well as to cooperate at an intracellular and intercellular level by adapting to an endogenous and exogenous exchange of information. These types of chemical reactions are short-range, as we know since the model of Heitler and London in 1927 (valence bond (VB) theory) on the formation of a hydrogen molecule starting from two elementary atoms [1] [2], *i.e.* they are activated at a distance between atoms or molecules that is equal to an atomic or molecular diameter. Yet, by focusing only on this point of view it turns out to be chemically inexplicable how in a living system molecules that are far more apart than a molecular diameter "look for each other" and "find each other" with absolute precision in the right moment and the right place, even though they have other molecules around them with which they could interact.

While it is true that in a chemical reactor, in other words, a container designed to make chemical reactions happen, a molecule reacts to the closest molecule with which it can bond, living systems are, indeed, not chemical reactors.

We therefore have to take certain aspects into account that have thus far been underestimated but could shed new light on the mechanisms that regulate living systems, and that fully include the biophysical paradigm that regulates medium and long-range exchange of information.

This way, we can follow another point of view which favors the search for the "logic" that controls the observed phenomena. We know very well, for instance, that the letters of the alphabet do not have any significance when considered individually and that knowing a single letter does certainly not mean knowing how to speak. The information, their meaning, lies in the relation with other letters and in the way they are linked together thanks to grammatical rules and syntax. Using this analogy with living systems, this means that in addition to the knowledge of the molecules involved and the physical-chemical forces that keep them together, it is necessary to understand the way in which these molecules interact on a short distance (short-range) as well as the interactions and ways of communication on long distances (long-range). In the case of living systems, we then

understand it is not just a simple exercise of acquiring the rules of grammar in order to construct words and then sentences, or the rules of chemistry for molecules and then connections between molecules, but the research of their *relations* becomes the very soul of science. As written by the great Henri Poincaré: “the value of science is not in the things themselves [...] but in the relations between them; without these relations, there is no knowable reality” [3]. And further: “we cannot consider an object if not in relation to the possibility of its connection to other things” [4].

Physics tries to come out of the schematization of planned processes according to linear sequences, precisely in order to elaborate an interpretation of the phenomena according to an overall view of the processes and events in question. Life itself can be seen as a structure of information which the whole is more important than the sum of the single parts.

2. The “Lock and Key” Model: Critical Issues

In immunology and biochemistry, one of the still strongly rooted cornerstones in the formation of students and in applied research is based on the so-called “Ehrlich dogma”, modified by Clark [5] in which all phenomena of molecular recognition, in particular the transmission of information from a properly biochemical point of view, follow a strictly geometric mode of operation known as the “key & lock” scheme, expressing the fact that the interaction between two molecules follows the comparison of a key that is perfectly compatible with one (and only that exact) lock.

The possibility, therefore, that two molecules can interact with or “ignore” each other is associated with “elements of information” seen as simple geometric-structural abilities in a globally static system, whether correlated or not to the presence of certain groups of atoms, that can allow these interactions to express themselves in the form of donor, acceptor or ligand, receptor bonds through hydrogen bridges, disulfide bridges, Van der Waals forces, polarity. It would be these abilities in a given molecule to determine its own potentiality to interact with another molecule, like compatibility or incompatibility in computer programmes. Following this logic, the activation of biological functions is therefore a “mediation” between the chemical exchange of information of the molecule-receptor type and the spatial characteristics of the two substances. It is believed that the cell can operate with a specific selection of a greatly varied number of chemical signals, thanks to a likewise great specificity of its own receptors.

This fact is reported not only in ordinary biochemical reactions, but also in the way medication intervenes in correcting “functional defects”.

Molecular biology, considered the conceptual basis for medical science, tends to concentrate all its attention to the interaction between molecules following a sequential process. The pharmacological action is aimed at favoring or preventing chemical communication by acting selectively on the emitters, the messen-

gers or the receptors, by acting on the adaptability of the structures (*i.e.* the “key” that enters the right “lock”). It is, for that matter, not sufficient to enumerate these steps if we do not also specify the modality of chemical selectivity, in other words an *identification map* must be introduced through which molecules can correctly interact (so that molecule A can “find” molecule B).

However, because of the complexity of biological systems and particularly the enormous quantity of molecules concerned, we almost never succeed at defining which are the “sick” molecules.

This rather complex action becomes even more complicated if we consider that not only the adaptability of the structure, but also the number of contacts between interacting molecules (speed of formation and dissociation) is important [6]. This leads us to a “new” variable that seems to be completely overlooked in Ehrlich’s dogma, which is time. The difficulties now broaden into space-time dynamics as it is not only important that molecule A “finds” molecule B, but also that it does so rapidly. This poses a divergence from the classic scheme of molecular biology which, dealing only with “close encounters” of molecules, is not capable of finding an answer to.

According to Rowlands, in the late ‘80s, it is inconceivable that molecules wander randomly in the cell until they (casually) manage to meet each other at the right time and the right place for a useful reaction [7]. Furthermore, Bistolfi confirmed around the same time [8] that biophysical research was moving increasingly towards an approach that took into account both the collective and cooperative properties of biological systems, as well as the ordered behaviour of dissipative structures, according to the work of Nobel Prize winner Prigogine. This approach has been confirmed in the work of various researchers and work groups [8] [9] [10] [11] [12].

3. Biophysics and Resonance Mechanisms

It is important to remember that when there is no correlation between molecules, the energy that is produced by the system will thermally disperse in the form of molecular kinetic energy. Whilst when molecules are associated, their movement is determined and stabilized by precisely those connections. We notice the same thing while observing a school of fish or a flock of birds: their apparently abrupt movements or sudden displacements are not commanded by one “leader of the pack”, but through the *tuning of collective characteristics* of the elements in the system. This means coordination constraints are introduced, reducing on the one hand the possibility of performing all possible movements (collisions between elements of the system for example are excluded), allowing on the other hand the formation of collective coordination criteria so that the system can have a proper *identification map*, and the first step is the one of phenomena of resonance [13].

Resonance is the condition that occurs when a forced oscillating system is subject to periodic stress with a frequency that is equal to that of the system it-

self.

In Physics and Biophysics we continuously observe oscillating and periodic processes (processes that follow a rhythm: circadian, monthly, etc...) and we always strive to describe them in the simplest way possible, like sinusoidal waves or their composition. A periodic oscillating motion can be assimilated into the movement of the pendulum, which is then nothing more than a “variation” of the uniform circular motion.

In this case, we know from classical physics that a body that moves in a uniform circular motion is subject to continuous variations in speed over time as it gradually completes the circumference span during its movement (speed is a vector, described by the number that measures its value, direction and way). A variation of speed in time is nothing more than an acceleration, so a body that moves in uniform circular motion is an accelerated system, and therefore moves in uniformly accelerated motion.

We know that atoms and molecules (more or less “large”) in a living system are not electrically neutral but present an unbalanced electric charge (such as positively or negatively charged ions and protein binding sites) to allow the formation of chemical bonds. From classical physics we know that an electric charge in uniformly accelerated motion is home to electromagnetic fields and quantum physics helps us to understand that these electromagnetic fields manifest themselves through the presence of photons (also called “quanta of electromagnetic radiation”). In living systems photons are called biophotons.

We begin to sense that biophotonic communication between one cell and another and between themselves and their environment forms the foundation of resonance mechanisms, where the endogenous electromagnetic field is the activator of such mechanisms [8] [11] [14]-[20].

Resonance is at the basis of cellular communication, hence the introduction of the biophysical paradigm which allows us to give a clear interpretation to molecular recognition that is extremely selective and harmonically synchronized in a living system, something that will not occur in a biochemical reactor.

As a result, also the so-called “lock and key” model finds an explanation that goes well beyond the “randomness” of ligand–receptor bonds, because of the interlocking of forms without any prior recognition that prepare the bond itself.

It is exactly on this initial base that a molecule becomes intelligent, because by resonating with physiological elements it interacts with, it is capable of identifying where to go and of recognising where it needs to act in order to either contrast an ongoing process or support a useful physiological action.

4. The “Lock and Key” Model: Overcoming Critical Issues

We know that proteins do not have a static structure but are dynamic, and thanks to their capability of taking on different, coherently linked forms, they can modify their functional activity. This characteristic, representing a regulatory mechanism in biological processes, is called allosterism and the proteins are

called allosteric [21]-[27].

This mechanism allows proteins to ensure that their internal hydrogen bridging bonds, the disulfide bridging (SH) bonds and the Van der Waals forces can assume alternative but energetically similar positions, which is why new spatial relationships between the “folds” of the secondary and tertiary structure of the proteins can be formed, and consequently a modification of their form at the external surface level, thus allowing a different modality of interaction with other molecules.

Keeping in mind that the lateral chains of a single protein have superficial binding sites allowing weak bonds with ligands (in order to be reversible), these only occur if the ligand perfectly matches the receptor. Therefore, the modelization of protein, ligand binding describes a dynamic process of morphological adaptation of the binding site of the “receptor” protein to the “ligand” molecule [8] [28]; it is not a purely mechanical or geometric mechanism, but instead this is all mediated by what we previously defined as “identification maps and codes”. To put it simply, proteins have binding sites (receptors) that can be structurally modified, form-wise, thanks to modifications of the lateral chain structure of the protein itself which are linked to signals coming from the molecule (the ligand) with which the protein interacts, thus to activated mechanisms of resonance.

5. Electromagnetic Fields and DNA Antenna

“How come we are not able to do what the lowest microbes can effortlessly accomplish?”. In a recent publication, Al-Khalili and McFadden asked themselves why matter behaves so differently when it has to build an animated creature compared to when it manifests itself in an inanimate subject like a stone [29]. These and related questions make us realize that the development of an organism is not just the simple sum of its parts, but infinitely much more. Although the human-machine model is extremely useful in certain situations, it has become clear that we have to go beyond. Being anchored exclusively to concepts of classical physics and chemistry, it fails to explain the complexity in the behaviour of a living system.

The idea that DNA would “simply” be some kind of protein-making machine, as well as a “rememberer” of genetic information, is a cognitive limitation. We know that only a small percentage (from 2% to 10%) of its structure codifies proteins, in a pleiotropic way. Until recently, the remaining non-coding part of DNA (between 90% and 98%) was considered useless as it seemed “not to do much”, leading to the term junk DNA. However, according to many researchers it is the non-coding part that controls the cellular complexity and regulates the behaviour of the coding part as it communicates through a grammatically and syntactically very precise and correct language which genes need to turn on or off for the synthesis of specific proteins [30].

A couple of new questions arise:

- How is it possible that DNA communicates with cytoplasm if it is seen as “just” a protein-producing machine?
- On the same premise, how can the nuclear DNA communicate with the mitochondrial DNA?

Let us briefly introduce a possible interpretation (working hypothesis).

Physically speaking, the spiral shape of DNA (double helix) represents:

- A solenoid, a coil of conducting wire wound in a spiral on a cylindrical-shaped support that generates a magnetic field when crossed by an electric current, consisting of a spiral winding of the external DNA skeleton;
- A series of capacitors, *i.e.* devices with parallel faces that store energy in an electrostatic field, consisting of the parallel faces of the spiral windings of the external structure.

This means that the DNA could be seen as a device that electrical engineers call an LC circuit, where L stands for the inductance of the equivalent solenoid and C for the capacity of the equivalent capacitor, which, at certain frequencies, is subject to the phenomenon of resonance.

DNA can store and release electromagnetic energy, thus information, in the form of biophotons.

This leads to think that the double helix structure of DNA allows this super-molecule to behave like a proper electromagnetic input/output antenna, capable of “reading” and “retransmitting” information signals of the electromagnetic type which come from various districts of the cytoplasm [8] [31] [32] [33].

It is exactly this electromagnetic information that forms the subject of communication between antenna DNA and cytoplasm. In this way, DNA can be informed about “how things are going” and whether it is necessary to proceed to replace or produce proteins in certain areas of the cell.

Moreover, the absorption spectra of DNA in the so-called “far infrared” region (more than 10 - 15 μm) indicate low-frequency molecular movements linked to the flexibility and deformation capacity of the double helix structure, which can then be bound up in the approximately 5 μm of the cell nucleus. This also allows the antenna to generate bio-phonons, or low-frequency fluctuating elastic waves [34].

The double helix structure as a transceiver antenna, combined with the deformability and flexibility of the structure [35], makes the DNA capable of encompassing an enormous range of frequencies and controlling the complexity of the cell in an extremely precise way. This lets the living system as a whole, as well as the component molecules, act like an intelligent structure capable of making decisions for its own (self-organization and self-regulation) based on exogenous and endogenous information flows.

On the other hand, this is a controversial issue, due to the experimental difficulty of making measurements on isolable DNA. In fact, in a paper of four years ago [36] based on an extensive investigation with both prokaryotic and eukaryotic purified DNA sample in concentrated or diluted form, to put in evidence electromagnetic properties inherent to it, the authors concluded that either there

were no intrinsic EM activity in the DNA materials or any such activity was so weak respect on measurements limits of instruments used in these experiments.

So this model remain a suggestive working hypothesis because it is coherent with the accepted paradigm relating to the biophysics of living systems, but it is necessary to develop controlled experiments to correlate quantum coherent resonance with modalities of possible electromagnetic interactions between DNA and molecules. The main issue is that the claim to isolate a molecule from its biological context risks showing a fictitious reality, that does not correspond to the real behaviour of “that” molecule within the living system. So we must be very clear about what we consider acceptable and inalienable and what is “expendable”, in making an element of biophysical investigation isolable, such as a protein, a nucleic acid, water itself (which in this paper is not considered but will be subject to an in-depth review in a new paper).

6. Conclusions

I hope that the scientific community doesn't reject this interpretation “tout court”, because it can be an opportunity for a better understanding of living systems, looking at the wonderful complexity of life from a different perspective.

In my opinion living systems, as well as single cells, can be described as autopoietic biological reactors in which each cell, in phase coherence with the others, is able to make conscious choices, thus expressing an adaptive intelligence. In fact, a living system can respond autonomously to external stimuli, reorganizing and adapting itself.

We tend to exclude weak signals, which are often difficult to detect compared to what we call background noise, but I think that precisely these weak signals can allow a coherent reorganization at the metabolic and functional cellular level.

These considerations, all based on our current level of knowledge, make us look at the wonderful complexity and incredible mystery that forms life with humility and respect.

“As science gradually develops, it becomes more and more complicated to have an overall vision; so we divide it up into different pieces and are satisfied with one part, in one word, we specialize.

Continuing like this would constitute a serious obstacle towards scientific progress. As said before: it is the unexpected connections between various scientific domains that make such progress possible.” (J.-H. Poincaré)

Conflicts of Interest

The author declares no conflicts of interest regarding the publication of this paper.

References

- [1] Bransden, B.H. and Joachain, C.J. (1984) *Physics of Atoms and Molecule*. Longman

- Group Limited Publisher, Harlow.
- [2] Majorana, E. and Sasso, A. (2006) On the Formation of Molecular Helium Ion. In: Bassani, G.F., Ed., *Ettore Majorana: Scientific Papers*. Springer, Berlin. https://link.springer.com/chapter/10.1007/978-3-540-48095-2_3
 - [3] Poincaré, J.H. (2012) *La scienza e l'ipotesi*. Dedalo, Bari. (In Italian)
 - [4] Von Baeyer, H.C. (2004) *Information: The New Language of Science*. Harvard University Press, Cambridge.
 - [5] Clark, A.J. (1933) *Mode of Action of Drugs on Cells*. Arnold, London.
 - [6] Paton, W.D. (1960) The Principles of Drug Action. *Proceedings of the Royal Society of Medicine*, **53**, 815-820. <https://doi.org/10.1177/003591576005301002>
 - [7] Rowlands, S. (1988) The Interaction of Living Red Blood Cells. In: Frölich, H., Ed., *Biological Coherence and Response to External Stimuli*, Springer-Verlag, Berlin, 171-191. https://doi.org/10.1007/978-3-642-73309-3_10
 - [8] Bistolfi, F. (1989) *Radiazioni non ionizzanti: Ordine, disordine e biostrutture*. Minerva Medica, Torino.
 - [9] Preparata, G. (1995) *QED Coherence in Matter*. World Scientific Publishing, Singapore. <https://doi.org/10.1142/2738>
 - [10] Preparata, G. (2002) *Dai quark ai cristalli. Breve storia di un lungo viaggio dentro la materia*. Bollati Boringhieri, Torino.
 - [11] Popp, F.A. (2002) Biophotonics—A Powerful Tool for Investigating and Understanding Life. In: Dürr, H.P., Popp, F.A., Schommers, W., Eds., *What Is Life? Scientific Approaches and Philosophical Positions*, World Scientific Publishing, Singapore, 279-306. https://doi.org/10.1142/9789812706560_0013
 - [12] Van Wijk, R. (2003) Cellular and Molecular Aspects of Integrative Biophysics. In: Popp, F.A. and Belousov, L.V., Eds., *Integrative Biophysics: Biophotonics*, Springer-Verlag, Berlin, 179-201. https://doi.org/10.1007/978-94-017-0373-4_4
 - [13] Bischof, M. and Del Giudice, E. (2013) Communication and the Emergence of Collective Behaviour in Living Organisms: A Quantum Approach. *Molecular Biology International*, **2013**, Article ID: 987549. <https://doi.org/10.1155/2013/987549>
 - [14] Del Giudice, E., Doglia, S., Milani, M. and Vitiello, G. (1988) Structures Connection and Electromagnetic Interaction in Living Matter. In: Frölich, H., Ed., *Biological Coherence and Response to External Stimuli*, Springer-Verlag, Berlin, 49-64. https://doi.org/10.1007/978-3-642-73309-3_3
 - [15] Colli, L. and Facchini, U. (1954) Light Emission by Germinating Plants. *Il Nuovo Cimento*, **12**, 150-153. <https://doi.org/10.1007/BF02820374>
 - [16] Musumeci, F. (2003) Physical Basis and Applications of Delayed Luminescence. In: Popp, F.A. and Belousov, L., Eds., *Integrative Biophysics: Biophotonics*, Springer-Verlag, Berlin, 203-230. https://doi.org/10.1007/978-94-017-0373-4_5
 - [17] Cordone, L., Privitera, G., Tudisco, S. and Musumeci, F. (2003) Delayed Luminescence and Motional Harmonicity. In: Musumeci, F., Brizhik, L.S., Ho, M.-W., Eds., *Energy and Information Transfer in Biological Systems*, World Scientific Publishing, Singapore, 14-23. https://doi.org/10.1142/9789812705181_0002
 - [18] Niggli, H.J. and Applegate, N.A. (2003) Biophotons: Ultraweak Photons in Cells. In: Popp, F.A. and Belousov, L., Eds., *Integrative Biophysics: Biophotonics*, Springer-Verlag, Berlin, 361-385. https://doi.org/10.1007/978-94-017-0373-4_11
 - [19] Rahnema, M., Tuszyński, J.A., Bokkon, I., Cifra, M., Sardar, P. and Salari, V. (2011) Emission of Mitochondrial Biophotons and Their Effect on Electrical Activity of

- Membrane via Microtubules. *Journal of Integrative Neuroscience*, **10**, 65-88. <https://doi.org/10.1142/S0219635211002622>
- [20] Chen, X., Wu, T., Gong, Z., Guo, J., Liu, X., Zhang, Y., Li, Y., Ferraro, P. and Li, B. (2021) Lipid Droplets as Endogenous Intracellular Microlenses. *Light: Science & Applications*, **10**, Article No. 242. <https://doi.org/10.1038/s41377-021-00687-3>
<https://www.nature.com/articles/s41377-021-00687-3>
- [21] Frauenfelder, H., Petsko, G.A. and Tsernoglou, D. (1979) Temperature-Dependent X-Ray Diffraction as a Probe of Protein Structural Dynamics. *Nature*, **280**, 558-563. <https://doi.org/10.1038/280558a0>
- [22] Parak, F., Frolov, E.N., Mössbauer, R.L. and Goldanskii, V.I. (1981) Dynamics of Metmyoglobin Crystals Investigated by Nuclear Gamma Resonance Absorption. *Journal of Molecular Biology*, **145**, 825-833. [https://doi.org/10.1016/0022-2836\(81\)90317-X](https://doi.org/10.1016/0022-2836(81)90317-X)
- [23] Knapp, E.W., Fischer, S.F. and Parak, F. (1983) The Influence of Protein Dynamics on Mössbauer Spectra. *The Journal of Chemical Physics*, **78**, Article No. 4701. <https://doi.org/10.1063/1.445316>
- [24] Wagner, G., Pardi, A. and Wuethrich, K. (1983) Hydrogen Bond Length and Proton NMR Chemical Shifts in Proteins. *Journal of the American Chemical Society*, **105**, 5948-5949. <https://doi.org/10.1021/ja00356a056>
- [25] Bu, Z. and Callaway, D.J. (2011) Proteins Move! Protein Dynamics and Long-Range Allostery in Cell Signaling. *Advances in Protein Chemistry and Structural Biology*, **83**, 163-221. <https://doi.org/10.1016/B978-0-12-381262-9.00005-7>
- [26] Srinivasan, B., Forouhar, F., Shukla, A., Sampangi, C., Kulkarni, S., Abashidze, M., Seetharaman, J., Lew, S., Mao, L., Acton, T.B., Xiao, R., Everett, J.K., Montelione, G.T., Tong, L. and Balaram, H. (2014) Allosteric Regulation and Substrate Activation in Cytosolic Nucleotidase II from *Legionella pneumophila*. *The FEBS Journal*, **281**, 1613-1628. <https://doi.org/10.1111/febs.12727>
- [27] Cuendet, M.A., Weinstein, H. and LeVine, M.V. (2014) The Allostery Landscape: Quantifying Thermodynamic Coupling in Biomolecular Systems. *Journal of Chemical Theory and Computation*, **12**, 5758-5767. <https://doi.org/10.1021/acs.jctc.6b00841>
- [28] Tripathi, A. and Bankaitis, V.A. (2017) Molecular Docking: From Lock and Key to Combination Lock. *Journal of Molecular Medicine and Clinical Applications*, **2**, 1-9. <https://doi.org/10.16966/2575-0305.106>
<https://www.ncbi.nlm.nih.gov/pmc/articles/PMC5764188/pdf/nihms856098.pdf>
- [29] Al-Khalili, J. and McFadden, J. (2014) *Life on the Edge: The Coming of Age of Quantum Biology*. Bantam Press, London.
- [30] Mantegna, R.N., Buldyrev, S.V., Goldberger, A.L., Havlin, S., Peng, C.-K., Simons, M. and Stanley, H.E. (1994) Linguistic Features of Noncoding DNA Sequences. *Physical Review Letters*, **73**, 3169-3172. <https://doi.org/10.1103/PhysRevLett.73.3169>
- [31] Blank, M. and Goodman, R. (2011) DNA Is a Fractal Antenna in Electromagnetic Fields. *International Journal of Radiation Biology*, **87**, 409-415. <https://doi.org/10.3109/09553002.2011.538130>
- [32] Montagnier, L., Del Giudice, E., Aïssa, J., Lavallee, C., Motschwiller, S., Capolupo, A., Polcari, A., Romano, P., Tedeschi, A. and Vitiello, G. (2015) Transduction of DNA Information through Water and Electromagnetic Waves. *Electromagnetic Biology and Medicine*, **34**, 106-112. <https://doi.org/10.3109/15368378.2015.1036072>

- [33] Doerfler, W. (2017) DNA and Its Epigenetic Potential, an Antenna for Cosmic Emission: Driving Force in Evolution and Energy Transmission? *Journal of Clinical Epigenetics*, **3**, Article No. 9. <https://www.linkwitzlab.com/Fitz/J.%20Clinical%20Epigenetics%203,%202017.pdf>
- [34] Sussmann, J.A. (1964) Phonon Induced Tunneling of Ions in Solids. *Physik der Kondensierten Materie*, **2**, 146-160. <https://doi.org/10.1007/BF02422872>
- [35] Pethig, R. (1979) Dielectric and Electronic Properties of Biological Materials. John Wiley & Sons Ltd., Hoboken.
- [36] Bukhari, M.H., Batool, S., Raza, D.Y., Bagasra, O., Rizvi, A., Shah, A., Razzaki, T. and Sultan, T. (2018) DNA Electromagnetic Properties and Interactions—An Investigation on Intrinsic Bioelectromagnetism within DNA. *Electromagnetic Biology and Medicine*, **37**, 169-174. <https://doi.org/10.1080/15368378.2018.1499032>

An Hybrid Model for Rectal Tumour Response Prediction during Radiotherapy

Apeke Sena^{1,2}, Gaubert Laurent^{1,3}, Boussion Nicolas^{1,4}, Visvikis Dimitris^{1,4}, Saut Olivier⁵, Colin Thierry⁵, Lambin Philippe⁶, Rodin Vincent², Redou Pascal^{1,3}

¹LaTIM, Unité Mixte de Recherche 1101, Institut National de la Santé et de la Recherche Médicale, Brest, France

²Immersive Natural User Interaction Team, Lab-STICC, Unité Mixte de Recherche CNRS 6285, Computer Science Department, Université de Bretagne Occidentale, Brest, France

³Centre Européen de Réalité Virtuelle, Brest, France

⁴Centre Hospitalier Régional Universitaire de Brest, Brest, France

⁵Institut de Mathématiques de Bordeaux, Talence, France

⁶The D-Lab & M-Lab, Department of Precision Medicine, GROW—School of Oncology and Developmental Biology, Maastricht University, Maastricht, The Netherlands

Email: apekekodjo@gmail.com, gaubert@enib.fr, nicolas.boussion@chu-brest.fr, dimitris@univ-brest.fr, Olivier.Saut@math.u-bordeaux1.fr, colin@math.u-bordeaux1.fr, philippe.lambin@maastrichtuniversity.nl, vincent.rodin@univ-brest.fr, redou@enib.fr

How to cite this paper: Sena, A., Laurent, G., Nicolas, B., Dimitris, V., Olivier, S., Thierry, C., Philippe, L., Vincent, R. and Pascal, R. (2022) An Hybrid Model for Rectal Tumour Response Prediction during Radiotherapy. *Open Journal of Biophysics*, 12, 245-264.

<https://doi.org/10.4236/ojbiph.2022.124012>

Received: September 10, 2022

Accepted: October 25, 2022

Published: October 28, 2022

Copyright © 2022 by author(s) and Scientific Research Publishing Inc.

This work is licensed under the Creative Commons Attribution-NonCommercial International License (CC BY-NC 4.0).

<http://creativecommons.org/licenses/by-nc/4.0/>



Open Access

Abstract

A hybrid model is proposed in this study to predict rectal tumour response during radiotherapy treatment. As the oxygen partial pressure distribution (pO_2) is a data which is naturally represented at the microscopic scale, we firstly estimate the optimal pO_2 distribution using both a diffusion equation and a discrete multi-scale model (that we proposed in a previous study). The aim is to use the effectiveness in algorithmic complexity of the discrete model and its multi-scale aspect in this work to estimate biological information at cellular scale and then construct them at macroscopic scale. Secondly, the obtained pO_2 distribution results are used as an input of a biomechanical model in order to simulate tumour volume evolution during radiotherapy. FDG PET images of 21 rectal cancer patients undergoing radiotherapy are used to simulate the tumour evolution during the treatment. The simulated results using the proposed hybrid model, allow the interpretation of tumour aggressiveness.

Keywords

Tumour, Treatment, Response, Discrete, Density, FDG PET, SUV, PDE, Simulation

1. Introduction

The simulation of tumour growth and tumour response to radiation therapy

remains a major research topic due to the overall impact of cancer [1] [2]. According to the World Health Organization (WHO), cancer burden rises to 18.1 million new cases and 9.6 million deaths worldwide in 2018. In this context, research on the treatment of malignant tumours is obviously a major concern and requires the mobilization of multidisciplinary research communities. In the literature, a wide series of mathematical or computational approaches to tumour growth modelling is proposed [3]-[8]. Such studies are generally theoretical and rarely tackle the individual specificities of real patients. Therefore, building relevant relationships between mathematical models and actual data like morphological or anatomical images corresponding to standard clinical use remains a real challenge. In addition to this macroscopic aspect, the microscopic scale of the tumour microenvironment should also be taken into account. For example, partial oxygen pressure (pO_2) is a very important local factor to consider when simulating tumour growth [9] [10]. Unfortunately, reliable and precise data concerning local pO_2 remain difficult to obtain for a given patient. The absence of such information makes it difficult to realistically evaluate simulation models. A potential solution is to build an autonomous model which calculates the oxygen partial pressure from available information and then uses it as an input for the main model, *i.e.* the one which predicts tumour growth. In the literature, several approaches to pO_2 modelling exist both at the microscopic scale [11] [12] and macroscopic scale [13]. Partial oxygen pressure is also of crucial importance for radiotherapy outcomes since hypoxic tumours, with a low level of oxygen, are known to be more resistant to radiation than non-hypoxic tumours. Ideally the dynamics and the heterogeneity of pO_2 distribution inside the tumour must be manageable. Furthermore, the impact of pO_2 and the response to radiation may differ according to the tumour cell types. The behaviour of the different types of tumour cells, either proliferative, hypoxic or quiescent, can be distinguished by the way they manage pO_2 . In this context, taking oxygen partial pressure heterogeneity into consideration in tumour growth modelling during treatment is important, because the microenvironment has a significant impact on the efficacy of radiotherapy. Generally, pO_2 modelling does not take into account the dynamic nature of his evolution during the entire treatment [14], it is considered constant across the whole tumour, or not taken into account at all [15]. We previously described a multi-scale approach allowing to take images and cellular cycle phases into account but pO_2 was considered constant inside the volume of interest and the tumour surface evolution was not addressed [16]. Typical cancer treatment generally consists of a combination of surgery, radiotherapy and chemotherapy. When radiotherapy is associated with the treatment, it is sometimes performed to reduce the size of the tumour before surgery [17]. After surgery, radiotherapy can still be used to reduce local recurrence risks. Surgery obviously requires careful planning, and indications leading to the least complicated therapeutic strategy are welcome. For this purpose, morphologic and metabolic images are used in order to get some characteristics of the tumour

without necessarily going through biopsies. Furthermore, a CT scan (x-ray computed tomography) and FDG PET images (fluorodeoxyglucose positron emission tomography) are acquired before radiotherapy in order to delineate target and organs at risk, and also for optimizing treatment planning through relevant ballistics. In cases of potential tumour evolution during radiotherapy, additional images are acquired in order to adapt treatment according to the new size or shape of the tumour. In this context, the main objective of this study is to build a numerical tool able to predict the evolution of the tumour during radiotherapy by using images of the patient as an input. The proposed methodology is built on our previously described multi-scale and discrete framework [16]. In this new approach, a dynamic and heterogeneous map of pO_2 is generated and combined with a system of partial differential equations for modelling the tumour volume evolution. This hybrid process is evaluated using real FDG PET images acquired at different moments of radiotherapy in 21 rectal cancer cases.

2. Materials and Methods

2.1. Model Description

The new dynamic model for tumour response to radiotherapy that is proposed in this study comprises two main steps. As a first step, a diffusion equation is used to model the pO_2 evolution in the tumour at each time step [13] [18]. This equation is incorporated into a previously described multi-scale framework in order to take the personalized images of the patient into account [16]. As a second step, an advection reaction equation is proposed in order to predict the tumour volume evolution during radiotherapy treatment. These two steps compose the proposed hybrid approach and are described separately in the following sections.

2.1.1. pO_2 Evolution Modelling

Oxygen transport in tissues via blood vessels obviously depends on vessels structure but also on other biological constraints linked to the tumour behaviour. In the present study, Equation (1) was chosen to locally model the pO_2 evolution [18]:

$$\frac{\partial pO_2}{\partial t} = \frac{2P_m}{R} (p_{cap} - pO_2) + \nabla \cdot (D \nabla pO_2) - c_{max} \cdot \frac{pO_2}{pO_2 + P_h} \cdot \rho \quad (1)$$

where, ρ represents the cell density in a voxel, with:

- $\frac{2P_m}{R} (p_{cap} - pO_2)$: the source term, P_m is the blood vessels permittivity and R the radius;
- $\nabla \cdot (D \nabla pO_2)$: the diffusion term, D is the diffusion coefficient;
- $c_{max} \cdot \frac{pO_2}{pO_2 + P_h}$: the oxygen consumption per unit cell density, c_{max} is the maximum consumption of pO_2 , and P_h is the pO_2 at $\frac{c_{max}}{2}$.

In order to provide personalized simulation according to patient specific data coming from images, a parameter controlling the source term was introduced. By denoting μ this parameter, pO_2 distributions for a given patient are obtained by solving Equation (2). The values of the fixed parameters are given in **Table 1**.

$$\frac{\partial pO_2}{\partial t} = \mu(p_{cap} - pO_2) + \nabla \cdot (D \nabla pO_2) - c_{max} \cdot \frac{pO_2}{pO_2 + P_h} \cdot \rho \quad (2)$$

Since pO_2 consumption is a process that takes place at the cellular scale, a multi-scale approach is used in order to estimate the optimal distributions from macroscopic PET image data. The diagram shown in **Figure 1** describes the operating steps of this multi-scale stochastic methodology, but full details can be

Table 1. List of parameters used in this work.

Parameter	symbol	Value and reference
Diffusion coefficient	\mathbf{D}	$2 \times 10^{-9} \text{ m}^2 \cdot \text{s}^{-1}$ [11]
Maximum consumption of pO_2	c_{max}	1 mmHg s^{-1} [11]
pO_2 at $c_{max}/2$	P_h	2.5 mmHg [11]
pO_2 in the arterie	P_{cap}	40 mmHg [20]
Radio-sensitivity coefficient	α	0.044 Gy^{-1}
Radio-sensitivity coefficient	β	0.089 Gy^{-2}
Hypoxic threshold	pO_2^h	fixed at 5 mmHg [3]

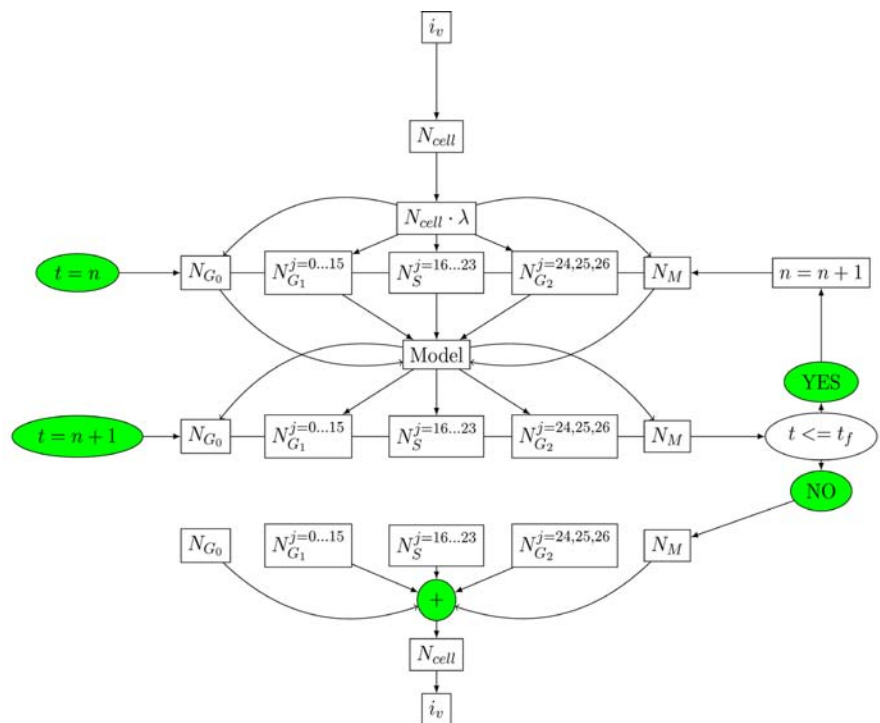


Figure 1. Diagram showing all the processes involved in the stochastic model, $[t_0, t_f]$ is the time interval between the beginning and the end of a cell cycle. In this case $t_f = 28 \text{ h}$.

found in [16]. The model is based on transitions between the successive phases of the cellular cycle. The total number of active tumour cells (N_{cell}) inside a voxel of the image is directly calculated from the voxel intensity (i_v). Then, the number of tumour cells in each cellular cycle phase ($N_{G_1}, N_S, N_{G_2}, N_M, N_{G_0}$) are deduced using a precomputed distribution (λ).

2.1.2. Estimation of the Optimal pO_2 Distributions

Optimal pO_2 distributions are estimated by minimizing a cost function which depends on the number of cells given by simulated and real data. These numbers are calculated from clinical and simulated FDG PET [19] images obtained at the 8th day following the beginning of radiotherapy. The simulated number of cells was derived from the multi-scale stochastic model. Let us now describe the optimization algorithm which consists of five steps:

1) an acceptability criterion is defined by means of a cost function F (Equation (3)); for every voxel index (l, n, m) :

$$F(P_1, P_2)(l, m, n) = \left(1 - \frac{N_8^s(l, m, n)}{N_8^c(l, m, n)}\right)^2 + \left(1 - \frac{N_{15}^s(l, m, n)}{N_{15}^c(l, m, n)}\right)^2 \quad (3)$$

where, N_8^s and N_{15}^c are the total numbers of tumour cells calculated respectively from simulated and clinical images. P_1 and P_2 are pO_2 distributions at day 0 and at day 8 respectively;

2) The capillary pressure is initialized at $t = t_0$ (t_0 corresponds to day 0) as $P_{cap} = 40$ mmHg (pO_2 in the arteries [20]);

3) Equation (2) is solved at each time step using finite difference method;

4) pO_2 distributions obtained in 3) are used as an input for the discrete model [16]; Then the results are used to calculate the cost function 1);

5) If the result of the cost function is less than a set threshold, the value of the parameter μ and the pO_2 distributions are saved, and the algorithm is stopped. Otherwise, the parameter μ is modified using simulated annealing method [21] and the algorithm is resumed from step 2.

The final optimal pO_2 maps are used as input of a biomechanical model that we describe now.

2.1.3. Description of the Biomechanical Model

We denote by $\mathbf{A} \subset \mathbf{R}^3$ an image containing a patient tumour at time $t \in [0, \Upsilon]$, where Υ is the time between the beginning of the first image acquisition (before treatment) and the last acquisition (15 days after the beginning of the irradiation for 17 patients, or after radiotherapy and just before surgery for 4 patients). Then, we denote by $\Omega(t)$, the tumour zone in the image \mathbf{A} (See **Figure 2**). $\Omega(t)$ is given by the set of standardized uptake values (SUV) calculated from FDG PET images [22]:

$$\Omega(t) = \{(x, y, z) \in \mathbf{A} / \rho(x, y, z, t) > 0\} \quad (4)$$

In this study, it is assumed that the tumour tissue is composed either of proliferative cells, quiescent cells, or necrotic cells [23] [24]. These cells densities

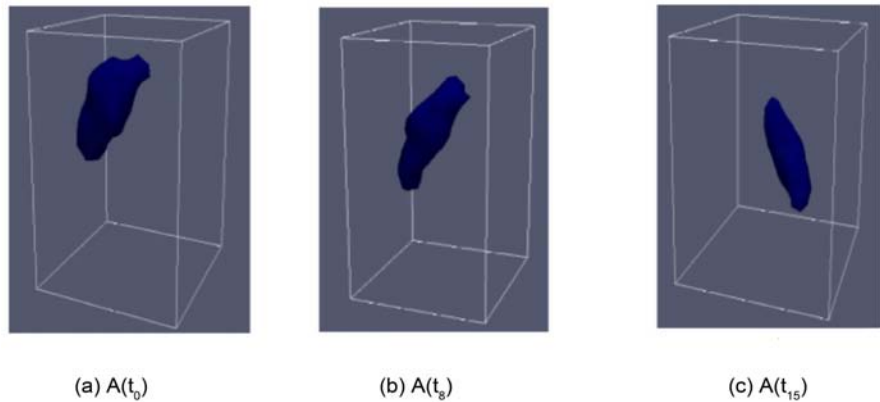


Figure 2. An example of data obtained from clinical images: (a) before the beginning of treatment A_0 , (b) after one week of treatment A_8 and (c) after two weeks of treatment A_{15} . The corresponding tumour zones are respectively $\Omega(t_0)$, $\Omega(t_8)$, $\Omega(t_{15})$.

are denoted by $\rho_p(\mathbf{x}, t)$, $\rho_q(\mathbf{x}, t)$ and $\rho_N(\mathbf{x}, t)$ respectively, ($\mathbf{x} = (x, y, z) \in \Omega(t)$). They satisfy an advection-reaction-diffusion equation [15] [25]:

$$\frac{\partial \rho_l}{\partial t} + \nabla \cdot \mathbf{K} = Sr(\rho_l) + \nabla \cdot \mathbf{J} - Tr(\rho_l) \tag{5}$$

where, $l = p, q, N$ and:

- Sr is the modelling tumour cells natural death and birth phenomena;
- $\nabla \cdot \mathbf{J}$ models migratory movements; with $\mathbf{J} = D(\mathbf{x})\nabla \rho_l$, D is the diffusion coefficient;
- T models the cell death caused by radiotherapy;
- $\nabla \cdot$ is the divergence operator. $\mathbf{K} = \mathbf{v} \cdot \rho_l$ is the physical flow given by the system advection (all cells have the same advective velocity \mathbf{v}).

Since rectal tumours are solid tumours, we assume that there is no migratory phenomenon caused by cells movement. Therefore, \mathbf{J} in Equation (5) vanishes. The only cell movements considered are the movements caused by the tumour volume variation. The source term Sr is modelled by a logistic function:

$$S(\rho_l) = \zeta(pO_2)\rho_l \left(1 - \frac{\rho_l}{\Phi}\right) \tag{6}$$

with,

$$\zeta(pO_2) = \sigma \cdot \frac{1 + \tanh(pO_2 - pO_2^h)}{2} \tag{7}$$

where, $\sigma > 0$ is the intrinsic growth rate, Φ is the maximum capacity of a voxel. pO_2^h is the hypoxic threshold and \tanh represents the classical hyperbolic tangent function. The term ζ gives a distinction between proliferating and quiescent cells, and was inspired by [26]. Cells survival probability after irradiation is given by the time-dependent linear quadratic model [27].

$$SF(pO_2) = \exp\left(-\alpha d \cdot pO_2 \cdot \left(1 + \iota \cdot \frac{\beta}{\alpha} \cdot d \cdot pO_2\right)\right) \tag{8}$$

where, ι is an adjustment parameter of radiotherapy d accumulation while α and β are classical radio-sensitivities parameters. Thus, tumour cells densities killed by irradiation are modelled as:

$$T(\rho_i) = (1 - SF(pO_2)) \cdot \rho_i \quad (9)$$

In this study, a macroscopic representation of the oxygen partial pressure in the tumour is considered. Indeed, according to the value of the pO_2 in the voxel, for methodological reasons, it exists either a density of proliferating and necrotic cells, or only a density of quiescent and necrotic cells. After normalization, we obtain the following Relation (10):

$$\rho_p(\mathbf{x}, t) + \rho_N(\mathbf{x}, t) = 1 \quad \text{or} \quad \rho_q(\mathbf{x}, t) + \rho_N(\mathbf{x}, t) = 1 \quad (10)$$

As one can notice, Equation (5) is not closed because it has two unknown variables: cell density and velocity \mathbf{v} ($\mathbf{K} = \mathbf{v} \cdot \rho_i$). To close this equation, it is assumed that tumour environment is isotropic and porous, allowing to use Darcy's law:

$$\mathbf{v} = -\nabla \Pi \quad (11)$$

where, Π represents the local pressure. Based on the previous descriptions, tumour cells densities evolution equation is given by ($\rho \in \{\rho_p, \rho_q\}$):

$$\begin{cases} \nabla \cdot (\mathbf{v}(\mathbf{x}, t) \rho(\mathbf{x}, t)) = S(\rho(\mathbf{x}, t)) - T(\rho(\mathbf{x}, t)) \\ \partial_t \rho_N + \nabla \cdot (\mathbf{v} \rho_N) = 0 \\ \mathbf{v}(\mathbf{x}, t) = -\nabla \Pi(\mathbf{x}, t) \end{cases} \quad (12)$$

The determination of pressure Π will lead to the knowledge of \mathbf{v} allowing to close the system (12). By summing the first two equations of this system and by using (10), we obtain:

$$\nabla \cdot \mathbf{v} = S(\rho) - T(\rho) \quad (13)$$

Then by replacing \mathbf{v} by its expression given by (11) in (13), we obtain:

$$-\Delta \Pi = S(\rho) - T(\rho) \quad (14)$$

The system (15) summarizes all the equations needed for the simulation:

$$\begin{cases} \partial_t \rho(\mathbf{x}, t) + \nabla \cdot (\mathbf{v}(\mathbf{x}, t) \rho(\mathbf{x}, t)) = S(\rho(\mathbf{x}, t)) - T(\rho(\mathbf{x}, t)) \\ \partial_t \rho_N + \nabla \cdot (\mathbf{v} \rho_N) = 0 \\ \mathbf{v}(\mathbf{x}, t) = -\nabla \Pi(\mathbf{x}, t) \\ -\Delta \Pi = S(\rho) - T(\rho) \\ \Pi(\mathbf{x}, t) = 0 \\ \rho(\mathbf{x}, 0) = \rho_0(\mathbf{x}) \end{cases} \quad (15)$$

2.2. Simulation of the Biomechanical Model

2.2.1. Meshing and Simulation Algorithm

For simulation purposes we used a finite volumes based method and a 3D cartesian grid $[0, I_x] \times [0, I_y] \times [0, I_z]$, where I_x , I_y and I_z are voxels numbers in

the x , y and z directions, respectively (see **Figure 3**). This grid corresponds to the distribution of cells densities in the SUV medical images. The simulation of the first equation in system (15) was performed by using the Strang splitting method [28] [29] and then by determining the fields of proliferating and quiescent cells densities. For this latter purpose, Equations (16) and (17) are simulated:

$$\frac{\partial \rho}{\partial t}(\mathbf{x}, t) + \nabla(\rho(\mathbf{x}, t) \mathbf{v}(\mathbf{x}, t)) = 0 \tag{16}$$

$$\frac{d\rho}{dt}(\mathbf{x}, t) = S(\rho(\mathbf{x}, t)) - T(\rho(\mathbf{x}, t)) \tag{17}$$

In practice, the two equations above are simulated by running the following algorithm:

- 1) Equation (14) is used to determine the pressure field Π ;
- 2) Equation (11) is used to compute the velocity field \mathbf{v} , knowing the pressure field Π ;
- 3) Proliferating (ρ_p) and quiescent (ρ_q) cells densities are computed by simulating Equations (16) and (17);
- 4) If necessary, necrotic cells densities were computed as follows:

$$\rho_N = 1 - \rho_p - \rho_q.$$

The discretization and numerical schemes used are presented in the Subsection 6.1.

2.2.2. Evaluation of the Model

The proposed model (Equation (15)) contains three parameters: σ , Φ and ι , which are analyzed using Sobol sensitivity indices [30].

The tumour volume at time t is calculated by:

$$V(t) = \int_{\Omega(t)} 1_{\{\mathbf{x} / \rho(t, \mathbf{x}) > 0\}} d\mathbf{x} \tag{18}$$

where, $1_{\{\mathbf{x} / \rho(t, \mathbf{x}) > 0\}}$ is the indicator function defined on $\{\mathbf{x} / \rho(t, \mathbf{x}) > 0\}$.

The correlation formula for clinical and simulated volumes comparison is:

$$Corr(\%) = \left(1 - \frac{|V_s - V_c|}{V_c}\right) \cdot 100 \tag{19}$$

where, $Corr$ is the correlation result, V_s and V_c are the simulated and clinical volumes, respectively.

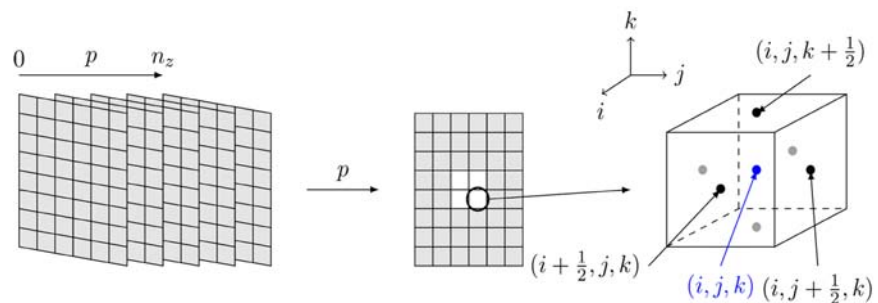


Figure 3. Meshing of the study domain.

3. Results

A clinical database containing 17 patients is used to evaluate the proposed model. First, optimal pO_2 distributions are estimated using the diffusion equation and the stochastic multi-scale model, as explained above. Second, the obtained pO_2 results are used as an input to the biomechanical model in order to simulate tumour volume evolution during radiotherapy. FDG PET images are used for both the pO_2 estimation and the tumour volume evolution for each patient.

3.1. Estimation of the pO_2 Distributions

The specific data for patient 5 and 12 are given as examples of obtained results. For these two patients, values for the parameter μ are 0.13 and 0.8 respectively. The distribution of oxygen partial pressure over time is given in **Figure 4** and **Figure 5**. In these figures, (a) and (c) show a cross-section of the pO_2 images at day 8 and day 15 after the beginning of irradiation; (b) and (d) are histograms over the whole volume of each of these pO_2 images. The estimation of pO_2 distributions for the whole set of patients is shown in **Table 2**. From this table one can see that oxygen partial pressure is increased for almost all patients after one week of treatment. This is an expected result but a validation cannot be put forward in the absence of a real pO_2 measurement. Nevertheless, the results suggest that the evolution of pO_2 should be taken into account for the tumour growth simulation, supporting published data [31].

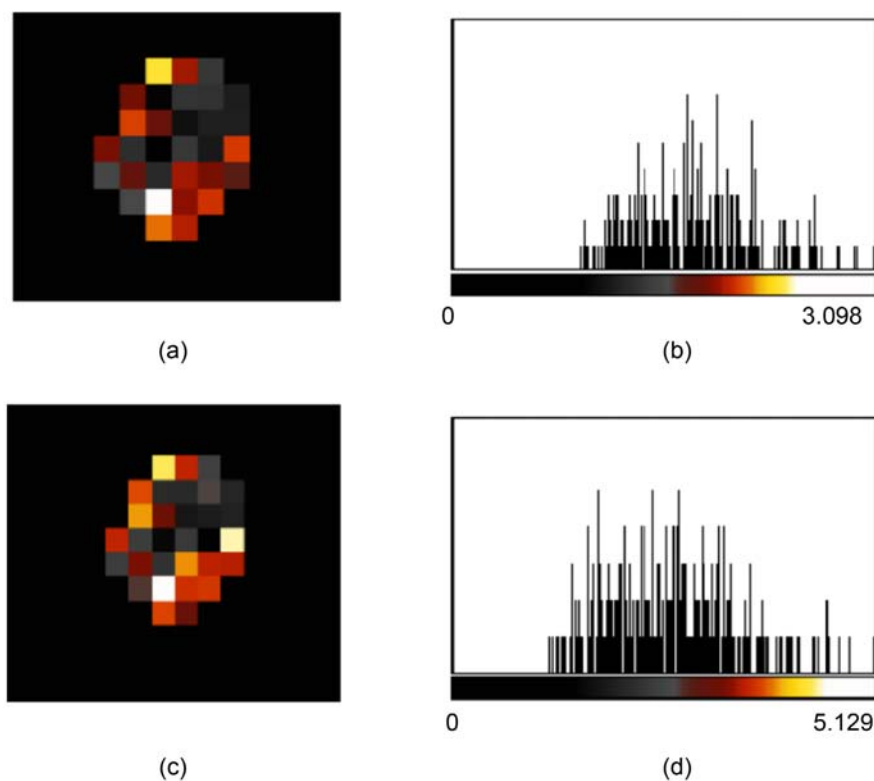


Figure 4. (a) and (c) sections of pO_2 distribution images, obtained at the 8th and 15th days, (b) and (d) histograms of these images for the patient 5 example.

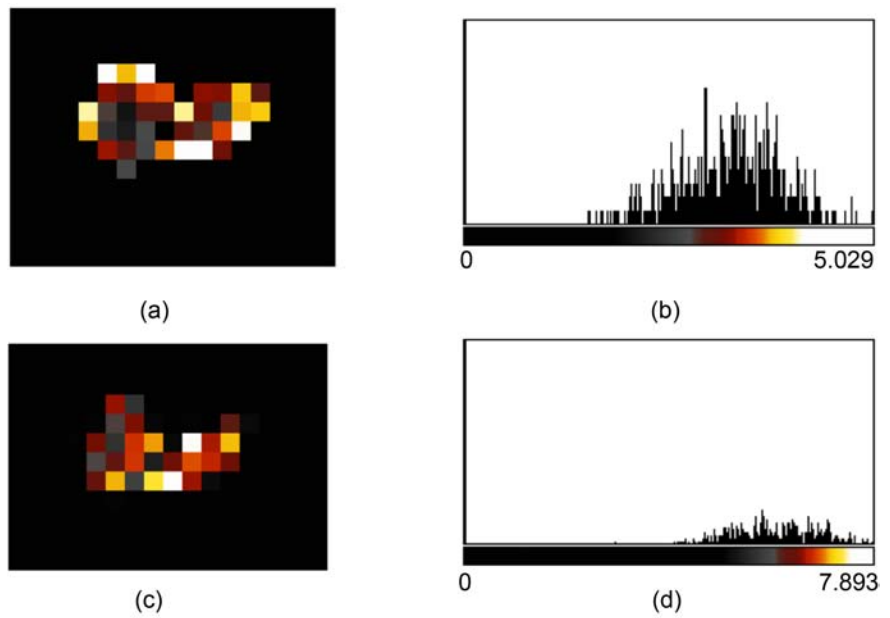


Figure 5. (a) and (c) sections of pO_2 distribution images, obtained at the 8th and 15th days, (b) and (d) histograms of these images of the patient 12 example.

Table 2. pO_2 optimal distributions results, at 8th (day 8) and 15th days (day 15) after the start of treatments. $\overline{pO_2,8}$ and $\overline{pO_2,15}$ are the pO_2 average values, respectively at the 8th and 15th days.

Patient #	day 8	$\overline{pO_2,8}$	day 15	$\overline{pO_2,15}$
1	$1.863 \leq pO_2 \leq 6.448$	4.525	$2.186 \leq pO_2 \leq 10.480$	6.787
2	$1.267 \leq pO_2 \leq 6.157$	3.59	$0.386 \leq pO_2 \leq 11.548$	6.886
3	$2.198 \leq pO_2 \leq 5.284$	3.688	$3.027 \leq pO_2 \leq 11.422$	8.281
4	$1.616 \leq pO_2 \leq 5.73$	3.646	$3.023 \leq pO_2 \leq 10.333$	6.991
5	$0.937 \leq pO_2 \leq 3.098$	1.768	$1.018 \leq pO_2 \leq 5.129$	2.696
6	$1.112 \leq pO_2 \leq 4.033$	2.656	$0.899 \leq pO_2 \leq 9.250$	5.717
7	$1.179 \leq pO_2 \leq 4.722$	3.043	$1.697 \leq pO_2 \leq 9.821$	6.345
8	$1.120 \leq pO_2 \leq 4.243$	2.308	$1.864 \leq pO_2 \leq 9.234$	5.236
9	$1.207 \leq pO_2 \leq 4.550$	2.969	$2.174 \leq pO_2 \leq 9.144$	6.129
10	$0.514 \leq pO_2 \leq 2.226$	1.185	$0.195 \leq pO_2 \leq 3.930$	0.670
11	$0.801 \leq pO_2 \leq 4.378$	1.812	$0.781 \leq pO_2 \leq 6.749$	3.275
12	$1.531 \leq pO_2 \leq 5.029$	3.257	$0.970 \leq pO_2 \leq 7.893$	6.717
13	$0.800 \leq pO_2 \leq 5.181$	2.449	$1.122 \leq pO_2 \leq 9.014$	5.053
14	$0.479 \leq pO_2 \leq 4.237$	1.602	$0.635 \leq pO_2 \leq 7.300$	3.187
15	$0.719 \leq pO_2 \leq 6.912$	3.003	$0.867 \leq pO_2 \leq 9.827$	5.338
16	$0.844 \leq pO_2 \leq 6.218$	3.100	$1.197 \leq pO_2 \leq 9.018$	5.129
17	$0.731 \leq pO_2 \leq 5.956$	2.439	$0.376 \leq pO_2 \leq 9.305$	4.887

3.2. Simulation of the Tumour Volume Evolution

According to the value of pO_2 in a voxel, the system of Equation (15) is simulated by considering only the proliferating and necrotic cells or only the necrotic and quiescent cells in the voxel. Sensitivities of biomechanical model parameters according to Sobol analysis are presented in **Table 3**. The results show that, contrary to parameters σ and ι , the parameter Φ can be fixed because a small disturbance of the latter does not influence the output of the model. Throughout the simulation and for all patients, we fixed $\Phi = 2$. The two other parameters are estimated using the annealing method [21] for each patient. As an illustration, tumour volume evolution during the treatment is showed, **Figure 6** illustrates the case of patient number 5 (and **Figure 7** shows a 2D section). Also, the

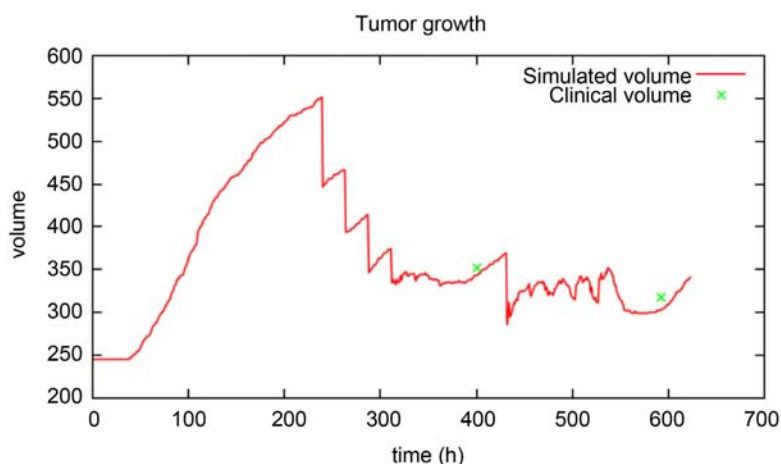


Figure 6. Tumour volume evolution, case of patient 5.

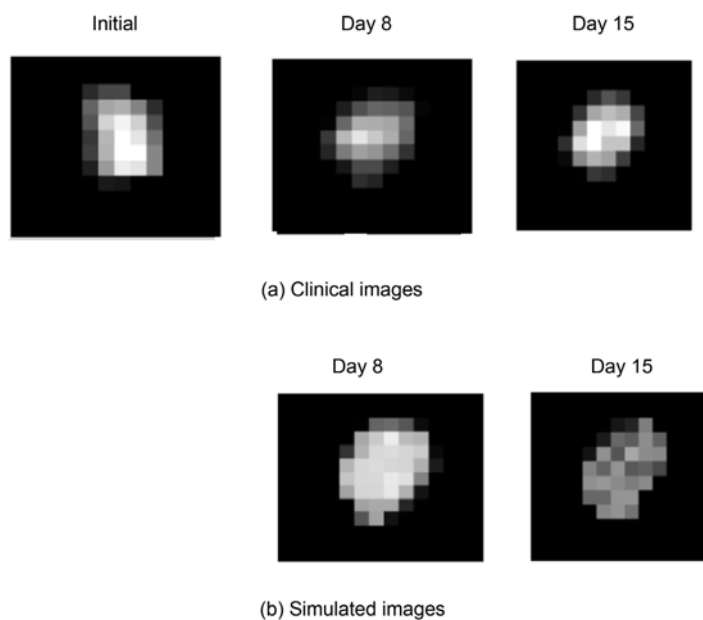


Figure 7. (a) Clinical SUV image and (b) Simulated SUV image, case of patient 5.

optimal adjustment parameters obtained for patients 5 and 12 are given in **Table 4**. The aim of **Table 5** is to give an overview of the correlations (using Equation (19)) between simulated and clinical images at day 8 and at day 15 after the beginning of radiotherapy. For day 15 one can observe that 10/17 of patients have a correlation superior to 90%, 4/17 of patients have an average correlation of 70% - 80%, 2/17 of patient have an average correlation of 60% - 70%, and 1/17 has an overall correlation <60.

Table 3. Sobol total sensitivity indices for the biomechanical model parameters.

Parameter #	Indice
σ	0.482031
Φ	0.020014
l	0.430759

Table 4. Optimal parameters obtained for patients 5 and 12.

Patient #	σ	Φ	l
5	0.028	2	0.001
12	0.00026	2	0.0016

Table 5. Results of correlations between clinical and simulated images at 8th and 15th days after the beginning of the irradiation.

Patient #	Correlations at day 8 (%)	Correlations at day 15 (%)
1	92.954	51.495
2	94.444	91.270
3	99.324	64.925
4	94.759	61.851
5	97.721	95.584
6	92.366	92.135
7	93.092	98.739
8	98.624	92.661
9	98.361	70.238
10	91.008	92.830
11	95.432	96.388
12	90.074	71.585
13	98.895	96.244
14	90.452	70.435
15	99.214	94
16	91.150	72
17	91.667	90.415

In order to compare the aggressiveness of tumours, the example of patient 12 is also given (see **Figure 9** and **Figure 10**). Additionally, **Figures 8-11** give a 3D representation of the simulation results for patients 5 and 12 respectively.

One of the objectives of this study is to build a model able to propose the potential extent of the tumour a few days before surgery in order to help resection planning. To this end, the model is also applied to four other patients who have one additional PET image a few days prior to surgery. Results can be seen on **Table 6** where correlations between simulated and clinical images are presented at day 8, day 15 and day 90 after the beginning of radiotherapy. Except for patient 19 who has a low correlation $<50\%$, the other three have a correlation $>90\%$.

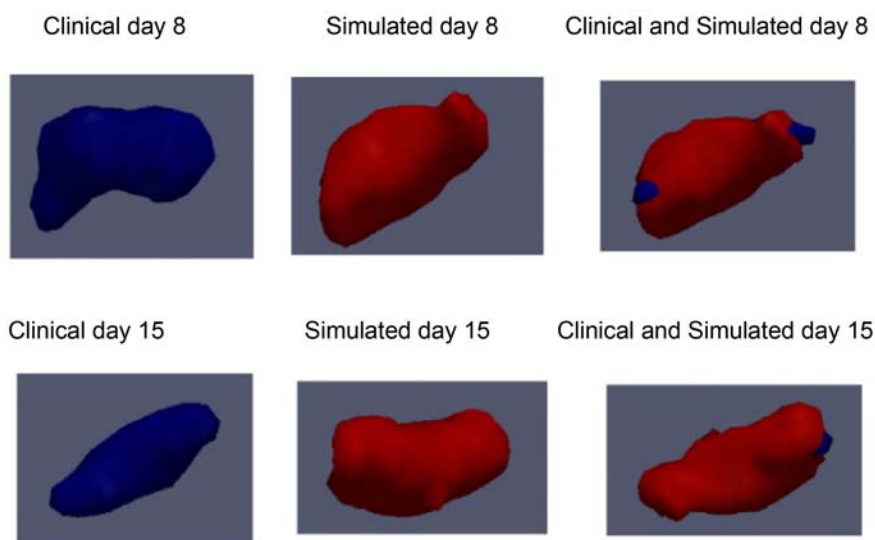


Figure 8. 3D illustration of clinical and simulated volumes, case of patient 5.

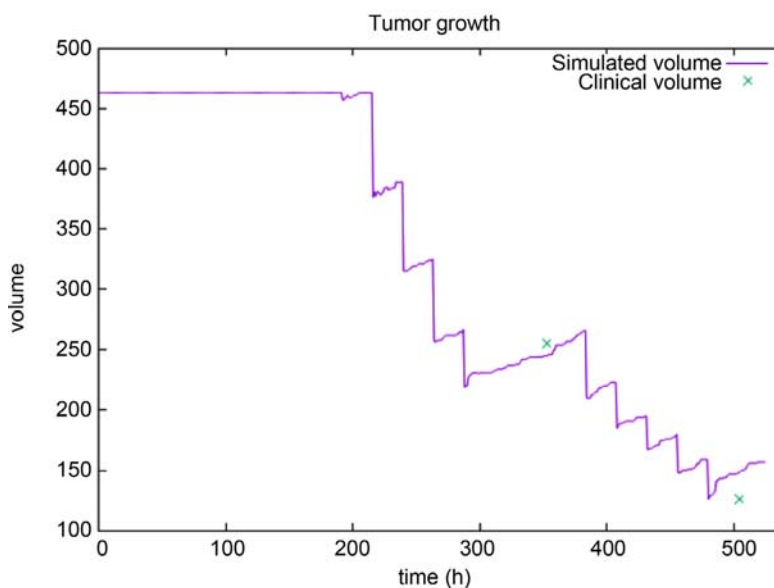


Figure 9. Tumour volume evolution, case of patient 12.

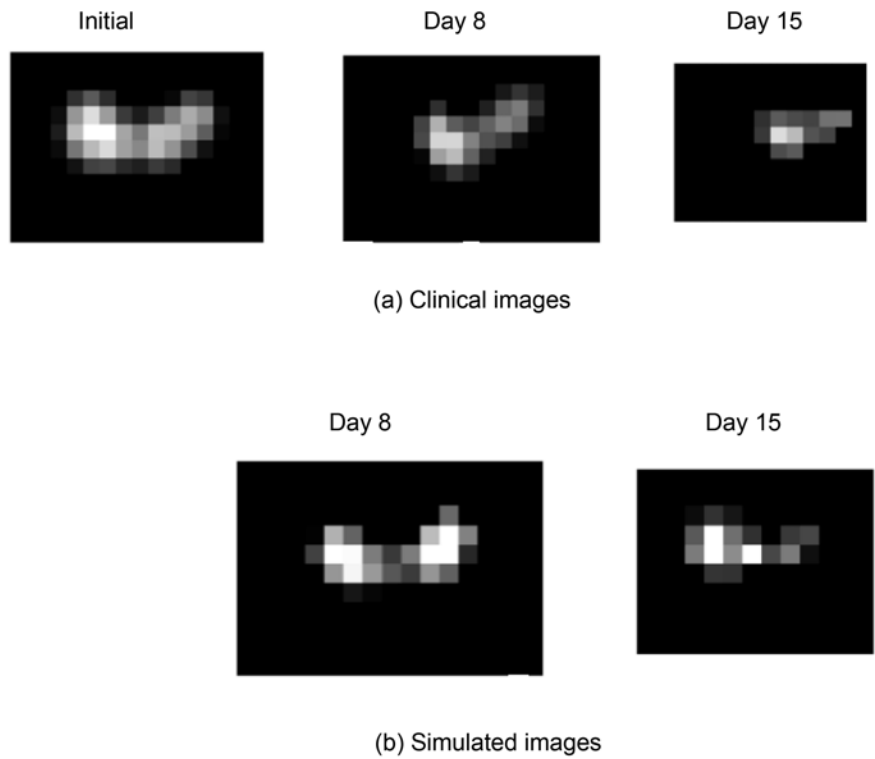


Figure 10. (a) Clinical SUV image and (b) Simulated SUV image, case of patient 12.

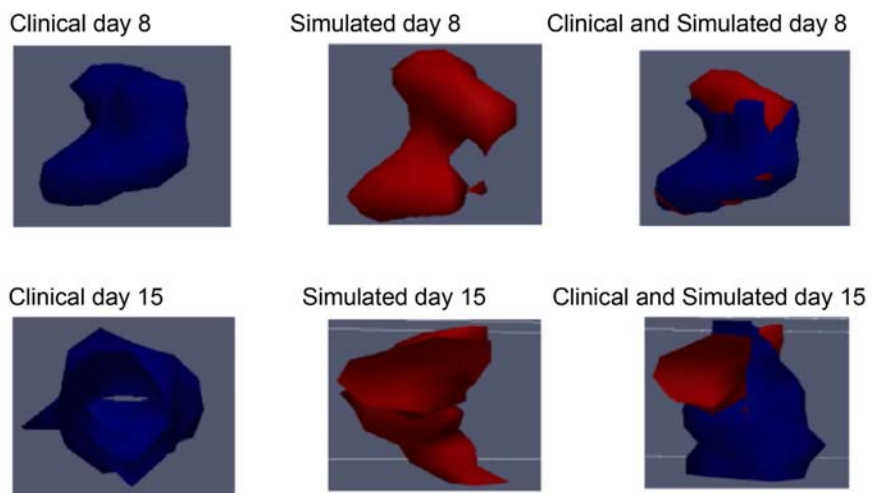


Figure 11. 3D illustration of clinical and simulated volumes, case of patient 12.

Table 6. Correlations results, between clinical and simulated images at the 8th (day 8), 15th (day 15) and 90th (day 90) days after the beginning of irradiation.

Patient #	day 8 (%)	day 15 (%)	day 90 (%)
18	97.861	86.186	90.698
19	98.540	90.0552	35.112
20	82.031	96.774	97.678
21	88.799	91.242	98.233

4. Discussion

The impact of pO_2 remains one of the most studied biological phenomena in simulations of tumour growth and tumour response to radiotherapy [32] [33]. Most of the latest studies focus either on space-time aspects via reaction-diffusion equations [34] or on purely biological aspects at the cellular level [35]. These algorithms are generally compared with each other [36] or challenged against theoretical models [37] or empirical information [38], but they are rarely confronted with real data. In the present work, we proposed a method based on fully-described reaction-diffusion equations driven by a cellular-based stochastic approach [16]. The obtained platform can be adapted to available clinical data and is evaluated by using a series of FDG PET images from 21 patients. The distribution of pO_2 inside the tumour is known to have an impact on radiotherapy effects, but it remains difficult to obtain personalized and reliable pO_2 information from images. Often, functional imaging during cancer monitoring only consists of FDG PET images depicting glucose metabolism. For this reason, we separated our simulation approach into two parts working concomitantly. The first part is a multi-scale model which simulates temporal and spatial evolution of oxygen concentration from available patient images. The second part simulates the tumour growth using a biomechanical approach based on the reaction-diffusion equations and the pO_2 knowledge as provided by the first step.

Concerning this second part, the source term is a logistic function whose growth rate depends on the oxygen partial pressure. This made the entire reaction term dependent on pO_2 , leading to an increased complexity. The challenge is to find the oxygen distribution that would provide the best prediction in terms of tumour volume evolution. This hybrid methodology is applied to a set of real data and the obtained results appeared satisfactory since a reasonably good agreement is observed between real and computed data (see **Table 5**). In addition to obtain information on the tumour volume evolution during radiotherapy, it is worth mentioning that the model also suggests a qualitative overview of the tumour aggressiveness. As an illustration, one can observe that the tumour of patient 5 is found more radioresistant than that of patient 12 (see **Figures 7-10**) while in the same time the simulated levels of oxygen partial pressure for patient 5 are found lower than those of patient 12 (**Table 2**). This difference in aggressiveness is also markedly observed before the beginning of treatments since tumour 5 appears to grow very rapidly while tumour 12 appears constant in volume. This general observation is in accordance with the obtained intrinsic growth rates, with σ values of 0.028 for patient 5 and 0.00026 for patient 12 (**Table 4**).

The above encouraging results suggest that this study will benefit from a validation on a larger database, including a comprehensive clinical follow-up of the patients. However, despite the variation of tumour cell densities between voxels, as driven by the computed flux, this model does not directly take into account tumour deformations. This is illustrated by the fact that according to Dice

Table 7. Dice index of simulated images on the 90th day after the beginning of irradiation, cases of patients 18, 19, 20 and 21.

Patient #	18	19	20	21
Dice	0.2456	0.1583	0.4062	0.5524

metric [39] the proposed hybrid model does not predict the tumour shape evolution accurately. Also known as an overlap index, the Dice metric is a similarity index that is widely used for volume comparison purposes. The values of Dice index for patients 18, 19, 20 and 21 are given in **Table 7** and show that simulated and real images at day 90 do not overlap (Dice < 0.6).

The mechanical constraints that are at the origin of the shape alteration are indeed difficult to control. This point clearly represents a potential improvement of our method, and in this context, it will be valuable to use anatomical information provided by CT or MRI images for example.

5. Conclusion

In this study, we proposed a methodology for simulating tumour growth and tumour response to radiation therapy. The adopted approach is based on the synergy between a discrete multi-scale stochastic model and a continuous model based on advection-reaction equations. This image-based process can be personalised according to available clinical data. The evaluation of the method on actual FDG images of patients suffering from rectal cancer is encouraging and opens several opportunities for improvement. The use of multi-modal images providing additional functional information instead of the single modality as presented here will certainly reinforce the robustness and the reliability of the simulations. Also, the introduction of morphological images like X-ray computed tomography is expected to help manage the mechanical constraints that can modify the shape of the tumour and influence its deformation.

Acknowledgements

The authors would like to thank the Bretagne Region and the LaTIM for their financial support.

Conflicts of Interest

The authors declare no conflicts of interest regarding the publication of this paper.

References

- [1] Bekker, R.A., Kim, S., Pilon-Thomas, S. and Enderling, H. (2022) Mathematical Modeling of Radiotherapy and Its Impact on Tumor Interactions with the Immune System. *Neoplasia*, **28**, Article ID: 100796. <https://doi.org/10.1016/j.neo.2022.100796>
- [2] Borkenstein, K., Levegrn, S. and Peschke, P. (2004) Modeling and Computer Simu-

- lations of Tumor Growth and Tumor Response to Radiotherapy. *Radiation Research*, **162**, 71-83. <https://doi.org/10.1667/RR3193>
- [3] Ribba, B., Colin, T. and Schnell, S. (2006) A Multiscale Mathematical Model of Cancer, and Its Use in Analyzing Irradiation Therapies. *Theoretical Biology and Medical Modelling*, **3**, 1-19. <https://doi.org/10.1186/1742-4682-3-7>
- [4] Lo, C.F. (2007) Stochastic Gompertz Model of Tumour Cell Growth. *Journal of Theoretical Biology*, **248**, 317-321. <https://doi.org/10.1016/j.jtbi.2007.04.024>
- [5] Iwata, K., Kawasaki, K. and Shigesada, N. (2000) A Dynamical Model for the Growth and Size Distribution of Multiple Metastatic Tumors. *Journal of Theoretical Biology*, **203**, 177-186. <https://doi.org/10.1006/jtbi.2000.1075>
- [6] Titz, B. and Jeraj, R. (2008) An Imaging-Based Tumour Growth and Treatment Response Model: Investigating the Effect of Tumour Oxygenation on Radiation Therapy Response. *Physics in Medicine & Biology*, **53**, 4471-4488. <https://doi.org/10.1088/0031-9155/53/17/001>
- [7] Titz, B., Kozak, K.R. and Jeraj, R. (2012) Computational Modelling of Anti-Angiogenic Therapies Based on Multiparametric Molecular Imaging Data. *Physics in Medicine & Biology*, **57**, 6079-6101. <https://doi.org/10.1088/0031-9155/57/19/6079>
- [8] Gerisch, A. and Chaplain, M.A.J. (2008) Mathematical Modelling of Cancer Cell Invasion of Tissue: Local and Non-Local Models and the Effect of Adhesion. *Journal of Theoretical Biology*, **250**, 684-704. <https://doi.org/10.1016/j.jtbi.2007.10.026>
- [9] Vaupel, P. (2004) Tumor Microenvironmental Physiology and Its Implications for Radiation Oncology. *Seminars in Radiation Oncology*, **14**, 198-206. <https://doi.org/10.1016/j.semradonc.2004.04.008>
- [10] Chen, Y.J., Cairns, R., Papandreou, I., Koong, A. and Denko, N.C. (2009) Oxygen Consumption Can Regulate the Growth of Tumors, a New Perspective on the Warburg Effect. *PLOS ONE*, **4**, e7033. <https://doi.org/10.1371/journal.pone.0007033>
- [11] Espinoza, I., Peschke, P. and Karger, C.P. (2013) A Model to Simulate the Oxygen Distribution in Hypoxic Tumors for Different Vascular Architectures. *Medical Physics*, **40**, Article ID: 081703. <https://doi.org/10.1118/1.4812431>
- [12] Grimes, D.R., Kannan, P., Warren, D.R., Markelc, B., Bates, R., Muschel, R. and Partridge, M. (2016) Estimating Oxygen Distribution from Vasculature in Three-Dimensional Tumour Tissue. *Journal of the Royal Society Interface*, **13**, Article ID: 20160070. <https://doi.org/10.1098/rsif.2016.0070>
- [13] Daşu, A., Toma-Daşu, I. and Karlsson, M. (2003) Theoretical Simulation of Tumour Oxygenation and Results from Acute and Chronic Hypoxia. *Physics in Medicine & Biology*, **48**, 2829-2842. <https://doi.org/10.1088/0031-9155/48/17/307>
- [14] Powathil, G.G., Gordon, K.E., Hill, L.A. and Chaplain, M.A.J. (2012) Modelling the Effects of Cell-Cycle Heterogeneity on the Response of a Solid Tumour to Chemotherapy: Biological Insights from a Hybrid Multiscale Cellular Automaton Model. *Journal of Theoretical Biology*, **308**, 1-19. <https://doi.org/10.1016/j.jtbi.2012.05.015>
- [15] Mi, H.M., Petitjean, C., Dubray, B., Vera, P. and Ruan, S. (2014) Prediction of Lung Tumor Evolution during Radiotherapy in Individual Patients with PET. *IEEE Transactions on Medical Imaging*, **33**, 995-1003. <https://doi.org/10.1109/TMI.2014.2301892>
- [16] Apeke, S., Gaubert, L., Bousson, N., Lambin, P., Visvikis, D., Rodin, V. and Redou, P. (2018) Multi-Scale Modeling and Oxygen Impact on Tumor Temporal Evolution: Application on Rectal Cancer during Radiotherapy. *IEEE Transactions on Medical Imaging*, **37**, 871-880. <https://doi.org/10.1109/TMI.2017.2771379>
- [17] Gérard, A., Buyse, M., Nordlinger, B., Loygue, J., Pène, F., Kempf, P., Bosset, J.F.,

- Gignoux, M., Arnaud, J.P. and Desaive, C. (1988) Preoperative Radiotherapy as Adjuvant Treatment in Rectal Cancer. Final Results of a Randomized Study of the European Organization for Research and Treatment of Cancer (EORTC). *Annals of Surgery*, **208**, 606-614. <https://doi.org/10.1097/00000658-198811000-00011>
- [18] Toma-Dașu, I. and Dașu, A. (2013) Modelling Tumour Oxygenation, Reoxygenation and Implications on Treatment Outcome. *Computational and Mathematical Methods in Medicine*, **2013**, Article ID: 141087. <https://doi.org/10.1155/2013/141087>
- [19] Gambhir, S.S., Czernin, J., Schwimmer, J., Silverman, D.H., Coleman, R.E. and Phelps, M.E. (2001) A Tabulated Summary of the FDG PET Literature. *Journal of Nuclear Medicine*, **42**, 1S-93S.
- [20] Bertout, J.A., Patel, S.A. and Simon, M.C. (2008) The Impact of O₂ Availability on Human Cancer. *Nature Reviews Cancer*, **8**, 967-975. <https://doi.org/10.1038/nrc2540>
- [21] Kirkpatrick, S., Gelatt, C.D. and Vecchi, M.P. (1983) Optimization by Simulated Annealing. *Science*, **220**, 671-680. <https://doi.org/10.1126/science.220.4598.671>
- [22] Kim, C.K., Gupta, N.C., Chandramouli, B. and Alavi, A. (1994) Standardized Uptake Values of FDG: Body Surface Area Correction Is Preferable to Body Weight Correction. *Journal of Nuclear Medicine*, **35**, 164-167.
- [23] Ferreira, S.C., Martins, M.L. and Vilela, M.J. (2002) Reaction-Diffusion Model for the Growth of Avascular Tumor. *Physical Review E*, **65**, Article ID: 021907. <https://doi.org/10.1103/PhysRevE.65.021907>
- [24] Wallace, D.I. and Guo, X.Y. (2013) Properties of Tumor Spheroid Growth Exhibited by Simple Mathematical Models. *Frontiers in Oncology*, **3**, Article No. 51. <https://doi.org/10.3389/fonc.2013.00051>
- [25] Konukoglu, E., Sermesant, M., Clatz, O., Peyrat, J.-M., Delingette, H. and Ayache, N. (2007) A Recursive Anisotropic Fast Marching Approach to Reaction Diffusion Equation: Application to Tumor Growth Modeling. *20th International Conference, IPMI 2007*, Kerkrade, 2-6 July 2007, 687-699.
- [26] Cornelis, F., Saut, O., Cumsill, P., Lombardi, D., Iollo, A., Palussiere, J. and Colin, T. (2013) La modélisation mathématique *in Vivo* de la croissance tumorale sur les données de l'imagerie: Un avenir proche? *Journal de Radiologie Diagnostique et Interventionnelle*, **94**, 610-617. <https://doi.org/10.1016/j.jradio.2013.02.008>
- [27] Brenner, D.J., Hlatky, L.R., Hahnfeldt, P.J., Huang, Y. and Sachs, R.K. (1998) The Linear-Quadratic Model and Most Other Common Radiobiological Models Result in Similar Predictions of Time-Dose Relationships. *Radiation Research*, **150**, 83-91. <https://doi.org/10.2307/3579648>
- [28] Castella, F., Chartier, P., Descombes, S. and Vilmart, G. (2009) Splitting Methods with Complex Times for Parabolic Equations. *BIT Numerical Mathematics*, **49**, 487-508. <https://doi.org/10.1007/s10543-009-0235-y>
- [29] Glowinski, R. and Le Tallec, P. (1989) Augmented Lagrangian and Operator-Splitting Methods in Nonlinear Mechanics. Society for Industrial and Applied Mathematics, University City. <https://doi.org/10.1137/1.9781611970838>
- [30] Nossent, J., Elsen, P. and Bauwens, W. (2011) Sobol' Sensitivity Analysis of a Complex Environmental Model. *Environmental Modelling & Software*, **26**, 1515-1525. <https://doi.org/10.1016/j.envsoft.2011.08.010>
- [31] Lyng, H., Sundfør, K. and Rofstad, E.K. (2000) Changes in Tumor Oxygen Tension during Radiotherapy of Uterine Cervical Cancer: Relationships to Changes in Vascular Density, Cell Density, and Frequency of Mitosis and Apoptosis. *International*

- Journal of Radiation Oncology, Biology, Physics*, **46**, 935-946.
[https://doi.org/10.1016/S0360-3016\(99\)00497-6](https://doi.org/10.1016/S0360-3016(99)00497-6)
- [32] Petit, S.F., Lambin, P., Seigneuric, R., Murrer, L., Riel, N.A.W., van Dekker, A.L.J. and Wouters, B.G. (2007) Realistic Cellular Oxygen Model Reveals High Potential Gains with Dose Painting and Offers a General Solution for Incorporating Cellular Distributions That Underlie Imaging Data. *International Journal of Radiation Oncology, Biology, Physics*, **69**, S69. <https://doi.org/10.1016/j.ijrobp.2007.07.126>
- [33] Harriss-Phillips, W.M., Bezak, E. and Potter, A. (2016) Stochastic Predictions of Cell Kill during Stereotactic Ablative Radiation Therapy: Do Hypoxia and Reoxygenation Really Matter? *International Journal of Radiation Oncology, Biology, Physics*, **95**, 1290-1297. <https://doi.org/10.1016/j.ijrobp.2016.03.014>
- [34] Roque, T., Risser, L., Kersemans, V., Smart, S., Allen, D., Kinchesh, P., Gilchrist, S., Gomes, A.L., Schnabel, J.A. and Chappell, M.A. (2018) A DCE-MRI Driven 3-D Reaction-Diffusion Model of Solid Tumor Growth. *IEEE Transactions on Medical Imaging*, **37**, 724-732. <https://doi.org/10.1109/TMI.2017.2779811>
- [35] Zangoeei, M.H. and Habibi, J. (2017) Hybrid Multiscale Modeling and Prediction of Cancer Cell Behavior. *PLOS ONE*, **12**, e0183810. <https://doi.org/10.1371/journal.pone.0183810>
- [36] Elaff, I. (2018) Comparative Study between Spatio-Temporal Models for Brain Tumor Growth. *Biochemical and Biophysical Research Communications*, **496**, 1263-1268. <https://doi.org/10.1016/j.bbrc.2018.01.183>
- [37] Sundstrom, A., Bar-Sagi, D. and Mishra, B. (2016) Simulating Heterogeneous Tumor Cell Populations. *PLOS ONE*, **11**, e0168984. <https://doi.org/10.1371/journal.pone.0168984>
- [38] Forster, J.C., Douglass, M.J.J., Harriss-Phillips, W.M. and Bezak, E. (2017) Development of an *in Silico* Stochastic 4D Model of Tumor Growth with Angiogenesis. *Medical Physics*, **44**, 1563-1576. <https://doi.org/10.1002/mp.12130>
- [39] Taha, A.A. and Hanbury, A. (2015) Metrics for Evaluating 3D Medical Image Segmentation: Analysis, Selection, and Tool. *BMC Medical Imaging*, **15**, Article No. 29. <https://doi.org/10.1186/s12880-015-0068-x>
- [40] Jiang, G.-S. and Wu, C.-C. (1999) A High-Order WENO Finite Difference Scheme for the Equations of Ideal Magnetohydrodynamics. *Journal of Computational Physics*, **150**, 561-594. <https://doi.org/10.1006/jcph.1999.6207>

Appendix

Discretization and Numerical Schemes

Denote by $\rho_{i,j,k}^n = \rho((x_i, y_j, z_k), t_n)$, the local cells densities at time t_n and at the position (x_i, y_j, z_k) , by $\mathbf{v}_{i,j,k}^n = \mathbf{v}((x_i, y_j, z_k), t_n)$ and $\Pi_{i,j,k}^n = \Pi((x_i, y_j, z_k), t_n)$ the corresponding advection velocity and local pressure respectively. The numerical approaches used for the simulation are as follows:

- A finite difference method based on an implicit Euler scheme is used for simulating Equation (14);
- A finite volume method with the 5th order WENO scheme (Weighted Essentially Non-Oscillatory [40]) is used for simulation of Equation (16). By re-writing this equation in the form:

$$\partial_t \rho + \partial_x (v_x \rho) + \partial_y (v_y \rho) + \partial_z (v_z \rho) = 0 \quad (20)$$

and by integrating it, we obtain:

$$\bar{\rho}_{ijk}^{n+1/2} = \bar{\rho}_{ijk}^n - \frac{\Delta t}{\Delta x} (F_{i+1/2} - F_{i-1/2}) - \frac{\Delta t}{\Delta y} (G_{j+1/2} - G_{j-1/2}) - \frac{\Delta t}{\Delta z} (H_{k+1/2} - H_{k-1/2}) \quad (21)$$

where, $\bar{\rho}_{ijk}^n$ is the mean local tumour cells densities, F_i , G_j and H_k , are their numerical flow, respectively in the x , y and z directions. For all i , j and k , we wrote $\Delta x_i = \Delta x$, $\Delta y_j = \Delta y$, and $\Delta z_k = \Delta z$, with Δx , Δy , and Δz representing voxel dimensions in the x , y and z directions. Δt is the time step;

- A finite differences method based on an explicit Euler scheme is used for simulating Equation (17), with a discretization given by:

$$\bar{\rho}_{ijk}^{n+1} = \bar{\rho}_{ijk}^{n+1/2} + \Delta t \cdot (S_{i,j,k}^{n+1/2} - T_{i,j,k}^{n+1/2}) \quad (22)$$

where, $S_{i,j,k}^{n+1/2} = S(\bar{\rho}(x_i, y_j, z_k, t+1/2))$, and $T_{i,j,k}^{n+1/2} = T(\bar{\rho}(x_i, y_j, z_k, t+1/2))$.

Study on Plant Radiation Signal Transduction for Human Self-Healing

Xinzhou Yuan, Jafeng Yuan, Qiao Bi*, Kongzhi Song

Shenzhen Xinzhou Bio-Information Technology Co., Ltd., Shenzhen, China

Email: *biqiao@gmail.com

How to cite this paper: Yuan, X.Z., Yuan, J.F., Bi, Q. and Song, K.Z. (2022) Study on Plant Radiation Signal Transduction for Human Self-Healing. *Open Journal of Biophysics*, 12, 265-283.

<https://doi.org/10.4236/ojbiphy.2022.124013>

Received: August 17, 2022

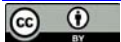
Accepted: October 25, 2022

Published: October 28, 2022

Copyright © 2022 by author(s) and Scientific Research Publishing Inc.

This work is licensed under the Creative Commons Attribution International License (CC BY 4.0).

<http://creativecommons.org/licenses/by/4.0/>



Open Access

Abstract

We selected 450 patients with chronic and difficult diseases as receptors, and selected edible and medicinal plant combinations as biological signal donors, and randomly participated in a new experiment. After adjusting the patient's biological field, the compensating bio information energy (CBE) high-tech is applied to transmit the signal of plant radiation to the patient's body. The physical therapy of this health care mode has the characteristics of no contact, no drugs, no intervention, no toxic side effects, no pain, and no electromagnetic radiation and so on. Before and after the experiment, the main function test, cell function, cell biochemistry and body temperature of each patient were used for the same body control and data statistical analysis, and then the comprehensive integration method was used to evaluate the effect. We found that after 1 - 4 courses of treatment (7 - 28 dx 2h), the potential disease risk of patients was significantly reduced, the relevant medical indicators improved rapidly, and the cell function and symptoms improved simultaneously. The effective rate was up to 90%, the significant efficiency was up to 57%. This experiment shows that this new physical therapy can treat both symptoms and root causes, make chronic and difficult diseases self-healing and rehabilitation, and has no ethical problems. It also shows that information on plant health can play an important role in reversing cell aging and restoring cell function. Therefore, it opens up a new field of natural therapy, which can be called cell information therapy.

Keywords

Plant Signal, DNA Communication, Cell Information Therapy, CBE Technology

1. Introduction

In the 1920s, the former Soviet biologist Gulovich first discovered biological

signals and non-contact biological effects through the famous onion experiment [1]. Jiangcan Zheng, a Chinese scientist in the former Soviet Union, has made many incredible achievements in improving human function and transferring genetic traits through allogeneic biological signal transmission by using the technology of physical shielding, which was once supported by the former Soviet Academy of Sciences and Chinese experts [2].

We have taken a different approach and applied CBE technology to directionally select the signal of plant radiation to deliver it to the human body, so that the functions of the organs, tissues and corresponding cell systems of patients with chronic and difficult diseases can achieve self-healing and recovery [3]. This is a method for directional transfer of plant information to achieve self-healing and recovery of cells. This information is expressed through the change of signal energy, which is the information “nutrient” needed by cells, and can reverse cell aging and restore cell function. Therefore, we can call this plant signal as information energy [4]. On the basis of this research, we discovered a natural therapy for compensating bioinformatic energy [5], which is a new type of physical therapy derived from plant (biological) information, which can realize cell self-healing and recovery, referred to as cell information therapy. Since 2018, we have tried to make 450 patients with chronic and difficult diseases randomly participate in the experiment of CBE technology transferring plant combined signals to human body by using double-blind method and same body control. During the experiment, according to the different conditions of their functional improvement, they were arranged to gradually reduce or stop the drugs without psychological induction and suggestion, and there were also no other therapies. We only focus on improving the basic function of patients, and making the same body control with the results of cell biochemical test, cell function and body temperature test; from qualitative to quantitative, the comprehensive integration method was used to determine the experimental results, and the effect was tracked for more than one year.

2. Materials and Methods

2.1. Information Donors and Receptor

In order to ensure that good information donors will provide good information of human cells in the experiment, we have strict standards for the selection of donor plants: give priority to the food and vegetable sprouts eaten by the human, and select the traditional Chinese medicine plants commonly used by the human body and verified by a large number of human experiments, which are beneficial, harmless and in the process of vigorous growth according to the different conditions of patients. Considering the fact that the famous onion experiment found that the biological signal comes from the process of cell division, we chose grain, vegetable buds and vigorous growth of traditional Chinese medicine plants as the donors of plant information, as shown in **Figure 1**. Our experimental results show that plants will radiate young and vigorous growth information in the

process of growth, and the information power density is large, that is, the amount of information is large, which can accelerate the reversal of cell aging and restore human cell function. In addition, the biological experimental results of many repeatable molecular transfer free genetic traits show that DNA signal is the most basic signal in biological signals [6]. According to the theory of atomic emission spectrum and absorption spectrum [7], we speculate that the change of atomic energy level in DNA macromolecules may be a process of controlling life activities. When the atoms in DNA molecules fall from high-energy state to low-energy state, DNA will release energy quantum, On the contrary, when it rises from low-energy state to high-energy state, DNA needs to receive energetic particles, which may be a reason for DNA radiation or absorption of signals, expression or acceptance of life information; biological information is expressed through some complex changes of biological signals. Therefore, we have developed biological radiation signal power detection equipment to detect the radiation signal power of selected plant signal donors, as shown in **Figure 2**. In the experiment, for the sake of rigor, we also made a strict selection for the selection of information donors, and formulated quantitative criteria.

The receptors in the experiment are randomly selected patients with various chronic and difficult diseases, all of whom are difficult to treat and cannot be cured by current medical treatment, including 241 male patients and 209 female patients, the youngest being 4 years old and the oldest being 84 years old; among them, about 20% of critically ill patients, about 70% of patients suffering from various underlying diseases and complications, and about 10% of difficult diseases.



Figure 1. It shows the selected hydroponic grain and vegetable sprouts on the left and the selected living traditional Chinese medicine plants on the right. What is put on the wooden frame is to put it into the equipment as an information donor according to the combination of hydroponic buds and traditional Chinese medicine plants prepared for each patient.



Figure 2. The equipment shown is a plant radiation signal power detector, and the staff is doing plant radiation signal power detection.

2.2. Experimental Equipment

All the experimental equipments are developed and manufactured by ourselves, and we have obtained relevant Chinese patents, as shown in **Figure 3**. Among them, the biological information self-healing and rehabilitation cabin is referred to as the rehabilitation cabin [8], as shown in **Figure 3(a)**; the biological information self-healing and rehabilitation machine [9], referred to as the rehabilitation machine, as shown in **Figure 3(b)**; the vision self-healing and rehabilitation machine [10], as seen in **Figure 3(c)**; the bio-field rehabilitation bed [11], can be seen in **Figure 3(d)**. The above-mentioned special equipments are all equipped with “the system for directional transfer of biological signals” [12], which are installed in the above-mentioned different equipments according to different treatment needs.

2.3. Basic Principle and Composition of CBE Technology

2.3.1. Basic Principles

When the functions or structures of cells, tissues, organs and other systems change, the biological signals radiated by them will change first, which can be used as an important basis for judging whether they are not ill (possible lesions), such as the application of cardiac and brain electrical signals. Moreover, we also found that when the signals radiated by cells, tissues, organs and other systems are modulated by external matched biological signals, it will also affect the changes of the function or structure of the original system [13], which is the basic principle on which CBE is used.



Figure 3. It shows the main equipment of cell information therapy. (a) Shows the biological information self-healing recovery cabin, referred to as the recovery cabin, whose function is to restore the immune function of the human body. (b) Shows the biological information self-healing rehabilitation machine, referred to as the rehabilitation machine, and its function is to treat human cell diseases. (c) Shows the vision self-healing rehabilitation machine, the function is to restore the vision function. (d) Shows the Bio-field Rehabilitation Bed, whose function is to adjust the human bio-field.

2.3.2. Three Part Composition

Through experiments, we have found that different plants will radiate different biological signals and have different improvement effects on different cells of the human body [14]. Therefore, we believe that DNA in different cells may radiate different life signals and receive corresponding life signals, so different life signal effects will be produced. The patients who participated in the experiment at random had different diseases. According to the different conditions of each patient, we choose different combinations of living plants to output their signals, including grain, vegetables, and bean sprouts; there are combinations of traditional Chinese medicine plants; and the combination of grain, vegetables and traditional Chinese medicine plants, we call it as a “recipe”. During the recovery process, the plant recipe must be adjusted according to their physical recovery and needs. The experimental results show that the correct recipe will accelerate the recovery of the patient’s function, which is similar to the traditional Chinese medicine formula for conditioning and curing diseases.

According to the basic principles of quantum physics and low-energy particle accelerator, we have invented the biological signal transfer system in CBE technology by using a variety of new technologies, which realizes the functions of directional acquisition, processing, acceleration, maximum signal-to-noise ratio

and directional transfer of plant signals to human cells. This new technology has developed a new structure and biological signal wave processing process, which greatly reduces the manufacturing cost. Through the directional acceleration of plant signal field, it realizes the maximum power density of plant signal output and increases the amount of information received by receptor cells per unit time. According to the different needs of patients, CBE signal transfer system can be installed on different equipment to facilitate the application of human treatment.

Furthermore, according to the theory of Chinese medicine and the successful practice of plant-based treatment of diseases for thousands of years, as well as the advantages of plant varieties such as diversification, universality, low cost and no ethical problems, we determine to give priority to grain, vegetable buds and seedlings, as well as traditional Chinese medicine plants in the growth process as the donors of biological signals. The experiments show that plants radiate stronger signals, greater and better information in the process of cell division, the role of repairing cells is more obvious [15], so we have strict technical standard control over the cultivation, management, detection and use of plants, and also pay attention to control the size and quantity of plants according to the equipment requirements.

2.4. CBE Plant Signal Processing Program

In the experiment, we processed the biological signals transferred by CBE technology as following **Figure 4**.

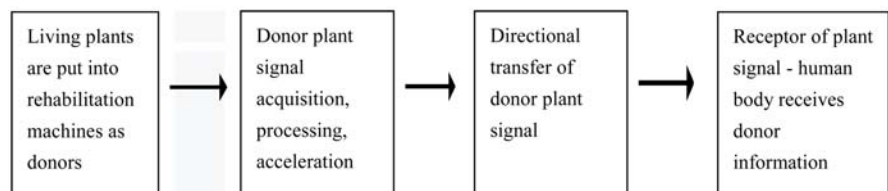


Figure 4. The biological signals transferred by CBE technology.

2.5. Experimental Methods

We used the TJQQ-ZDJTEQAM quantum resonance detector to determine the efficacy of plant information [16], and screened out several groups of grains, vegetable hydroponic plants, and living traditional Chinese medicine plants that have high efficacy in improving patient function and are beneficial and harmless, as shown in **Figure 2**; the biological signal radiation power detector developed by us is applied, as shown in **Figure 3**. The radiation power of each plant can be used only after reaching a certain value.

In the above experimental equipment, different varieties and quantities of the above plants selected according to the experimenter's different symptoms are used as information donors and placed on the special rack in the equipment, as shown in **Figure 3(a)** and **Figure 3(b)**. The patients participating in the experiment receive plant signals for 40 min each time in the rehabilitation cabin, as shown in **Figure 3(a)**, to realize the overall conditioning of the whole body and

mind, and restore or improve the immune function. Patients generally need to lie still in the rehabilitation machine for 30 - 40 min, as shown in **Figure 3(b)**. During this period, plant signals are directed to different parts of the patient's body, so that cells in different organs can also receive signals. The experimenter of vision rehabilitation receives the selected plant information on the biological information vision self-healing rehabilitation machine for 30 min, as shown in **Figure 3(c)**. Some patients need to regulate the body biological field on the rehabilitation bed for 40 minutes to improve the function of body cell radiation signal and increase cell activity (*i.e.* detoxification in traditional Chinese Medicine), as shown in **Figure 3(d)**. Generally, patients take 7 days as a course of treatment, and the cell recovery time is about 14 hours (7 dx 2h). However, patients with a long course of disease and older age need to be extended to 3 - 4 courses of treatment (21 - 28 dx 2h). Usually, young people or patients with short course of disease and less medication improve their function faster while those with older age and longer course of disease need to prolong the treatment time.

2.6. Effect and Analysis

2.6.1. Improvement of Function and Symptoms

450 people participated in the experiment randomly. After 1 - 4 courses of cell information therapy (7 - 28 dx 2h), 405 of them improved their function and symptoms, as shown in **Figure 5**, the orange column area, accounting for 90% of the total number of people; among them, 256 people have obvious improvement, which is the blue column area, accounting for 57% of the total number. Another 10% did not improve, as shown in the light green column area in **Figure 5**, because no biological information donor plant for the patient's disease was found.

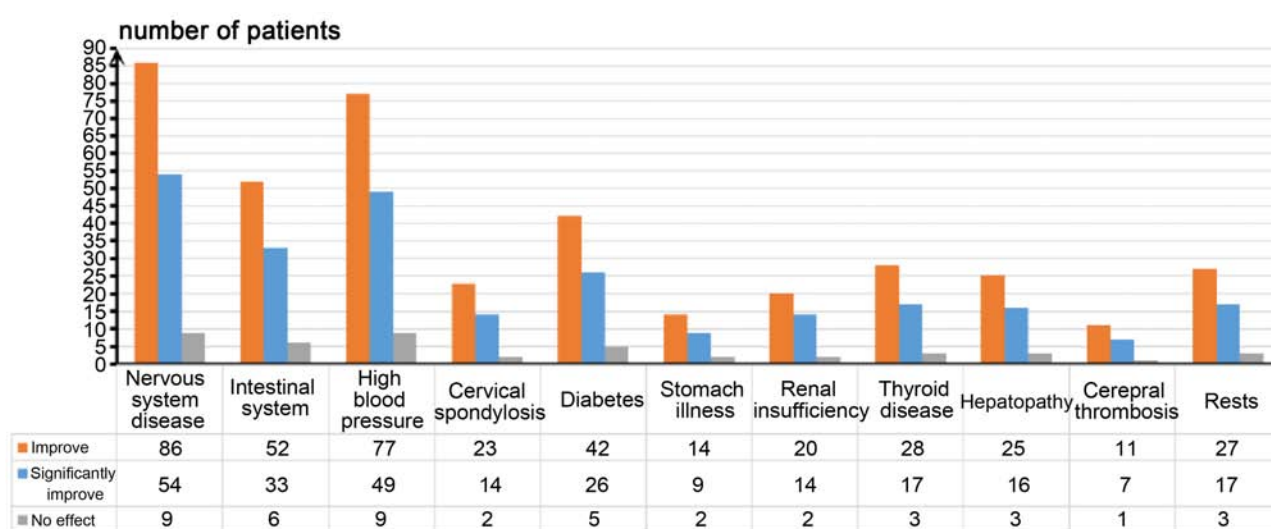


Figure 5. It shows the statistical graph of the effect of 450 patients with chronic and intractable diseases participating in cell information therapy. There are 405 patients with functional improvement, see the orange column, and the effective rate reaches 90%; 256 patients have obvious improvement, see the blue column area, and the effective rate is as high as 57%; 45 patients have no effect, see light black columnar area.

It is very important to find the correct biological information donor plant for the patient's disease. At present, we have accumulated some experience and related technical patents in this regard. **Figure 6** is a summary chart of the visual acuity test of a group of ten people after 6 days of cell information therapy. From the table, we can see that the vision of these ten people was significantly improved after 6 days of the therapy.

2.6.2. Reduce the Risk of Major Diseases

Patients with chronic diseases and difficult diseases are at risk of cerebral infarction and myocardial infarction. Cell information therapy can quickly reduce the risk of these two common serious diseases. In order to protect against unexpected events, we use cardiovascular disease risk prediction equipment to test each patient before treatment. The above picture in **Figure 7** is a patient who was found to be at risk of stroke after 5 days of cell information treatment. The risk of stroke disappeared; the lower picture in **Figure 7** shows a patient who was at risk of myocardial infarction due to the discomfort of the heart area. After the electrocardiographic (ECG) examination, he was found to be in danger of myocardial infarction. Then after a course of cell information therapy, his ECG returned to normal and his suffering symptoms disappeared. So far, we have completed the experiment of more than 10,000 cases of chronic and critical patients, which not only did not have any medical accidents, but also extended the life of critical patients with quality.

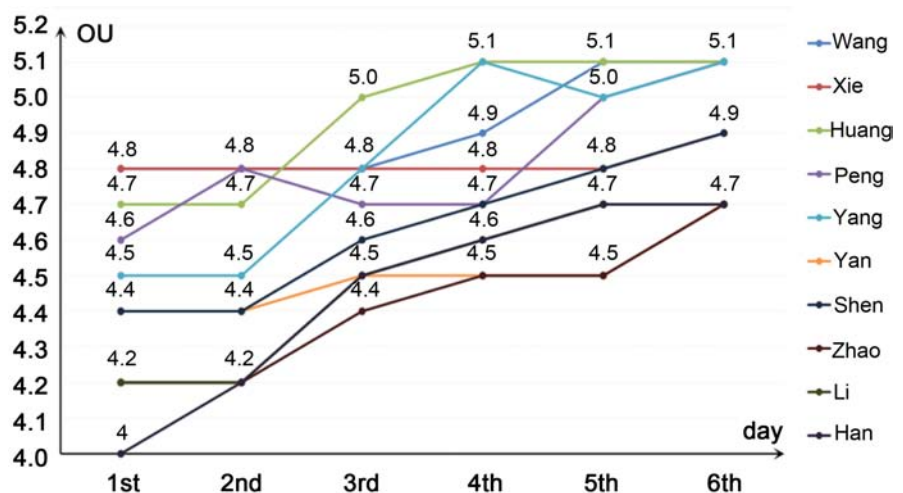


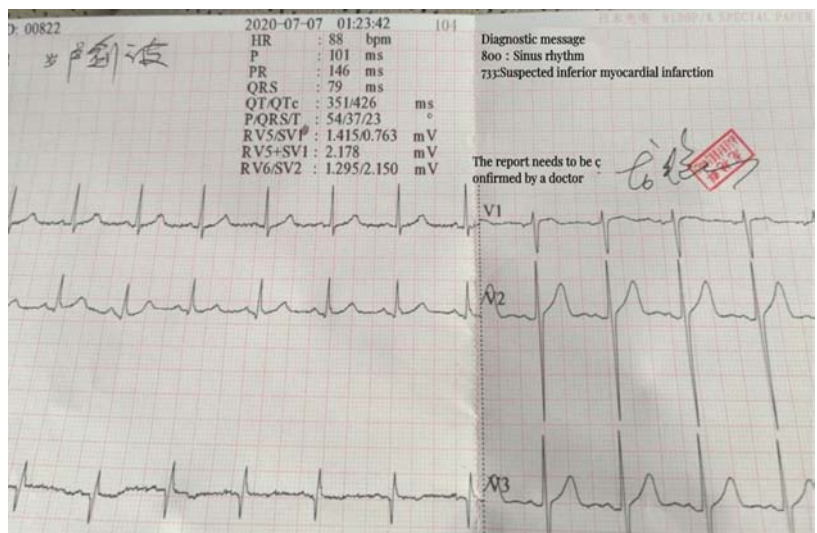
Figure 6. It shows the statistical chart of the self-healing and rehabilitation effect of vision in ten patients with chronic and difficult diseases after participating in cell information therapy. From the data point of view, these ten patients have different visual acuity starting points, ranging from 4 to 4.7. After six days and six times of information treatment, their visual acuity increased to 5.1, indicating that their visual acuity has improved, and some are fast. The visual acuity improved to 5.1 in four days; some were slow, for example, Xie's visual acuity improved from 4.7 to 4.9 after the sixth day; other patients gradually improved every day, which shows that the effect varies from person to person. The effect of self-healing and rehabilitation of vision forms 10 broken lines with different colors. The general trend is that the vision is improving after the treatment every day.



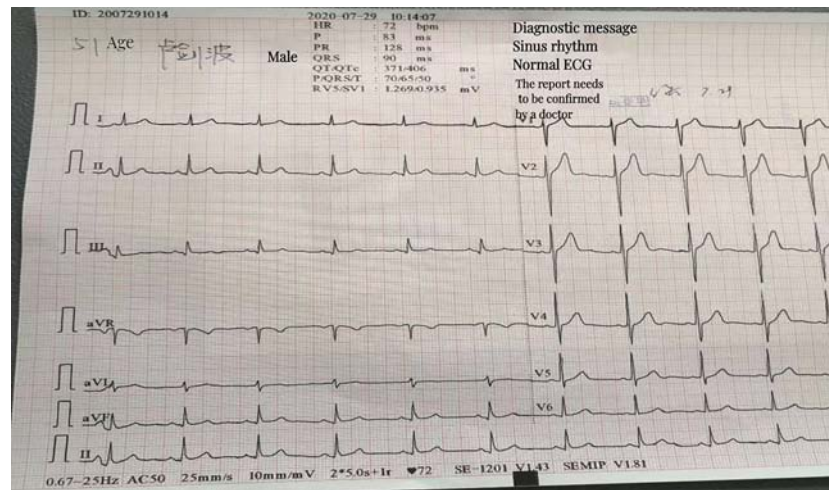
(a)



(b)



(c)



(d)

Figure 7. The picture above shows the comparison report of serious disease risk detection before and after a patient's cell information therapy. The green circle is normal, and the yellow indicates that there is a risk of disease. One can see the upper left picture of the patient's test report. The stroke risk and cardiovascular function appear yellow, indicating that the patient is at risk of serious illness; the upper right picture is after 5 days of treatment, both yellow circles have turned green, indicating that reduced risk of serious illness. The picture below is the comparison report of the ECG test before and after the cell information therapy for patients with myocardial infarction. The picture below on the left shows that the ECG has myocardial infarction and the patient has obvious symptoms. The picture below on the right shows the normal ECG after a course of treatment improves consistency.

2.6.3. The "Three Highs" Indicators Have Dropped Significantly

The patients with chronic diseases participating in the experiment generally suffer from hypertension, hyperglycemia, hyperlipemia, low immunity and other diseases. Over the years, they have been taking various drugs and various treatments. The effect is not ideal, their physical functions are low, and even they can't take care of themselves. After 3 - 4 courses of cell information therapy (21 - 28 dx 2h), their higher indexes decreased significantly, as shown in **Figure 8**. For example, when the patient's blood pressure drops to about 120/90 mmHg and they start to stop or reduce the dosage, the blood pressure and other indicators will have different repetitions. Then continue the treatment, and it is found that the indicators gradually drop to the safe range. We can see from **Figure 8** that the decline of blood glucose and blood pressure has a fluctuating process and a nonlinear decline. At the same time, the experimenter's diet, digestive function, physical fitness, sleep and other aspects have been significantly improved. Even patients who were unable to take care of themselves before in life have now become able to take care of themselves.

2.6.4. Body Temperature Increased Significantly and Heart Function Improved

The previous research results of Chinese experts show that after the human body receives plant information, the immune function is improved [17]. **Figure 9** is

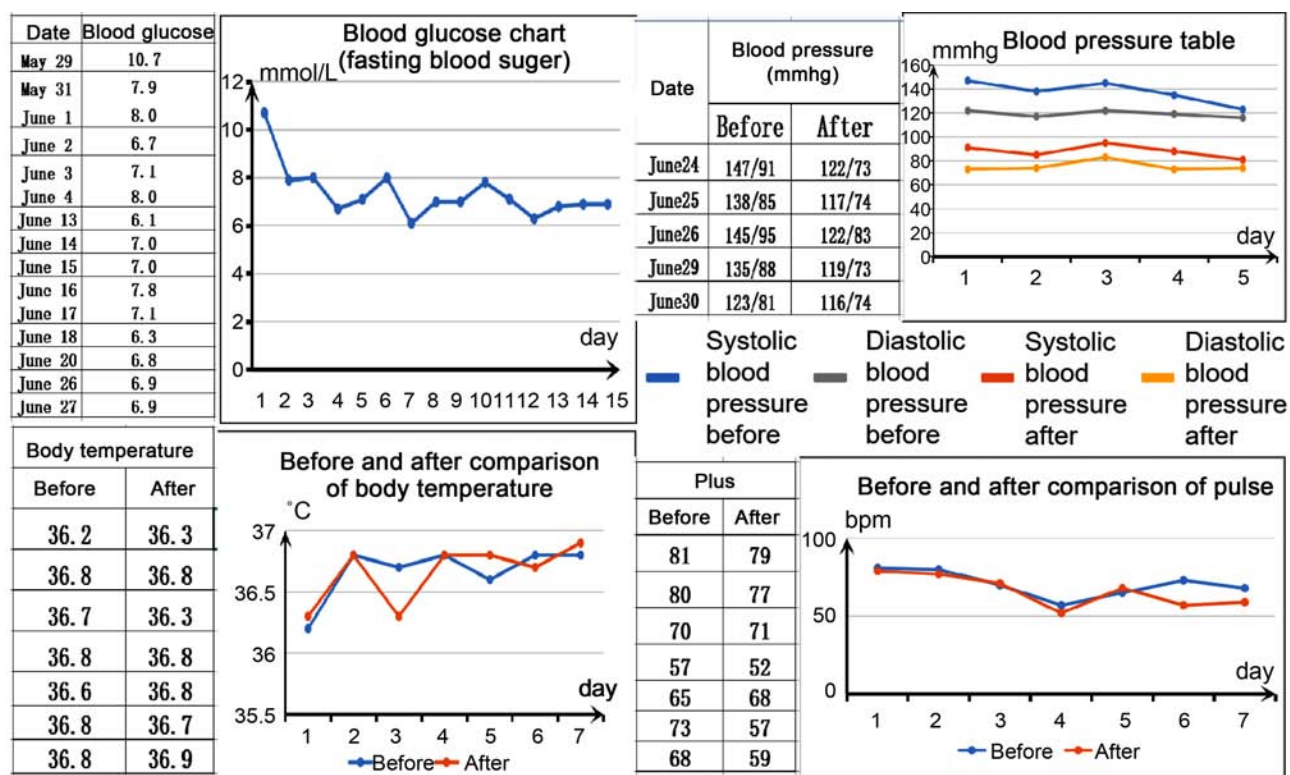


Figure 8. It shows the improvement chart of blood glucose, blood pressure, body temperature, and pulse before and after a patient's cell information therapy. After the previous treatment, the patient has stopped taking the drug. It can be seen from the upper left picture that the fasting blood sugar value of the patient decreased with the number of days of treatment. After 15 days of treatment, the fasting blood sugar dropped from 10.7 to 6.9; from the upper right picture, it can be seen that the blood pressure also decreases with the number of days of treatment. After 6 days of treatment, the blood pressure drops from 147/91 mmHg to 116/79 mmHg, indicating that the cardiovascular function has improved; the patient's body temperature is low but rises faster, see the lower left picture. The patient's body temperature should be checked every day before treatment, see the blue line. Body temperature should be checked after treatment on the same day, see the yellow line. The patient's body temperature before treatment was 36.5°C, and the temperature rose from 35.5°C to 37.5°C on the second day after treatment. After 7 treatments over 7 days, the patient's body temperature remained basically normal at around 37.5°C. The bottom right graph is the patient's pulse, which decreased from 80 beats per minute to 59 beats per minute after 7 days of treatment. It shows that the blood supply function of the heart has been improved to some extent.

the result of testing by the Biology Teaching and Research Office of Hunan Medical University. The report shows that the number of NK and T cells increases significantly after the human body receives plant information. For this reason, we have also done the results of NK cell detection in 31 patients after receiving biological information, and found that there is also a significant increase, $p < 0.05$; using TJQQ-ZDJTEQAM quantum resonance detector detection also found that the immune function has improved, $p < 0.001$ [18]; further, heart function was also significantly improved in patients with heart disease after receiving plant information [19]. Taking these results into consideration, in this experiment, the patient's body temperature was monitored every day before and after health care treatment. From **Figure 8**, we can see that the patient's body temperature was low before health care, and the body temperature increased significantly after health care. After treatment, the body temperature increased

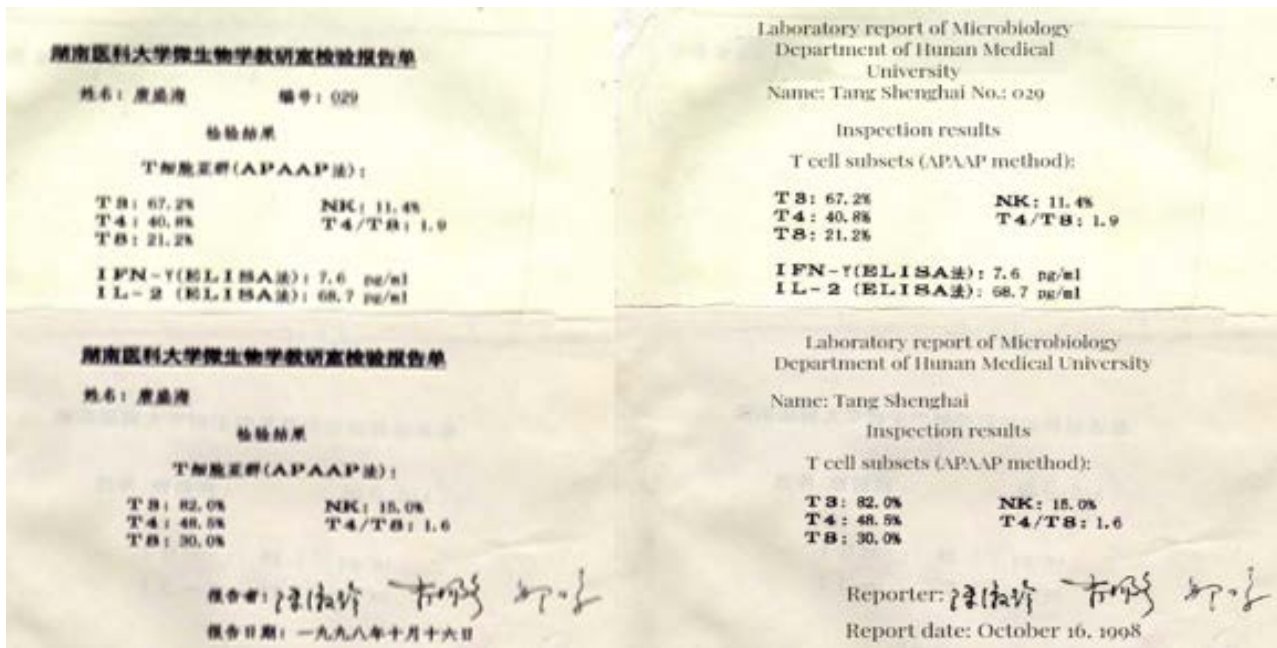


Figure 9. It shows the detection report of NK and T cells before and after the chronic disease patient Tang received plant information. The picture on the left is the comparison report of the microbiology laboratory of Hunan Medical University (the picture on the right is the translation). The upper left picture is the detection result of immune cells before treatment, and the lower left picture is the detection result of immune cells after treatment. The comparison report showed that after information therapy, T3 increased from 67.2% to 82.0%, T4 increased from 40.8% to 48.5%, T8 increased from 21.2% to 30.0%, and the number of NK cells increased from 11.4% to 15.0%, indicating that cell information therapy can increase the number of immune cells in the body.

by more than 90%. This increase in body temperature indicates that the patient's immunity has been improved and improved significantly. This shows that the research results of this experiment are consistent with the previous research results, indicating that information therapy is indeed to possess the effect of significantly improving the immune function and heart function of the human body.

2.6.5. Self-Healing, Rehabilitation of Human Function and Reversing Cellular Aging

The relevant results of previous information experiments also show that plant information can significantly improve or enhance the functions of human digestion, grip strength, physical fitness, vision and sexual desire, which is the performance of reversing human cell aging. In 2019, we cooperated with Guangzhou Jinshaiyou hospital and used our technology and equipment to conduct a clinical experiment to restore the male function of patients with chronic diseases. Before treatment, the patients with chronic diseases who participated in the experiment almost lost their male function. After 1 - 3 courses of cell information therapy, their sexual function was restored to varying degrees without adverse reactions. On October 20, 2019, a Guangdong andrology expert appraisal meeting was held in Guangzhou Biological Island. The experts at the meeting fully affirmed our "cooperative clinical experiment" and believed that this new information therapy can significantly improve the male function of patients with

chronic diseases.

In the course of this treatment, more than 90% of the patients have improved appetite, increased grip strength, increased physical fitness, improved vision, sexual function, etc.; their skin has become moist and bright, the wrinkles on the face are reduced, and the ratio of beard to hair turns out that the growth is fast, and even the hair of the elderly in the 80s is obviously darkened. These improved effects show that cell information therapy can reverse cellular aging and achieve a certain degree of rejuvenation in the human body.

2.6.6. Cell Function Improvement

Using the SCIO biofeedback instrument (Certified Drug (Jin) Letter 2012 No. 2213148 of the China Food and Drug Administration) for cell function detection, the improvement of cell function can be judged, as shown in **Table 1**. The values in the chart are the results of the comparison before and after cell information therapy. Different colors and values represent different functional states of cells; red means high values indicate that the cell function is in danger or sick. When the color in the chart on the right changes, the value becomes smaller, or the color becomes lighter, or the red disappears, it means that the cell function is restored. We believe that diseases all start from the decline of cell function. The signals that are transferred to human cells through CBE technology can directly pass through different cells of the human body without obstacles. The cells can choose to absorb the information they need. After receiving a certain amount of information, the problematic cells recover their function and communicate the information inside and outside the cells, so all kinds of cell-related diseases have been recovered or even cured. The test results can be seen in **Tables 1-3** below.

Table 1 shows the comparison of the data detected by SCIO biofeedback instrument before and after treatment. From the color and data, we can see the improvement or significant improvement of the patient's cells after treatment. **Table 2** shows the comparative data of cell biochemical tests and follow-up records of a group of patients in Taiwan, China before and after cell therapy. Those patients go to Taiwan hospital for examination before and after treatment, so the data in the table is different from that in Chinese Mainland. We can see from the data that the cell biochemical test data of Taiwan patients have significantly improved after treatment. The follow-up one to three years also found that the response effect is getting better and better. **Table 3** is a comparative report of biochemical test data of a 4-year-old girl with gene mutation before and after cell therapy. From the data, many cell functions of the little girl have been significantly improved. In conclusion, the changes of the above cell data show that cell information therapy is that plant information restores the function of cells. The general procedure for the end of cell information therapy is: patients should go to the corresponding hospital for testing 1 - 2 months after the end of their health care course, then return to the self-healing and rehabilitation center, submit the test report of the corresponding hospital, and then do the cell function test, and do the same test requirements one year later to judge the effect.

Table 1. Comparison table of cell function test reports.

Name: Song Age: 54

Gender: Man first test: 2021/11/23

Second test: 2021/11/27

Detection equipment: cell information detector

Test instructions:

1) Do a test before conditioning, and then do a test after conditioning, and compare the results of the two tests

2) Red: the cell function is significantly reduced; Yellow and dark yellow indicate varying degrees of decline in cell function

Project name	Before	Later	Evaluation of effects	Project name	Before	Later	Evaluation of effects
Risk of vascular damage to the brain	5	0.9	Substantial improvement	Function of tendon	2.6	0.8	Substantial improvement
Poor circulation	2.8	1.6	Improvement	Risk of fibrositis	2.5	0.7	Improvement
Lung function	3.3	2.9	Improvement	The lumbar spine	2.6	2.2	Improvement
The small intestine function	2.8	2.1	Improvement	Risk of abnormal cholesterol metabolism	3.2	2.4	Substantial improvement
Jejunum function	2.8	1.4	Improvement	Alanine deficiency	2.5	1.2	Improvement
Indigestion	4	3.8	Improvement	Magnesium deficiency	3.4	3.2	Improvement
Protein dyspepsia	4	3.8	Improvement	Deficiency of the mineral calcium	3.1	2.5	Improvement
Disturbance of intestinal flora	3.6	1.7	Substantial improvement	Mineral potassium deficiency	2.5	2.4	Improvement
Hormone imbalance	4.4	3.3	Improvement	Vitamin C deficiency	4.8	2.6	Substantial improvement
Testosterone	4.4	0.8	Substantial improvement	Deficiency of vitamin B1	2.7	2.4	Improvement
Endocrine disorder	4.5	3.3	Improvement	Vitamin E deficiency	2.7	2.1	Improvement
Thyroid stimulating hormone releasing hormone	4.5	1.2	Substantial improvement				

2.7. Evaluation of the Effect of Cell Information Therapy

Qian Xuesen, a famous Chinese scholar, once put forward this view: the human body is an open giant complex system. Neither the Prigogine method nor the Haken method can be used to study it. Those methods cannot be used. Only the qualitative to quantitative comprehensive integration method can be used, that is, the general principles of system theory method can be combined with the

Table 2. Comparison of biochemical examination reports of Taiwan patients before and after cellular information therapy. Red: outlier light; blue: improved; dark blue: significantly improved green: normal.

No	Name	Sex	Age	Project	Date of examination	Prior treatment	Date of examination	After treatment	Normal values	Track record
1	Li	Man	76	Cholesterol	2010.2.26	5.6	2010.3.12	4.9	2.9 - 5.2	2011.8—good 2012.9—good
				Intermediate cell content		17.6		14.7	3 - 16	
				Absolute value of neutrophil		1.7		0.6	2 - 7	
				Neutrophil percentag		43.52		50.6	50 - 70	
2	Zheng	Man	60	Uric acid	2011.2.15	8	2011.3.11	7.7	4 - 7.5	2012.9—good
				Blood sugar before meal		106		95	70 - 100	
				Total cholesterol		225		206	<200	
				LDL cholesterol		135		112	<100	
3	Shi	Woman	54	Triglyceride	2011.2.15	202	2011.3.11	176	<150	2012.9—good
				Total cholesterol		216		169	<200	
				LDL cholesterol		114		102	<100	
4	Yan	Man	64	Total cholesterol	2010.2.18	212	2010.4.2	172	0 - 200	
				Blood sugar before meal		119		96	70 - 100	
5	Feng	Man	64	Cholesterol	2010.02.15	236	2010.03.10	217	135 - 200	2012.9—good 2015.3—good
				Triglyceride		168		111	50 - 150	
				Blood sugar before meal		117		102	70 - 110	
				White blood cells		10,800		9400	4500 - 10,000	
6	Lin	Woman	57	TSH	2011.11.11	92.217	2011.11.21	11.221	0.35 - 5.5	2012.9—good 2014.10—good
				LDL-C (calc)		*TG > 400		141	<100	
				T-CHOL/HDL-C		14.44		4.56	<5	
				Total cholesterol		520		228	<200	
				Blood fat		2586		186	<100	
				Mean RBC volume MCV		92.8		92.2	80 - 92 fl	
				White blood cell count WBC		3.2		4.7	(4 - 9) × 10 ⁹ /L	

development of computer-based modern information technology to form a specific method system, To solve the problem of such a complex giant system as the human body [20]. The process of this experiment described above follows the

Table 3. Comparison of biochemical test reports of the patient.

Date of examination	2020/10/22		2021/4/8		2021/5/13	
Project	Former	Reference value	In the treatment	Reference value	After	Reference value
The urea	2.61		2.36		3.96	2.9 - 8.2
Creatinine	24		27		28	45 - 84
Uric acid	245		243		225	155 - 357
Bicarbonate root	22.5		22.3		24.7	22 - 29
Endogenous creatinine clearance	147.3		134.2		108.8	75 - 115
The elf inhibition C	0.53		0.58		0.71	0 - 1.03
Retinol binding protein	24.7		30.2		25.9	25 - 70
Albumin/globulin	1.5	1.5 - 2.5	1.4	1.2 - 2.4	1.6	1.2 - 2.4
Y-glutamyl transpeptidase	25	0 - 50	27	0 - 50	37	0 - 50
Alanine aminotransferase	87	7 - 45	43	7 - 45	44	7 - 45
Ratio of millet straw to mille propyl	0.9		1.7		1.6	
Before the albumin	138.5	250 - 400	161	250 - 400		170 - 420
Cholinesterase	2965		3752			5000 - 12,000
Aspartate aminotransferase	80	13 - 40	74	13 - 40	69	13 - 40
Total bile acid	6.5		7.4		5.7	0 - 10
Alkaline phosphatase	369	40 - 750	352	40 - 750		20 - 500
Lactic acid	11.54	12 - 16	1.55	0.63 - 2.44	1.87	0.63 - 2.44
Plasma ammonia determination	77	18 - 72	46	18 - 72	56	18 - 72
Activated partial thrombin time	42.7	23 - 40	34	23 - 40	33.6	23 - 40
Fibrinogen	2.19	2 - 5	1.83	2 - 5	1.78	2 - 5
Prothrombin time	18.6	9 - 15	12.5	9 - 15	12.8	9 - 15
International standardized ratio	1.7	0.8 - 1.4	1.06	0.8 - 1.4	1.09	0.8 - 1.4

Note: red is abnormal item, green is improved item after treatment; no filling color is within the normal value range.

principle of comprehensive integration method to deal with and solve the problems of this experiment. In fact, the patients who randomly participated in the cell therapy experiment in this experiment are patients with chronic or difficult diseases who have failed to be treated for a long time by modern medical treatment, and they all suffer from a variety of diseases and can't even take care of themselves. The comparative data of the improvement of various functional test results after their own experiment is a convincing proof. Therefore, the identification of this experimental effect attempts to use the method from qualitative to quantitative, and then use the comprehensive integration method to compare the same body effect. The participants of cell therapy take videos and photos for qualitative comparative observation before and after each course of treatment.

Each time, they make detailed medical records, enter into the database, and analyze, evaluate and track the effect.

3. Conclusions and Prospect

1) In this experiment, the improvement of multiple functions of patients is parallel to the results of cell biochemistry and other tests, and there are follow-up effects, which shows that: the macro and micro effects of patients have achieved self-healing and rehabilitation, and the process can be carried out at the cell level, that is, cell information therapy has achieved both symptoms and root causes, which is an effect that is difficult to achieve in general medical treatment.

2) Many chronic diseases and intractable diseases belong to polygenic problems, thus becoming medical and health problems. The results of the rapid and obvious improvement of the patient's function by plant information in this experiment show that the cell information therapy has a certain repair effect on the patient's genes not only at the cellular level but also at the gene level. In this experiment, we found that if the plant information is compensated for the human body in time, it can reverse human aging to some extent.

3) The cell information therapy in this experiment is aimed at patients using plant formulas to transmit plant information. Human organs and cells receive some biophysical signals of plant radiation. Under the effective control of plant formulas, these signals have no adverse effects on human organs and cells. Of course, continuously exploring and improving the "prescription" of plant information combination should be an important direction of future research.

Acknowledgements

The author thanks the Science and Technology Committee of Liaoning Old Professors Association and Shenzhen Health Management Association for their support!

Availability of Data and Materials

The datasets obtained and analyzed for this study will be made available from the corresponding author in a reasonable request.

Authors' Information

Xinzhou Yuan, Jafeng Yuan, Qiao Bi, and Kongzhi Song are researchers in the Shenzhen Xinzhou Biological Information Technology Co., LTD., Zip code: 518115, Shenzhen, China.

Contributions

Xinzhou Yuan, Jafeng Yuan, Qiao Bi, and Kongzhi Song wrote the main manuscript text, and Xinzhou Yuan and Jafeng Yuan prepared the experimental data, forms and related figures. Four authors all reviewed the manuscript.

Consent for Publication

All authors contributed to the article and approved the submitted version for publication.

Funding

This study is supported by the Shenzhen Xinzhou Biological Information Technology Co., LTD. The Shenzhen Xinzhou Biological Information Technology is a high tech company.

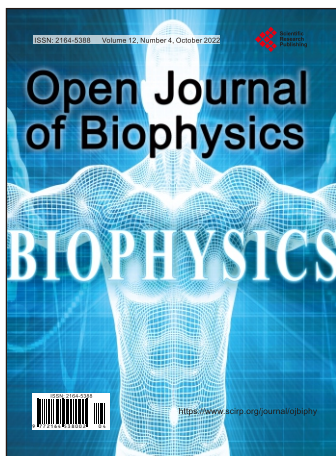
Competing Interests

There are no competing interests with this article.

References

- [1] Gu, Q. (2014) Biophotonics. Science Press, Beijing. (In Chinese)
- [2] Jiang, C. and Yuan, X. (2010) Bioelectromagnetic Wave Disclosure—Field Conductance Discovery. Dakang Publishing House, Taiwan, 83-308. (In Chinese)
- [3] Yuan, X. (2017) Experimental Research on Bioinformatics (Energy) Self-Healing Therapy. Compilation of Papers on Research Progress in Human Science, Beijing. (In Chinese)
- [4] Yuan, X., *et al.* (2010) It Is Urgent to Compensate the Biological Information Energy. *Medical Information*, **22**, 228-239. (In Chinese)
- [5] Yuan, X. (2010) Compensating Bioinformatics Energy—New Natural Therapy. *Medical Information*, **23**, 334. (In Chinese)
- [6] Yuan, X. (2016) Exploration and Discovery of Life Signals. Compilation of Papers on the Progress of Human Science Research, Beijing. (In Chinese)
- [7] Wang, H., Zhang, W. and Li, G. (2000) University Basic Physics. China Higher Education Press, Beijing, 394-397. (In Chinese)
- [8] Yuan, X. (2010) Combined Biological Information Energy Compensation Device. Chinese Patents, cn201020667266.92010. (In Chinese)
- [9] Yuan, X. (2014) Bioinformatics Rehabilitation Machine. Chinese Patents, cn2014-20045965.82014. (In Chinese)
- [10] Yuan, X. and Yuan, J. (2021) Vision Rehabilitation Machine. Chinese Patents, cn202122075836.62021. (In Chinese)
- [11] Yuan, X. (2012) Bioinformatics Energy Health Bed. Chinese Patents, cn2012-20688206.42012. (In Chinese)
- [12] Yuan, X. (2017) Directional Transfer of Bioinformatics Energy. Chinese Patents, cn201710842076.2. (In Chinese)
- [13] Yuan, X. (2017) Exploration and Discovery of Biological Fields. *Frontier Science*, **11**, Article No. 85. (In Chinese)
- [14] Yuan, X., *et al.* (2009) Natural Physical Therapy, Compensation for Plant Information Energy—A New Trend of Health Care and Medicine Approach. *China Health Monthly*, **29**, 203-205. (In Chinese)
- [15] Xia, Z., *et al.* (2000) Preliminary Study on the Effect of Plant Electromagnetic Wave on Human Body. *Journal of Hunan Medical University*, **25**, 151-153. (In Chinese)

- [16] Jiang, C., Zheng, Q. and Yuan, X. (2008) Effect of Biological Electromagnetic Field on Human Anti-Aging and Health Care. *China Practical Medicine*, **7**, 45-46. (In Chinese)
- [17] Jiang, C., Zheng, Q. and Tang, B. (2000) Health Care and Anti-Aging Effects of Biological Electromagnetic Fields of Plant Seedlings on Human Body. *Chinese Journal of Applied Physiology Research*, **16**. (In Chinese)
- [18] Jiang, C., Zheng, Q. and Yuan, X. (2008) Effect of Bioelectromagnetic Field on Improving Human Immune Function. *China Practical Medicine*, **9**, 31 p. (In Chinese)
- [19] Jiang, C., Zheng, Q. and Yuan, X. (2008) Improving Effect of Bioelectromagnetic Field on Human Myocardial Ischemia. *China Practical Medicine*, **4**, 72-73. (In Chinese)
- [20] Qian, X. (1991) Selected Letters of Qian Xuesen. People's Publishing House, Beijing. (In Chinese)



Call for Papers

Open Journal of Biophysics

ISSN Print: 2164-5388 ISSN Online: 2164-5396

<https://www.scirp.org/journal/ojbiphy>

Open Journal of Biophysics (OJBIPHY) is an international journal dedicated to the latest advancement of biophysics. The goal of this journal is to provide a platform for scientists and academicians all over the world to promote, share, and discuss various new issues and developments in different areas of biophysics.

Subject Coverage

All manuscripts must be prepared in English, and are subject to a rigorous and fair peer-review process. Accepted papers will immediately appear online followed by printed hard copy. The journal publishes original papers including but not limited to the following fields:

- Bioelectromagnetics
- Bioenergetics
- Bioinformatics and Computational Biophysics
- Biological Imaging
- Biomedical Imaging and Bioengineering
- Biophysics of Disease
- Biophysics of Photosynthesis
- Cardiovascular Biophysics
- Cell Biophysics
- Medical Biophysics
- Membrane Biophysics
- Molecular Biophysics and Structural Biology
- Physical Methods
- Physiology and Biophysics of the Inner Ear
- Proteins and Nucleic Acids Biophysics
- Radiobiology
- Receptors and Ionic Channels Biophysics
- Sensory Biophysics and Neurophysiology
- Systems Biophysics
- Theoretical and Mathematical Biophysics

We are also interested in: 1) Short Reports—2-5 page papers where an author can either present an idea with theoretical background but has not yet completed the research needed for a complete paper or preliminary data; 2) Book Reviews—Comments and critiques.

Notes for Intending Authors

Submitted papers should not have been previously published nor be currently under consideration for publication elsewhere. Paper submission will be handled electronically through the website. All papers are refereed through a peer review process. For more details about the submissions, please access the website.

Website and E-Mail

<https://www.scirp.org/journal/ojbiphy>

E-mail: ojbiphy@scirp.org

What is SCIRP?

Scientific Research Publishing (SCIRP) is one of the largest Open Access journal publishers. It is currently publishing more than 200 open access, online, peer-reviewed journals covering a wide range of academic disciplines. SCIRP serves the worldwide academic communities and contributes to the progress and application of science with its publication.

What is Open Access?

All original research papers published by SCIRP are made freely and permanently accessible online immediately upon publication. To be able to provide open access journals, SCIRP defrays operation costs from authors and subscription charges only for its printed version. Open access publishing allows an immediate, worldwide, barrier-free, open access to the full text of research papers, which is in the best interests of the scientific community.

- High visibility for maximum global exposure with open access publishing model
- Rigorous peer review of research papers
- Prompt faster publication with less cost
- Guaranteed targeted, multidisciplinary audience



**Scientific
Research
Publishing**

Website: <https://www.scirp.org>

Subscription: sub@scirp.org

Advertisement: service@scirp.org